DISSERTATIONES MATHEMATICAE UNIVERSITATIS TARTUENSIS
46

OPTIMIZATION OF INELASTIC PLATES WITH CRACKS

ANNELY MÜRK

TARTU UNIVERSITY
PRESS

Faculty of Mathematics and Computer Science, University of Tartu, Tartu, Estonia

Dissertation is accepted for the commencement of the degree of Doctor of Philosophy (PhD) in mathematics on May 12, 2006 by the Council of the Faculty of Mathematics and Computer Science, University of Tartu.

Thesis adviser:
Dr. Phys. and Math., Professor — Jaan Lellep
University of Tartu,
Institute of Applied Mathematics,
Tartu, Estonia

Opponent:
Dr. Phys. and Math., Professor
Member of Latvian Academy of Science — Vitauts Tamužs
University of Latvia,
Institute of Polymer Mechanics,
Riga, Latvia

Commencement will take place on June 19, 2006.

Publication of this dissertation is granted by the Institute of Applied Mathematics, University of Tartu (project HMTRM)

ISSN 1024–4212
ISBN 9949–11–360–1 (trükis)
ISBN 9949–11–361–X (PDF)

Tartu Ülikooli Kirjastus
www.tyk.ee
Tellimus nr. 301

CONTENTS

REVIEW OF LITERATURE

Thin walled plates and shells have a lot of practical applications in civil engineering and machinery. Annular plates are used as internal watertight bulkheads in submersibles in order to isolate a damaged compartment in the case of an accident.

The dynamic plastic behaviour of annular and circular plates subjected to dynamic loadings was studied by several authors. Probably the first investigations in dynamic plastic response of circular plates are by Hopkins and Prager (1954), also Wang and Hopkins (1954) and Wang (1955) making use of the concept of a rigid-plastic body and Tresca yield hexagon. Hopkins and Prager (1954) considered a simply supported circular plate subjected to the uniformly distributed transverse pressure which is suddenly applied and removed at a certain instant of time. Wang and Hopkins (1955) considered circular plates subjected to initial impulsive loading. This concept was used by many researchers in studying of the plastic behaviour of various beams, plates and shells. Reviews of these works can be found in the books and review papers by Jones (1980, 1989), also Stronge and Yu (1993) and Martin (1975), Kaliszky (1985, 1989), Nurick and Martin (1989), Chakrabarty (2000).

As regards annular plates, e.g. circular plates with central concentric hole, the investigation of the plastic response to dynamic loads is quite complicated even in the case of a rigid-plastic Tresca material. Shapiro (1959) examined the dynamic behaviour of annular plates which are fully clamped around the inner edge and completely free at the outer edge. As a result of the initial impact the outer edge is subjected to a constant axisymmetric transverse velocity which is removed at certain time instant.

A similar problem was studied by Florence (1965) except that the outer edge was subjected to a transverse impulse rather than a constant velocity being maintained for a short time.

An approximate solution to the problem of dynamic loading of annular plates was given by Aggarwal and Ablow (1971). A rigorous solution procedure was developed later by Mazalov and Nemirovski (1976).

However, in many cases even this approach appeared to be too complicated. A simplification which retains reasonable exactness was suggested by Martin and Symonds (1966). The so-called method of mode form motions was later used in the optimization of beams, plates and shells subjected to dynamic loadings by Lepik (1982) and by Lepik and Mroz (1977), also in the further works Lellep and Mürk (1997, 1999).

Problems of strength of non-homogeneous composite materials have been studied by many authors. Tamuzs, Romalis and Petrova (2000), also Tamuzs and Romalis (1989) investigated fracture of non-homogeneous solids and solids with microdefects. Starting from the maximum shear stress theory of plastic failure Lance and Robinson (1972, 1973) derived simple yield surfaces for

composite materials composed of stiff fibers arranged in a uniform array in a ductile matrix. In the present study these yield surfaces are used in order to get simple approximations for deflections of plates of variable thickness made of composite materials.

Sandwich annular plates made of an inelastic composite material which obeys the yield surface derived by Lance and Robinson (1972, 1973) were studied by Lellep and Mürk (1997, 1999, 2002, 2003). The last paper is devoted to the determination of bounds of applicability of the mode form motions with triangular modes.

Failure modes and criteria of plastic beams, plates and shells are presented by Yu and Chen (1998). Dynamic response of fully clamped and simply supported circular plates to impact and distributed pressure loading applied in a central area of the plate is investigated by Liu and Stronge (1996) in the case of a Tresca material. Wang et al. (2005), Ma et al. (1999) studied circular plates on the base of unified strength theory. The unified yield criterion includes as particular cases both, the Tresca and Mises yield criteria. Clamped circular plates subjected to impulsive loading were examined by Wen, Yu, Reddy (1995).

Shen and Jones (1993) developed an approximate analysis of dynamic plastic deformations of fully clamped circular plates under impulsive loading. The analysis employs an interaction yield surface and uses the Cowper – Symonds constitutive equation which enables to prescribe the strain rate sensitivity of the material. Li and Jones (1994), also Liu and Stronge (1996); Jones, Kim and Li (1997) investigated shear and bending behaviour of circular plates subjected to various types of loading. Li and Jones (1994) considered blast loaded plates and Liu and Stronge (1996) plates subjected to a distributed pressure loading applied in a central area of the plate. Jones, Kim and Li (1997) presented a theoretical analysis to predict the dynamic behaviour of circular plates struck normally by blunt solid cylindrical masses at the centre.

In the papers mentioned above circular and annular plates of constant thickness have been investigated. Plastic response of structures to dynamic loading and optimization of beams, plates and shells were investigated by Lepik (1982). In the book by Lepik (1982) exact and approximate theoretical methods are used for determination of the stress-strain state of structures of variable thickness.

Although, there is a quite rich literature on the dynamic plasticity of structural elements, the most of authors have studied the dynamic behaviour of beams and axisymmetric plates (see Jones, 1989; Yu and Chen, 1998). However, the only exact theoretical solution on dynamic response of a non-axisymmetric plastic plate is obtained by Cox and Morland (1959) who investigated within the framework of thin plate theory the behaviour of square plates subjected to rectangular pressure pulse.

It is shown that the analysis for simply supported square plates may be adopted with slight modifications to the case of regular n-sided polygonal

plates. This problem is not only of practical interest but it is of mathematical interest, as well. Evidently, this solution includes, as limiting cases, the solutions of the square and circular plate problems.

Several authors (among these Cox and Morland) have studied square plates of constant thickness made of a Johansen's material. Blast loaded square plates are investigated by Olson et al. (1993). Approximate techniques are presented by Baker (1975). Zhu (1997) obtained both, theoretical numerical predictions and experimental results for transient deformation modes of square plates subjected to explosive loadings. Numerical predictions showed a good agreement with experimental results.

The phenomenon of saturated impulse in elastic- plastic square plates is studied by Zhu and Yu (1997) in the case of a fully clamped plate.

Approximate procedures for investigation of rigid- plastic rectangular plates subjected to dynamic loadings are developed by Jones et al. (1970, 1971), Yu and Chen (1992). Theoretical predictions suggested by Jones (1970, 1971) and Symonds (1980, 1982) give surprisingly good agreement with corresponding experimental results. Lellep and Mürk (2003, 2004) used this approach for determination of residual deflections of stepped annular and square plates subjected to impulsive loadings. Lellep and Mürk (2003) investigated the dynamic plastic response of annular plates to the initial impact loading. The authors considered stepped plates with following support conditions: (i) plates clamped at the outer edge and free at the inner edge, (ii) annular plates clamped at the inner edge with free outer edge. Making use of numerical experiments lower bounded to the thickness was established in the case of single step.

Lellep and Mürk (2004) developed an approximate theoretical method for prediction of the problem of the behaviour of inelastic square plates under dynamic loading. The plates of piece wise constant thickness are studied whereas the material of plates obeys Johansen's yield condition. Numerical results are presented for plates with single step.

Inelastic behaviour and optimal design of beams, plates and shells was investigated by Lepik (1982) in the case of dynamic loading. Various approaches to the optimization of thin-walled structures are discussed in review by Kruzelecki and Życzkowski (1985), Lellep and Lepik (1985), Życzkowski (1992). In the work by Lepik (1982) also by Lellep and Hein (2002) methods on non-linear programming have been used for optimal design of structures of piece wise constant thickness in the case of initial impulsive loading.

An alternative approach which is based on variational methods of the theory of optimal control was suggested for optimization of shells under quasistatic loading by Lellep and Puman (2001), Lellep and Tungel (2005).

Optimal design of rigid-plastic structural elements subjected to dynamic loadings was initiated by Lepik and Mroz (1977). The authors considered rigid plastic circular plates of piece wise constant thickness and converted the problem into a constrained minimization problem. Lepik (1982) has solved a large variety of problems of optimal design of rigid plastic structures subjected

to dynamic loading. Lellep and Hein (2002) studied clamped shallow shells of piece wise constant thickness subjected to impulsive loading. The shell under consideration has a central hole and its material obeys the "limited interaction yield surface". The designs of shallow shells are established under the condition that the maximal residual deflection attains its minimal value for given material consumption. Lellep and Puman (1999, 2000) developed optimal designs for stepped conical shells. Lellep and Puman (1999) established optimal designs of inelastic conical shells with step-wise varying cross-section. It is assumed that the material of the shell obeys a "limited interaction yield surface" and associated flow law. The problem of minimum weight under given load carring capacity is transformed into a problem of non-linear programming and it is solved by the use of Lagrange multipliers.

Similar problem is solved by Lellep and Puman (2000) in the case of a conical shell loaded by the rigid boss. The material of the shells obeys the generalized diamond yield condition suggested by Ich and Jones (1973).

An alternative approach was suggested by Lellep and Hannus (1995), Lellep and Puman (2001), Lellep and Tungel (2005) on the basis of the theory of optimal control. In earlier works by Lellep and Mürk (1997, 1999, 2002, 2003) dynamic plastic response of stepped annular plates of sandwich cross-section was studied.

Methods of the optimal control theory are given in books by Bryson, 1975; Hocking, 2001; Hull, 2003. Variational methods of the theory of optimal control are used in order to get necessary conditions of optimality for annular plates subjected to impulsive loading by Lellep and Mürk (in press). Numerical results are presented for plates with single step in the thickness.

The aim of the work is to develop approximate theoretical methods for predictions of residual deflections of square plates and annular plates, also the use of these predictions in optimization of inelastic plates.

Current thesis consists of five original research papers of the author co-authored with the supervisor and of the introduction to contributing papers. Three of these (Chapters 1–3) regard to annular plates, the rest of papers to square plates (Chapters 5 and 6).

1. INTRODUCTION TO CONTRIBUTING PAPERS

1.1. Formulation of the problem

In papers [1]–[8] the dynamic response and optimization of stepped plates is considered. The plates are made of a homogeneous or composite material which can be regarded as a rigid- plastic material.

1.1.1. Annular plates clamped at the outer edge

Axisymmetric plates subjected to the initial impulsive loading are studied. Plates clamped at the outer edge of radius *R* with the free inner edge of radius *a* will be considered (Fig.1).

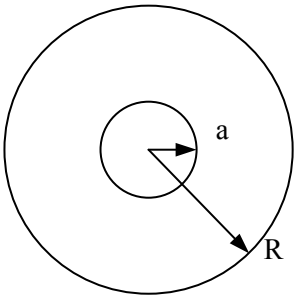

Fig. 1. Annular plate

It is assumed that the thickness is piece wise constant, e.g. $h = h_j$ for $r \in \left(a_j, a_{j+1}\right)$, where $j = 0,...,n$. Here $a_0 = a$ and $a_{n+1} = R$. The quantities h_j ($j = 0,...,n$) and a_j ($j = 1,...,n$) are treated as preliminarily unknown constant parameters to be defined so that a cost criterion attains its minimal value. It is assumed that at the re-entrant corners of steps (Fig. 2) symmetrical cracks of length c_j ($j = 1,...,n$) are located.

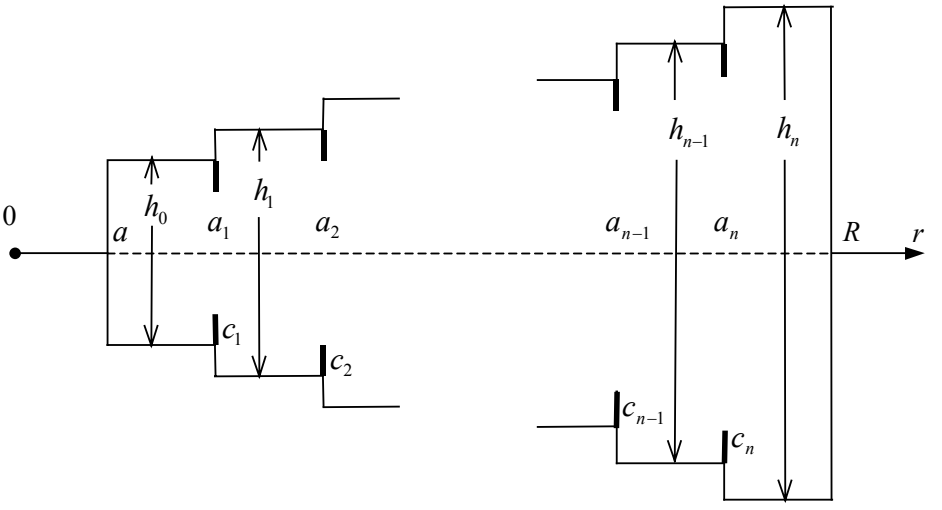

Fig. 2. Stepped annular plate

The cracks are assumed to be stable cracks, we neglect the crack propagation during the process of deformation. Generally speaking, the crack located at $r = a_j$ is not of constant length for each $\theta \in [0,2\pi]$, where θ stands for the polar angle. We call the length c_j of the crack the maximal length of this circular crack over $\theta \in [0,2\pi]$.

In the paper [1] we are looking for the design of the plate so that the maximal residual deflection of the plate attains the minimum value. Evidently, if the initial velocity distribution does not differ substantially from the uniform distribution then the maximum of deflections is attained at the outer edge of the plate. The cost criterion to be minimized can be written as

$$J = W(a_0, t_f)$$

where t_f is the time instant when the motion of the plate is completed. It appears that the maximal residual deflection depends on the design parameters $h_0,...,h_n$ and $a_1,...,a_n$ and on the acceleration of the free edge $\dfrac{\partial^2 W_0}{\partial t^2}$, as well, e.g.

$$J = \Phi_*\left(\frac{\partial^2 W_0}{\partial t^2}, a_1,...,a_n, h_0,...,h_n\right),$$

where $W_0 = W(a_0, t)$ and Φ_* is a given function which will be defined later. The cost criterion will be minimized for given weight or volume of the plate, e.g.

$$V = \pi \sum_{j=0}^{n} h_j \left(a_{j+1}^2 - a_j^2 \right),$$

where V is a given constant.

In the paper [5] an approximate method for determination of residual deflections of stepped plates is developed. This method is used in [1] for calculating of optimal designs of stepped plates clamped at the edge.

1.1.2. Annular plates clamped at the inner edge

Consider an axisymmetric plate clamped at the inner edge of radius a. The outer edge of radius R is absolutely free. Assume that $h = h_j$ for $r \in (a_j, a_{j+1})$ where $j = 0,...,n$. Here h_j ($j = 0,...,n$) and a_j ($j = 1,...,n$) are the design parameters. The cost criterion is

$$J = W(R, t_f),$$

where t_f is the response time of the plate. The weight or material volume of the plate is

$$V = \pi \sum_{j=0}^{n} h_j \left(a_{j+1}^2 - a_j^2 \right).$$

We are looking for the design of the plate of given weight so that the maximal residual deflection attains the minimal value.

Making use of method of mode form motions the cost criterion can be put into the form

$$J = \Phi_* \left(\frac{\partial^2 W_0}{\partial t^2}, a_1, ..., a_n, h_0, ..., h_n \right),$$

where $W_0 = W(R, t)$ and Φ_* is a given function.

In the paper [2] the design of the plate is established which minimizes maximal residual deflection for given weight.

1.1.3. Square plates

Let a square plate with a side length *2L* (Fig. 3.) be subjected to the initial impact loading. We assume that the initial kinetic energy K_0 is given whereas the initial transverse velocity field may be unknown.

Stepped plates will be considered, e.g. $h = h_j$ for $(x, y) \in D_j$; $j = 0,...,n$. The attention will be focused on the concentric case when the inner and outer boundaries of regions D_j are squares. Let the boundaries of regions of constant thickness intersect *x*- and *y*- axis at points $\alpha_0\sqrt{2}L$, $\alpha_1\sqrt{2}L$,..., $\alpha_{n+1}\sqrt{2}L$ (Fig. 3). Here

$$\alpha_0 = \frac{a}{L}, \quad \alpha_{n+1} = 1,$$

provided *2a* is the length of the internal edge of the plate. Note that in the case of a full plate without cut out $\alpha_0 = a = 0$.

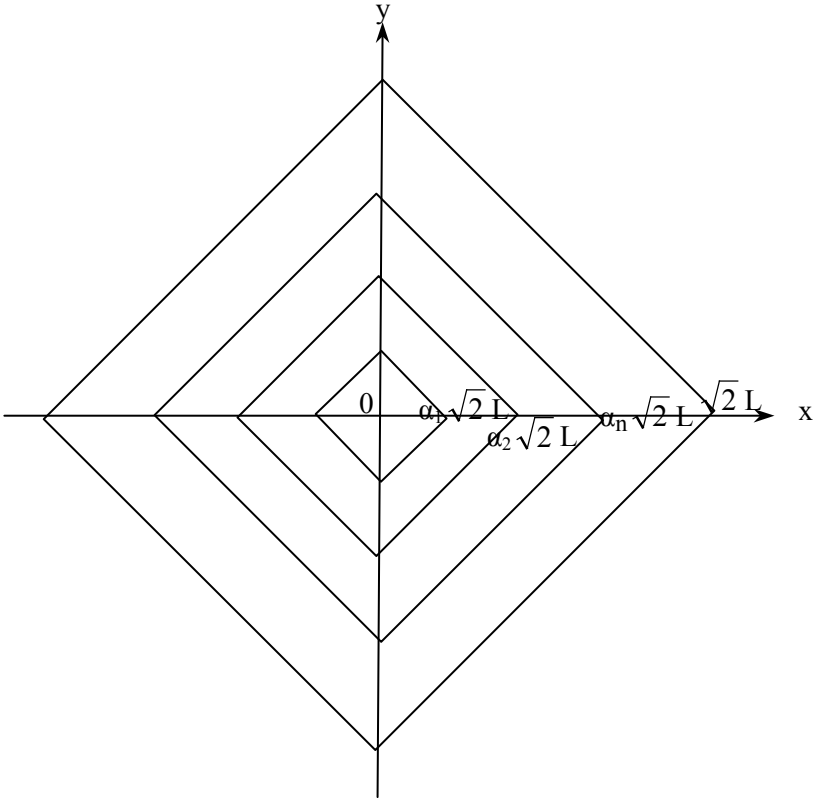

Fig. 3. Square plate

1.1.4. Optimization of square plates

Let the stepped square plate (Fig. 3) be subjected to the initial impact loading. The initial kinetic energy K_0 is assumed to be given whereas the initial transverse velocity field may be unknown.

We are considering plates with piece wise thickness, e.g.

$$h = h_j$$

for $(x, y) \in D_j$; $j = 0,...,n$. We restrict our attention to the concentric case when the inner and outer boundaries of regions D_j are squares.

It is assumed that the plates under consideration have cracks at re-entrant corners of steps. Let c_j be the length (deepness) of the straight crack located at the inner boundary of the region D_j. Cracks are treated as stable part trough surface cracks. The propagation of cracks is neglected.

The material volume of the plate is

$$V = 4L^2 \sum_{j=0}^{n} h_j \left(\alpha_{j+1}^2 - \alpha_j^2 \right)$$

We are looking for the design of the plate for which the maximal residual deflection W_1 attains its minimal value for fixed weight or material volume of the plate.

1.2. Basic equations and assumptions

1.2.1. Annular plates

In the case of axisymmetric plates the equilibrium equations and deformation rates of a plate element can be presented as (Jones, 1989)

$$\frac{\partial}{\partial r}\left(\frac{\partial}{\partial r}(rM_1) - M_2 \right) = rQ$$

$$\frac{\partial}{\partial r}(rQ) = \mu h_j r \frac{\partial^2 W}{\partial t^2}$$

for $r \in (a_j, a_{j+1})$; $j = 0,...,n$ and

$$\frac{\partial \kappa_1}{\partial t} = -\frac{\partial^3 W}{\partial r^2 \partial t}, \quad \frac{\partial \kappa_2}{\partial t} = -\frac{1}{r}\frac{\partial^2 W}{\partial r \partial t}.$$

Here M_1, M_2 stand for principal moments and κ_1, κ_2 — principal curvatures.

The material of the plate is assumed to be an ideal rigid plastic material. Plastic yielding of the material is controlled by the yield condition suggested by Lance and Robinson (1972). These yield locusci correspond to unidirectionally

reinforced ductile composites with ductile fibers and ductile matrix. In the foregoing analysis we assume that the stress profile corresponds to horizontal sides EA' of rectangles A'BC'E. The rectangles are considered as circumscribed approximations to hexagons presented by Lance and Robinson (Fig. 4, 5). Fig. 4 corresponds to a composite reinforced in the circumferential direction whereas Fig. 5 is associated with a radially reinforced plate.

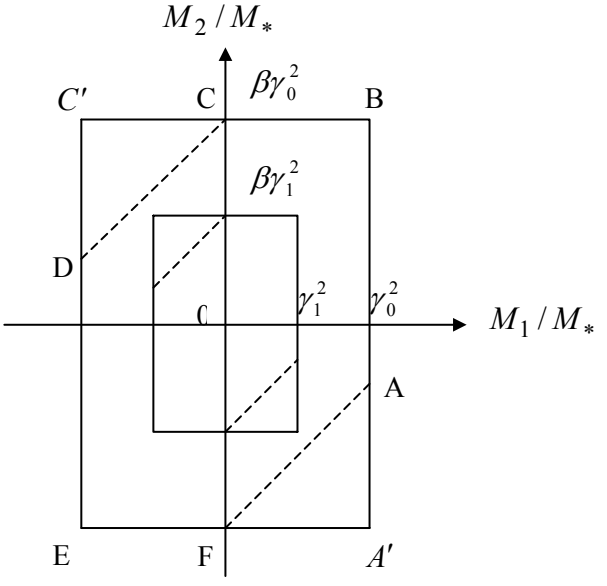

Fig. 4. Yield condition for circumferentially reinforced solid plates

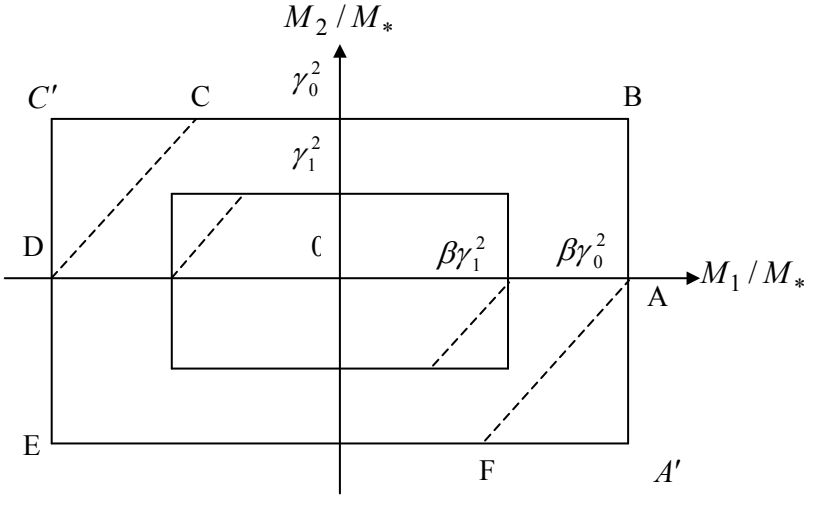

Fig. 5. Yield condition for radially reinforced solid plates

According to the associated flow law $\frac{\partial \kappa_1}{\partial t} = 0$. Thus,

$$\frac{\partial W}{\partial t} = \frac{\partial W_0}{\partial t}\frac{r-a}{R-a}.$$

When deriving the last equation the kinematical boundary condition

$$\frac{\partial W}{\partial t}(a,t) = 0$$

is taken account.

It is reasonable to assume that the stress state of the plate corresponds to the flow regime EA' one has

$$M_2 = -\beta M_j$$

in the case of circumferential orientation of fibers and

$$M_2 = -M_j$$

for $\rho \in (a_j, a_{j+1})$; $j = 0,...,n$ in the case of radially reinforced plate. Here $M_j = \sigma_0 h_j^2 / 4$ in the case of solid plates and $M_j = \sigma_0 H h_j$ in the case of sandwich plates whereas σ_0 is the yield stress of the matrix material.

The initial kinetic energy K_0 is defined as

$$K_0 = \pi \sum_{j=0}^{n} \int_{D_j} \mu h_j \left(\frac{\partial W}{\partial t} \right)^2 \Big|_{t=0} r dr,$$

where μ is the density of the material.

1.2.2. Square plates

The material of plates is an isotropic homogeneous material which can be treated as an ideal plastic material obeying Johansen's yield condition (Fig. 6). Here M_1, M_2 stand for the principal moments which are coupled with moments M_x, M_y by relations (see Jones, 1989)

$$M_1 = \frac{1}{2}\left[M_x + M_y + \sqrt{(M_x - M_y)^2 + 4M_{xy}^2} \right],$$

$$M_2 = \frac{1}{2}\left[M_x + M_y - \sqrt{(M_x - M_y)^2 + 4M_{xy}^2} \right].$$

The moments M_x, M_y, M_{xy} with shear forces Q_x, Q_y have to satisfy equilibrium equations

$$\frac{\partial Q_x}{\partial x} + \frac{\partial Q_y}{\partial y} + p = \mu\, h \frac{\partial^2 W}{\partial t^2}$$

$$\frac{\partial M_x}{\partial x} + \frac{\partial M_{xy}}{\partial y} - Q_x = 0$$

$$\frac{\partial M_y}{\partial y} + \frac{\partial M_{xy}}{\partial x} - Q_y = 0$$

Here μ stands for the material density, p is the intensity of transverse loading and W is the transverse deflection. Since we consider the motion of the plate due to inertia we can take $p = 0$. Eliminating shear forces Q_x, Q_y from the last system one obtains a single equation as

$$\frac{\partial^2 M_x}{\partial x^2} + 2\frac{\partial^2 M_{xy}}{\partial x \partial y} + \frac{\partial^2 M_y}{\partial y^2} = \mu\, h \frac{\partial^2 W}{\partial t^2}$$

It is well known that the curvatures have the form (see Ventsel and Krauthammer, 2001)

$$\kappa_x = -\frac{\partial^2 W}{\partial x^2},\ \kappa_y = -\frac{\partial^2 W}{\partial y^2},\ \kappa_{xy} = -\frac{\partial^2 W}{\partial x \partial y}$$

The method of mode form motions will be used. Perhaps the simplest kinematically admissible transverse velocity distribution is

$$\frac{\partial W}{\partial t} = \dot{W}_0(t)(1 - z)$$

where $z = (x + y)/\sqrt{2}L$.

Here $\dot{W}_0(t)$ stands for is the transverse velocity of the central point of the plate.

Boundary conditions at the edge can be obtained from the relation for the moment with respect to an inclined edge (see Ventsel and Krauthammer, 2001)

$$(M)_n = M_x \sin^2\beta + M_y \cos^2\beta + M_{xy} \sin 2\beta$$

where β stands for the angle of inclination with respect to the *x*-axis. In the case of a square plate $\beta = \pi/4$. Therefore the last relation takes the form

$$(M)_n = \frac{1}{2}(M_x + M_y)^2 + M_{xy}.$$

Similarly, for the shear force one has

$$(Q)_n = \frac{1}{\sqrt{2}}(Q_x + Q_y).$$

We are looking for the solution of the equation of motion as

$$M_x = M_j + x^2 F_j(z),$$

$$M_y = M_j + y^2 F_j(z),$$

$$M_{xy} = xyF_j(z),$$

for $(x, y) \in D_j$ ($j = 0,...,n$). Here F_j ($j = 0,...,n$) stand for unknown functions.

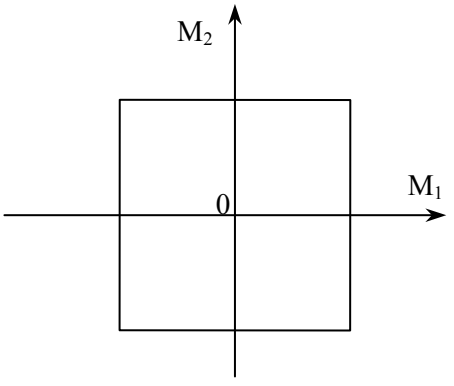

Fig. 6. Johansen's yield condition

In the paper [4] a method of determination of residual deflections of stepped plates was developed. It was used in [3] for determination of optimal designs of stepped plates.

References

1. Jones N (1989) Structural Impact. Cambridge University Press, Cambridge
2. Lance RH, Robinson DN (1972) Limit analysis of ductile fiber-reinforced structures. Proc ASCE, EM98, 195–209
3. Lellep J, Mürk A Optimization of inelastic annular plates with cracks. Struct Multidisc Optim (in press)
4. Lellep J, Mürk A Optimization of axisymmetric plates with cracks. Int J Solids Structures (in press)
5. Lellep J, Mürk A Optimization of inelastic square plates with cracks. Eng Optim (in press)

6. Lellep J, Mürk A (2004) Inelastic behaviour of stepped square plates. In: Kienzler R, Altenbach H, Ott I (eds) Theories of Plates and Shells. Critical Review and New Applications (Euromech Colloquium 444 held in Bremen 2002), Springer, Berlin Heidelberg New York, 133–140
7. Lellep J, Mürk A (2003) Inelastic stepped plates under impulsive loading. In: Gupta NK (ed) Plasticity and Impact Mechanics (Implast 2003 held in New Delhi), Phoenix Publishing House, New Delhi, 577–588
8. Lellep J and Myrk A (2002) Optimization of stepped plates under dynamic loading. Engineering Design Optimization. Proc 4th ASMO-UK/ISSMO Conf (Ed P. Gosling). Newcastle, 119–125
9. Lellep J and Mürk A (1999) Optimization of axisymmetric plates of composite materials. Impact and Damage Tolerance Modelling of Composite Materials and Structures. Proc Euromech Colloq 400 (Ed Soutis C, Guz IA). Imperial Colledge of Science, Technol Medic London, 146–153
10. Lellep J, Mürk A (1997) Optimization of annular plates of composite materials. Polymeric Composites-Expanding the Limits. Proc 18-th Riso Int Symposium on Materials Science, (Eds Andersen SI et al.), Roskilde, 405–410
11. Ventsel E, Krauthammer T (2001) Thin Plates and Shells. Theory, Analysis and Applications. Marcel Dekker, New York

2. INELASTIC STEPPED PLATES UNDER IMPULSIVE LOADING

J. Lellep and A. Mürk
Institute of Applied Mathematics, Tartu University
Tartu, Estonia

ABSTRACT

Axisymmetric plates made of a fiber reinforced composite are studied. The plates are subjected to the initial impulsive loading which imparts to the plates a fixed amount of the kinetic energy. Making use of the method of mode form motions simple theoretical predictions of maximal residual deflections are developed. Limits of the applicability of current approach are established.

2.1. INTRODUCTION

Dynamic plastic response of circular plates was investigated by Hopkins and Prager (1954) making use of the concept of a rigid-plastic body and Tresca yield hexagon. This concept was used by many researchers in studying of the plastic behaviour of various beams, plates and shells. Reviews of these works can be found in the books and review papers by Jones (1980, 1989), also by Stronge and Yu (1993) and Martin (1975), Kaliszky (1989).

However, in many cases even this approach appeared to be too complicated. A simplification which retains reasonable exactness was suggested by Martin and Symonds (1966). The so-called method of mode form motions was later used in the optimization of beams, plates and shells subjected to dynamic loadings by Lepik and Mroz (1977), also in the further works by Lellep and Mürk (1999, 2002).

Starting from the maximum shear stress theory of plastic failure Lance and Robinson (1972) derived simple yield surfaces for composite materials composed of stiff fibers arranged in a uniform array in a ductile matrix. In the present paper these yield surfaces are used in order to get simple approximations for deflections of plates of variable thickness made of composite materials.

2.2. FORMULATION OF THE PROBLEM AND ASSUMPTIONS

Consider an axisymmetric plate of variable thickness with the outer edge of radius R and inner edge of radius a. Assume that the plate is subjected to the initial impulsive loading so that at the initial moment of time the plate has the kinetic energy K_0. The subsequent motion is due to inertia until the energy K_0 is absorbed in plastic work.

The thickness of the plate is approximated with a piece wise constant distribution, e.g.

$$h = h_j \tag{1}$$

for $r \in (a_j, a_{j+1})$, where $j = 0,...,n$. It is reasonable to define $a_0 = a$ and $a_{n+1} = R$.

We consider both, homogeneous plates and ideal sandwich - type plates. In the latter case the thickness of carrying layers is piece wise constant whereas the thickness of the core material is assumed to be constant.

Material of the plates is a fiber reinforced composite which obeys the yield condition suggested by Lance and Robinson (1975). It is well known that the material behaviour strongly depends on the orientation of fibers in the solid under consideration.

That is why it is not possible to draw a single yield surface for different values of the angle of orientation of fibers. In the present paper we consider only the plates with radial and circumferential orientation of fibers in the matrix material. Corresponding yield conditions are presented in Fig. 2.1 and 2.2.

The aim of the paper is to evaluate the dynamic plastic response of plates making use of the method of mode form motions. This approach was developed by Martin and Symonds (1966, 1975). Later it was established by several authors (see Jones, 1989) that the results obtained by the method of form motions compare favourably with other theoretical predictions and with experimental data.

The plates clamped at inner edge (with free outer edge) and plates clamped at outer edge (inner edge is free) are considered from the unique point of view. The transverse velocity field is assumed to be given as

$$\frac{\partial W}{\partial t} = \frac{dW_0}{dt}\frac{R-r}{R-a} \tag{2}$$

for the plate clamped at the outer edge and

$$\frac{\partial W}{\partial t} = \frac{dW_0}{dt}\frac{r-a}{R-a} \tag{3}$$

for the plate with clamped inner edge. Here $W_0(t)$ stands for the deflection of the free edge.

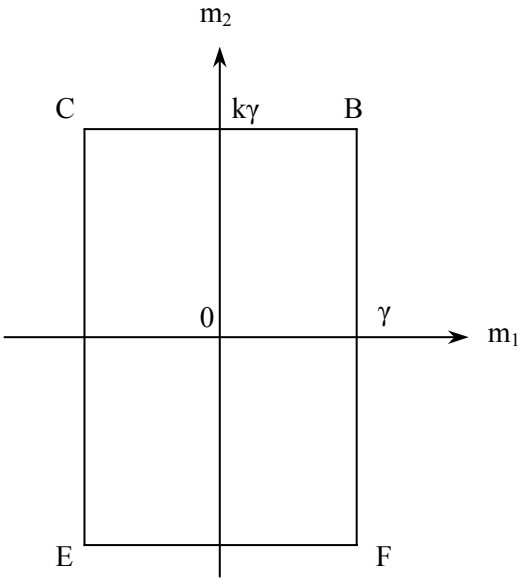

Fig. 2.1. Yield locus-circumferential reinforcement

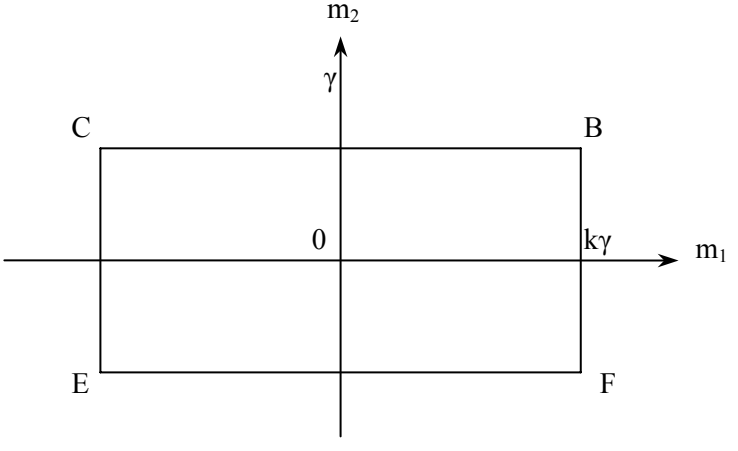

Fig. 2.2. Yield locus-radial reinforcement

2.3. GOVERNING EQUATIONS

Equilibrium equations of a plate element can be put into the form (Hopkins and Prager, 1954; Jones, 1989)

$$\frac{\partial}{\partial r}\left[\frac{\partial}{\partial r}(rM_1) - M_2\right] = -pr + \mu hr\frac{\partial^2 W}{\partial t^2} \tag{4}$$

where M_1, M_2 stand for the principal moments in the radial and circumferential direction, respectively. Here μ is the density of the material and h is defined by (1). Note that in the case of impulsive loading $p = 0$.

The curvatures in the principal directions are

$$\kappa_1 = -\frac{\partial^2 W}{\partial r^2}, \quad \kappa_2 = -\frac{1}{r}\frac{\partial W}{\partial r}. \tag{5}$$

According to the associated flow law the vector of curvature rates is to be directed along the outward normal to the yield surface. It can be easily shown that the associated flow law is fulfilled in the case of a linear mode form solution. Indeed, differentiating (2) and (3) twice with respect to r one can see that

$$\frac{\partial \kappa_1}{\partial t} = 0 \tag{6}$$

in both cases.
However,

$$\frac{\partial \kappa_2}{\partial t} = \frac{1}{r}\frac{1}{R-a}\frac{dW_0}{dt} \tag{7}$$

and

$$\frac{\partial \kappa_2}{\partial t} = -\frac{1}{r}\frac{1}{R-a}\frac{dW_0}{dt} \tag{8}$$

for plates clamped at the outer or inner edge, respectively. Thus, the associated flow law is satisfied, if the flow regimes BC or EF are used in the cases of plates clamped at the outer or inner edge, respectively.

The initial kinetic energy can be calculated as

$$K_0 = \pi \sum_{j=0}^{n} \int_{a_j}^{a_{j+1}} \mu h_j \left[\frac{\partial W(r,0)}{\partial t} \right]^2 r dr \,. \tag{9}$$

It appears to be reasonable to introduce following non-dimensional variables

$$\begin{aligned} &\rho = \frac{r}{R}, \quad \alpha_j = \frac{a_j}{R}, \quad \gamma_j = \frac{h_j}{h_*}, \quad \alpha = \frac{a}{R}, \\ &m_{1,2} = \frac{M_{1,2}}{M_*}, \quad w_0 = \frac{W_0}{h_*}, \quad \tau = \sqrt{\frac{M_*}{\mu h_*^2 R^2}}\, t, \quad K = \frac{K_0}{\pi M_* h_*}. \end{aligned} \tag{10}$$

Here h_* stands for a reference thickness of a plate of constant thickness and M_* is the limit moment of the plate of thickness h_*.

Thus, in the case of a solid plate $M_* = \sigma_0 h_*^2 / 4$ and in the case of a sandwich plate $M_* = \sigma_0 h_* H$ where H is the thickness of the core material and σ_0 stands for the yield stress of the material.

Making use of (10) the equilibrium equation can be presented as

$$\left(\left(\rho m_1 \right)' - m_2 \right)' - \rho \gamma_j \ddot{w} = 0 \tag{11}$$

for $\rho \in \left(\alpha_j, \alpha_{j+1} \right)$, where prims and dots denote the differentiation with respect to ρ and τ, respectively.

The initial kinetic energy (9) can be put into the form

$$K = \sum_{j=0}^{n} \int_{a_j}^{a_{j+1}} \gamma_j \dot{w}^2 (\rho,0) \rho d\rho \tag{12}$$

whereas the modal velocities (2) and (3) take the form

$$\dot{w} = \dot{w}_0 \frac{1-\rho}{1-\alpha} \tag{13}$$

and

$$\dot{w} = \dot{w}_0 \frac{\rho-\alpha}{1-\alpha} \tag{14}$$

respectively.

2.4. RESIDUAL DEFLECTIONS

It is known that the method of mode form motions leads to motions with constant accelerations (see Lepik and Mroz, 1977; Martin and Symonds, 1966). Thus, $\ddot{w}_0 = const$. Integrating this equation twice with respect to time yields

$$\dot{w}_0 = \ddot{w}_0 \tau + v_0 \tag{15}$$

and

$$w_0 = \frac{1}{2} \ddot{w}_0 \tau^2 + v_0 \tau \tag{16}$$

where the initial conditions $\dot{w}_0(0) = v_0$ and $w_0(0) = 0$ are taken into account.

The motion ceases at the moment $\tau = \tau_1$ when the velocity vanishes, e.g.

$$\tau_1 = -\frac{v_0}{\ddot{w}_0} \tag{17}$$

Making use of (16), (17) one obtains the maximal residual deflection $w_1 = w_0(\tau_1)$ as

$$w_1 = -\frac{v_0^2}{2\ddot{w}_0} \tag{18}$$

Note that in (15)–(18) the quantity v_0 is an unknown constant. It can be determined from the requirement that the initial kinetic energy is fixed. Making use of (12)–(14) one can easily to recheck that

$$v_0^2 = \frac{12 K_0 (1-\alpha)^2}{\sum_{j=0}^{n} \gamma_j \left[6\left(\alpha_{j+1}^2 - \alpha_j^2\right) - 8\left(\alpha_{j+1}^3 - \alpha_j^3\right) + 3\left(\alpha_{j+1}^4 - \alpha_j^4\right) \right]} \tag{19}$$

in the case of the plate clamped at the outer edge and

$$v_0^2 = \frac{12K_0(1-\alpha)^2}{\sum_{j=0}^{n}\gamma_j\left[6\alpha^2\left(\alpha_{j+1}^2-\alpha_j^2\right)-8\alpha\left(\alpha_{j+1}^3-\alpha_j^3\right)+3\left(\alpha_{j+1}^4-\alpha_j^4\right)\right]} \tag{20}$$

in the case of the clamped inner edge.

In a particular case $n=1$ relations (18) – (20) lead to results

$$w_1 = \frac{-6K(1-\alpha)^2}{\left[(\gamma_0-\gamma_1)\left(3\alpha_1^4-8\alpha_1^3+6\alpha_1^2\right)-\gamma_0\left(3\alpha^4-8\alpha^3+6\alpha^2\right)+\gamma_1\right]\ddot{w}_0} \tag{21}$$

and

$$w_1 = \frac{-6K(1-\alpha)^2}{\left[(\gamma_0-\gamma_1)\left(3\alpha_1^4-8\alpha_1^3\alpha+6\alpha_1^2\alpha^2\right)+\gamma_1\left(3-8\alpha+6\alpha^2\right)-\gamma_0\alpha^4\right]\ddot{w}_0} \tag{22}$$

which hold good for plates clamped at the outer or inner edge, respectively.

2.5. ANNULAR PLATE CLAMPED AT THE INNER EDGE

Let us consider a sandwich plate with clamped inner and absolutely free outer edge. Consider first the case of circumferential arrangement of fibers in the matrix material.

As it was mentioned above we assume that the flow regime EF (Fig. 2.1) takes place, e.g.

$$m_2 = -\gamma_j k \tag{23}$$

for $\rho\in(\alpha_j,\alpha_{j+1});\ j=0,..,n$.

Substituting (23) with (14) in (11) after integration one obtains

$$(\rho m_1)' + k\gamma_j = \gamma_j\frac{\ddot{w}_0}{1-\alpha}\left(\frac{\rho^3}{3}-\alpha\frac{\rho^2}{2}\right)+B_j \tag{24}$$

and

$$\rho m_1 + k\gamma_j\rho = \frac{\gamma_j\ddot{w}_0}{1-\alpha}\left(\frac{\rho^4}{12}-\alpha\frac{\rho^3}{6}\right)+B_j\rho+C_j \tag{25}$$

for $\rho\in(\alpha_j,\alpha_{j+1});\ j=0,..,n$.

Constants of integration B_j, C_j are to be determined so that the bending moment m_1 and the shear force

$$q = \frac{1}{\rho}\left[(\rho m_1)' - m_2\right] \tag{26}$$

are continuous at each boundary point α_j for $j = 0,..,n$. Moreover, the boundary conditions

$$m(\alpha,\tau) = -\gamma_0, \quad m(1,\tau) = 0, \quad q(1,\tau) = 0 \tag{27}$$

are to be satisfied, as well.

In the case of a single step in the thickness constants of integration in (24), (25) can be determined as

$$\begin{aligned}
B_0 &= \frac{\gamma_1\ddot{w}_0}{1-\alpha}\left(\frac{\alpha_1^3}{3} - \frac{\alpha\alpha_1^2}{2} + \frac{\alpha}{2} - \frac{1}{3}\right) - \frac{\gamma_0\ddot{w}_0}{1-\alpha}\left(\frac{\alpha_1^3}{3} - \frac{\alpha\alpha_1^2}{2}\right)\\
B_1 &= \frac{\gamma_1\ddot{w}_0}{1-\alpha}\left(\frac{\alpha}{2} - \frac{1}{3}\right)\\
C_0 &= \frac{\gamma_1\ddot{w}_0}{1-\alpha}\left(-\frac{\alpha_1^4}{4} + \frac{\alpha\alpha_1^3}{3} - \frac{\alpha}{3} + \frac{1}{4}\right) - \frac{\gamma_0\ddot{w}_0}{1-\alpha}\left(-\frac{\alpha_1^4}{4} + \frac{\alpha\alpha_1^3}{3}\right) +\\
&\quad + k\gamma_0\alpha_1 + k\gamma_1(1-\alpha_1)\\
C_1 &= k\gamma_1 + \frac{\gamma_1\ddot{w}_0}{1-\alpha}\left(-\frac{\alpha}{3} + \frac{1}{4}\right)
\end{aligned} \tag{28}$$

The acceleration takes according to (24)–(28) the form

$$\ddot{w}_0 = \frac{-12(1-\alpha)\left[\gamma_0\alpha + k\gamma_0(\alpha_1 - \alpha) + k\gamma_1(1-\alpha_1)\right]}{(\gamma_0 - \gamma_1)\left(3\alpha_1^4 + 6\alpha^2\alpha_1^2 - 8\alpha\alpha_1^3\right) + \gamma_1\left(6\alpha^2 - 8\alpha + 3\right) - \gamma_0\alpha^4}. \tag{29}$$

Making use of (29) one can present the maximal residual deflection as

$$w_1 = \frac{K(1-\alpha)}{2\left[\gamma_0\alpha + k\gamma_0(\alpha_1 - \alpha) + k\gamma_1(1-\alpha_1)\right]}. \tag{30}$$

Consider now the case of radial orientation of fibers in the matrix. The yield surface corresponding to the radial reinforcement is presented in Fig. 2.2. If the flow regime EF takes place then

$$m_2 = -\gamma_j \tag{31}$$

for $\rho \in (\alpha_j, \alpha_{j+1})$.

The integration of the equilibrium equation (11) is similar to that in the previous case. However, one has to take into account that now the maximal admissible bending moment in the radial direction is $k\gamma_0$. Thus the first boundary condition in (27) is to be replaced by the requirement

$$m(\alpha, \tau) = -k\gamma_0 . \tag{32}$$

For the plate with one step in the thickness one obtains the acceleration as

$$\ddot{w}_0 = \frac{-12K(1-\alpha)\left[k\gamma_0\alpha + \gamma_0(\alpha_1 - \alpha) - \gamma_1(\alpha_1 - 1)\right]}{(\gamma_0 - \gamma_1)\left(3\alpha_1^4 + 6\alpha^2\alpha_1^2 - 8\alpha\alpha_1^3\right) + \gamma_1\left(6\alpha^2 - 8\alpha + 3\right) - \gamma_0\alpha^4} . \tag{33}$$

The maximal residual deflection takes the form

$$w_1 = \frac{K(1-\alpha)}{2\left[k\gamma_0\alpha + \gamma_0(\alpha_1 - \alpha) + \gamma_1(1 - \alpha_1)\right]} . \tag{34}$$

2.6. ANNULAR PLATE CLAMPED AT THE OUTER EDGE

Consider a sandwich plate with clamped outer edge and free inner edge. In the case of the circumferential reinforcement according to the flow regime BC (Fig. 2.1) one has

$$m_2 = k\gamma_j \tag{35}$$

for $\rho \in (\alpha_j, \alpha_{j+1})$; $j = 0,..,n$.

Substituting (35) in the equilibrium equation (11) one can easily find the integrals of (11). For the plate with one step of the thickness one obtains

$$\ddot{w}_0 = \frac{-12K(1-\alpha)\left[k\gamma_0(\alpha_1-\alpha)+k\gamma_1(1-\alpha_1)+\gamma_1\right]}{(\gamma_0-\gamma_1)\left(3\alpha_1^4-8\alpha_1^3+6\alpha_1^2\right)-\gamma_0\left(3\alpha^4-8\alpha^3+6\alpha^2\right)+\gamma_1}. \qquad (36)$$

Substituting (36) in (21) leads to the maximal residual deflection of the plate with circumferential orientation of fibers

$$w_1 = \frac{K(1-\alpha)}{2\left[k\gamma_0(\alpha_1-\alpha)+k\gamma_1(1-\alpha_1)+\gamma_1\right]}. \qquad (37)$$

Similarly, in the case of radial reinforcement one has according to Fig. 2.2

$$m_2 = \gamma_j \qquad (38)$$

in each part of the plate. Now according to (38), (11), (13) one has

$$\ddot{w}_0 = \frac{-12K(1-\alpha)\left[\gamma_0(\alpha_1-\alpha)+\gamma_1(1-\alpha_1)+k\gamma_1\right]}{(\gamma_0-\gamma_1)\left(3\alpha_1^4-8\alpha_1^3+6\alpha_1^2\right)-\gamma_0\left(3\alpha^4-8\alpha^3+6\alpha^2\right)+\gamma_1}. \qquad (39)$$

When deriving (39) the boundary conditions

$$m(\alpha,\tau)=0, \quad m(1,\tau)=-k\gamma_1, \quad q(\alpha,\tau)=0$$

have been taken into account. In the present case the maximal residual deflection has the form

$$w_1 = \frac{K(1-\alpha)}{2\left[\gamma_0(\alpha_1-\alpha)+\gamma_1(1-\alpha_1)+k\gamma_1\right]}. \qquad (40)$$

2.7. DISCUSSION

Results of calculations are presented in Fig. 2.3–2.8 and Tables 2.1–2.2. In Fig. 2.3–2.8 distributions of the bending moment m_1 are presented for different thicknesses and different locations of the step. Fig. 2.3, 2.4, 2.7 correspond to plates clamped at the inner edge and free at the outer edge whereas Fig. 2.5, 2.6, 2.8 are associated with plates clamped at the outer edge. Different curves in Fig. 2.3–2.8 are obtained for the thickness γ_1 or γ_0 equal to 0.1, 0.2,…,0.9, respectively. In Fig. 2.3 and 2.4 $\alpha = 0.1$ whereas $\alpha_1 = 0.3$ and $\alpha_1 = 0.5$, respectively.

The bending moment m_1 is shown for plates clamped at the outer edge in Fig. 2.5, 2.6. Here $\alpha = 0.1$ whereas in $\alpha_1 = 0.2$ and $\alpha_1 = 0.3$, respectively.

It can be seen from Fig. 2.3–2.6 that the bending moment distributions are admissible, e.g. $|m_1| \le \gamma_j$ for $\rho \in D_j$.

At the boundary between these regions the slope of the curve has a finite jump.

In Fig. 2.7, 2.8 the maximal residual deflections are presented for plates clamped at the inner and outer edge, respectively. The matter that the curves intersect at the unique point is not surprising. Vice versa, it is natural because when the point where the jump takes place moves towards the clamped edge the solution for a stepped plate tends to that corresponding to the plate of constant thickness.

It was checked numerically if the solutions obtained above met statical conditions of admissibility. Calculations carried out showed that in the case of the plate clamped at the inner edge the solution (23)–(28) was statically admissible for $\gamma \ge \gamma_*$. The values of the parameter γ_* are accommodated in Table 2.1. It can be seen from Table 2.1 that the limits of applicability of the mode form solution are more severe in the cases if the step is located near to the internal edge of the plate. Note that the upper part of Table 2.1 is empty because of the natural constraint $\alpha_1 > \alpha$.

Similar bounds for γ_0 in the case of the plate clamped at the outer edge are presented in Table 2.2.

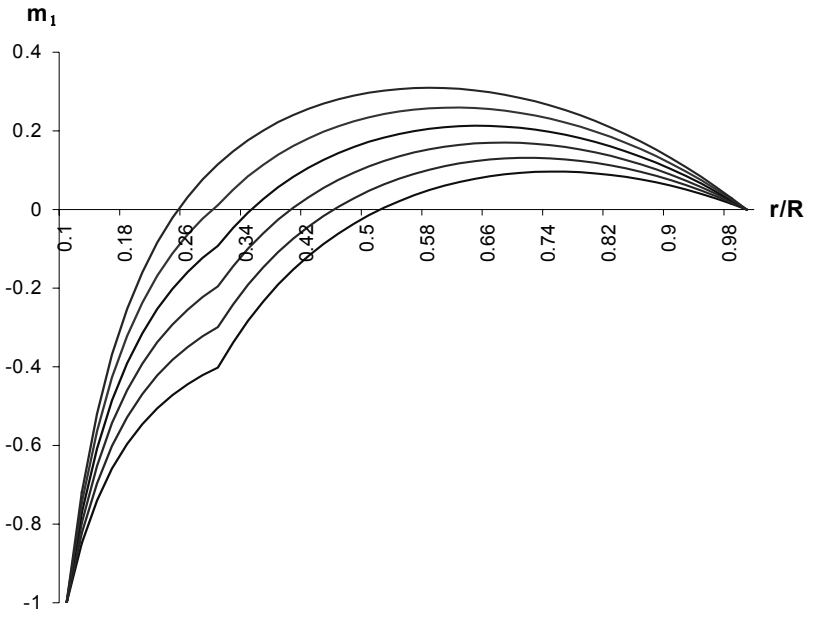

Fig. 2.3. Bending moment for the plate clamped at the inner edge (α=0.1, α_1=0.3)

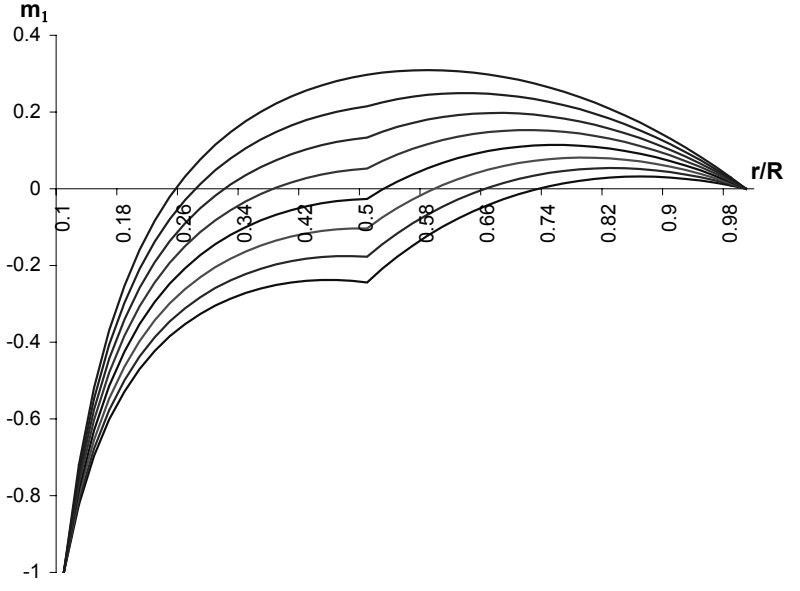

Fig. 2.4. Bending moment for the plate clamped at the inner edge (α =0.1, α_1=0.5)

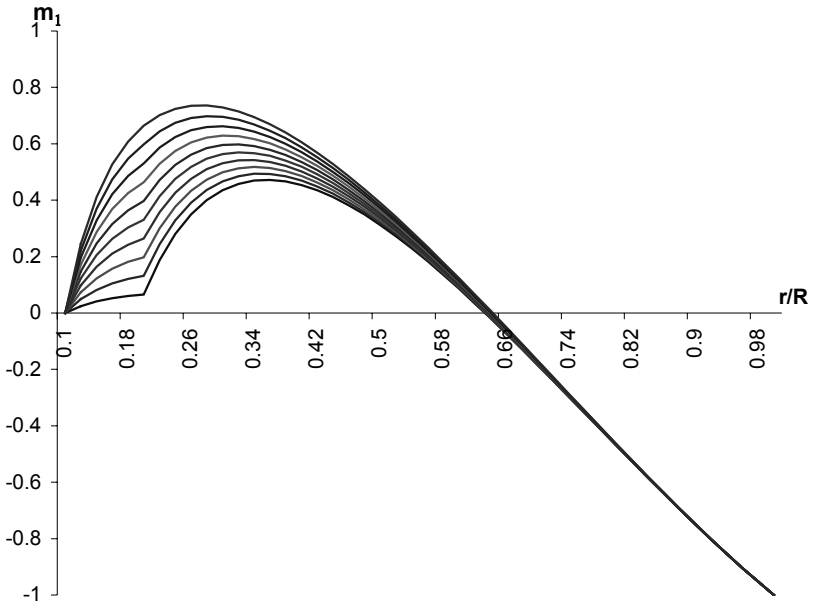

Fig. 2.5. Bending moment for the plate clamped at the outer edge (α =0.1, α_1=0.2)

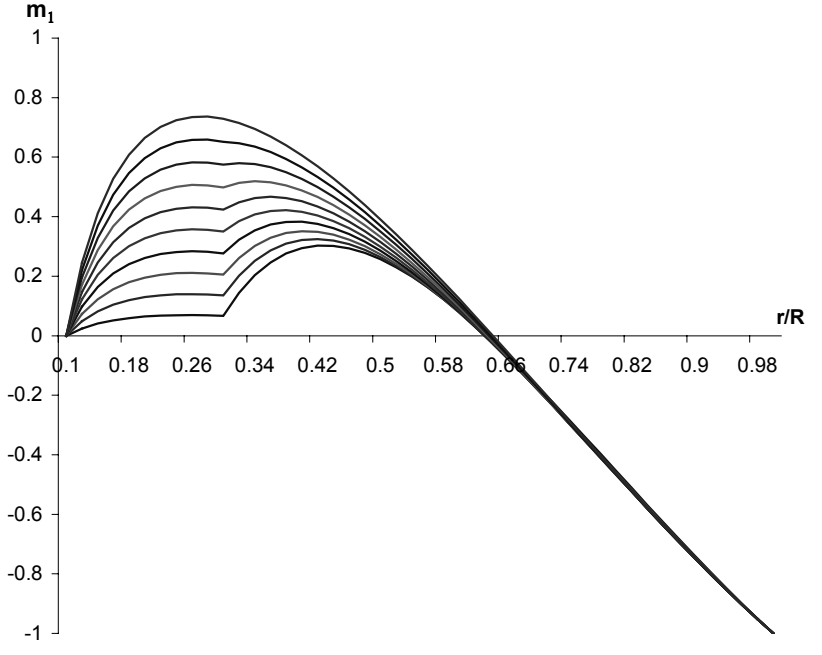

Fig. 2.6. Bending moment for the plate clamped at the outer edge (α =0.1, α_1=0.3)

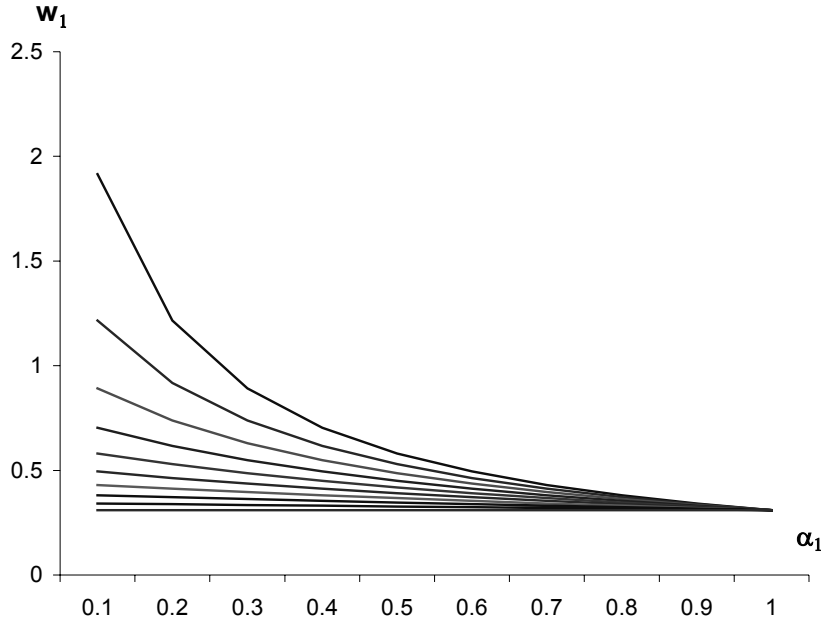

Fig. 2.7. Maximal deflection of the plate clamped at the inner edge, α =0.1

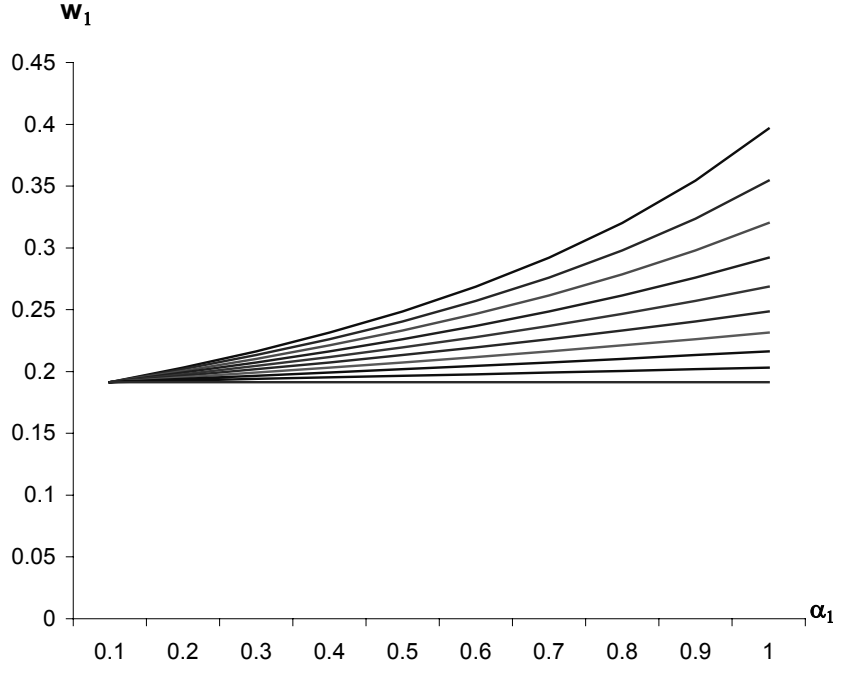

Fig. 2.8. Maximal deflection of the plate clamped at the outer edge, α =0.1

Table 2.1. Lower bounds for the thickness in the outward region

α_1 \ α	0.1	0.2	0.3	0.4	0.5	0.6	0.7	0.8	0.9
0.2	0.5578	–	–	–	–	–	–	–	–
0.3	0.4517	0.6032	–	–	–	–	–	–	–
0.4	0.3654	0.4596	0.6222	–	–	–	–	–	–
0.5	0.2650	0.3410	0.4477	0.6218	–	–	–	–	–
0.6	0	0.2014	0.2914	0.4126	0.6019	–	–	–	–
0.7	0	0	0	0	0.3426	0	–	–	–
0.8	0	0	0	0	0	0	0	–	–
0.9	0	0	0	0	0	0	0	0	–

Table 2.2. Lower bounds for the thickness in the internal region

α_1 \ α	0.1	0.3	0.5	0.7
0.5	0	0	0	0
0.6	0.2330	0	0	0
0.65	0.3533	0.2210	0	0
0.7	0.4553	0.3665	0	0
0.75	0.5464	0.4865	0.2547	0
0.8	0.6313	0.5914	0.4373	0
0.85	0.7143	0.6888	0.5860	0.2509
0.9	0.7998	0.7852	0.7204	0.5322

2.8. CONCLUDING REMARKS

A method for evaluation of stresses and displacements for plates of variable thickness has been developed. The thickness of the plate has been approximated with a piece wise constant distribution. The method of mode form motions based on the energy balance was used.

The applicability of the simplest method of mode form motions in the case of stepped plates was investigated numerically. It was established that the lower bound for the thickness is essential in the cases, if the step in the thickness is relatively large and it is located relatively near to the clamped edge.

ACKNOWLEDGEMENT

The partial support of the research via grant № 4377 of the Estonian Science Foundation is gratefully acknowledged.

2.9. REFERENCES

1. Hopkins, H. G and Prager, W. On the dynamics of plastic circular plates. ZAMP, 1954, 5, 317–330.
2. Jones, N. Structural Impact. Cambridge University Press, Cambridge, 1989.
3. Jones, N. Dynamic plastic response of structures. Recent Adv. Struct. Dyn. Proc. Int. Conf. Southampton, 1980, 677–689.
4. Kaliszky, S. Plasticity. Theory and Engineering Applications. Elsevier, Amsterdam, 1989.
5. Lance, R. H. and Robinson, D. N. A maximum shear stress theory of plastic failure of fiber-reinforced materials. J. Mech. Phys. Solids, 1972, 19, 49–60.
6. Lance, R. H. and Robinson, D. N. Limit analysis of ductile fiber-reinforced structures. Proc. ASCE, 1972 EM 98, 195–209.
7. Lellep, J. and Myrk, A. Optimization of stepped plates under dynamic loading. Engineering Design Optimization. Proc. 4th ASMO-UK/ISSMO Conf. (Ed. P. Gosling). Newcastle, 2002, 119–125.
8. Lellep, J. and Mürk, A. Optimization of axisymmetric plates of composite materials. Impact and Damage Tolerance Modelling of Composite Materials and Structures. Proc. Euromech Colloq. 400 (Ed. C. Soutis and I. A. Guz). Imperial Colledge of Science, Technol. Medic. London, 1999, 146–153.
9. Lepik, Ü. and Mroz, Z. Optimal design of plastic structures under impulsive and dynamic pressure loading. Int. J. Solids Structures, 1977, 13, 657–674.
10. Martin, J. B. Plasticity. Fundamentals and General Results. MIT Press, Cambridge, 1975.
11. Martin, J. B. and Symonds, P. S. Mode approximation for impulsively loaded rigid-plastic structures. Proc. ASCE, EM92, 1966, 43–66.
12. Stronge, W. and Yu, T. X. Dynamic Models for structural Plasticity. Springer, London, 1993.

3. OPTIMIZATION OF INELASTIC ANNULAR PLATES WITH CRACKS

J. Lellep, A. Mürk
Institute of Applied Mathematics,
University of Tartu, Tartu 50409, Estonia
Telephone: +372 737 5868
Fax: +372 737 5862
E-mail addresses: jaan.lellep@ut.ee, annely.murk@ut.ee

Abstract

Stepped plates made of a fiber reinforced composite material are studied. The plates are subjected to the initial impulsive loading which imparts the plates given kinetic energy. Optimal designs corresponding to the minimum of the maximal residual deflections are established making use of the variational methods of the theory of optimal control. Maximal deflections are evaluated with the method of mode form motions.

Keywords: Annular plate. Impulsive loading. Inelastic material. Optimization. Crack.

3.1. Introduction

Axisymmetric plates are structural elements which have a lot of practical applications. The quasistatic and dynamic behaviour of annular and circular plates was studied under various assumptions by many authors. An exhaustive review of investigations of this kind can be found in the book by Jones (1989). Earlier works on dynamic plasticity are cited by Nurick and Martin (1989), also by Kalizky (1985, 1989).

Optimal design of rigid-plastic structural elements subjected to dynamic loadings was initiated by Lepik and Mroz (1977) who converted the problem into a constrained minimization problem. Lepik (1982) has solved a large variety of problems of optimal design of rigid plastic structures subjected to dynamic loading. Lellep and Hein (2002) studied clamped shallow shells of piece wise constant thickness subjected to impulsive loading whereas Lellep and Puman (1999, 2000) developed optimal designs for stepped conical shells. An alternative approach was suggested by Lellep and Hannus (1995), Lellep and Puman (2001), Lellep and Tungel (2005) on the basis of the theory of optimal control. In earlier works by Lellep and Mürk (2003, 2004) dynamic

plastic response of stepped annular plates of sandwich cross-section was studied.

In the present paper variational methods of the control theory (see Hocking, 2001; Hull, 2003) are used in order to get necessary conditions of optimality for annular plates subjected to impulsive loading. Numerical results will be presented for plates with single step in the thickness.

3.2. Formulation of the problem

Let us consider an annular plate of radius R with the free inner edge of radius a. Let the outer edge of the plate be clamped. We shall consider plates of piece wise constant thickness whereas (Fig. 3.1)

$$h = h_j$$

for $r \in (a_j, a_{j+1})$ where $j = 0,...,n$. Here $a_0 = a$ and $a_{n+1} = R$. At $r = a_j$ ($j = 1,...,n$) stable symmetrical cracks of constant length c_j are located (Fig. 3.1). The quantities h_j ($j = 0,...,n$) and a_j ($j = 1,...,n$) are treated as preliminarily unknown constant parameters to be defined so that a cost criterion attains its minimal value.

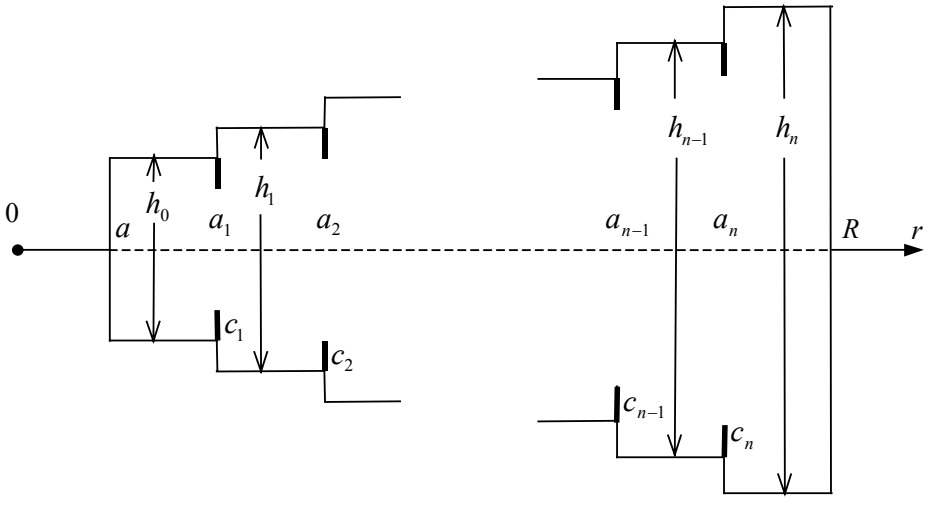

Figure 3.1. Annular plate with cracks

It is assumed that the plate is subjected to an initial impulsive loading which imparts the plate the initial kinetic energy K_0, whereas

$$K_0 = \pi \sum_{j=0}^{n} \int_{D_j} \mu h_j \left(\frac{\partial W}{\partial t} \right)^2 \Big|_{t=0} r dr . \qquad (1)$$

Here $W = W(r,t)$ stands for the transverse deflection, t is time, r-current radius of the plate, μ density of the material and $D_j = (a_j, a_{j+1})$.

Material of the plate is a fiber reinforced composite material with strong ductile fibers embedded in a metal matrix. It is assumed that the behaviour of the composite can be prescribed with the model of a rigid-plastic body. It is well known (see Jones, 1999) that the behaviour of a composite strongly depends on the orientation of fibers in the matrix material. In the present study we restrict our attention to the cases of circumferential and radial arrangements of fibers only. Corresponding yield surfaces for these materials have developed by Lance and Robinson (1972). These yield surfaces can be presented as hexagons ABCDEF on the plane of principal moments M_1, M_2 (Fig. 3.2, 3.3). Fig. 3.2 corresponds to the case of circumferential arrangement of fibers, Fig. 3.3 is associated with the radial orientation of fibers. In the present study rectangular approximations of hexagons are used.

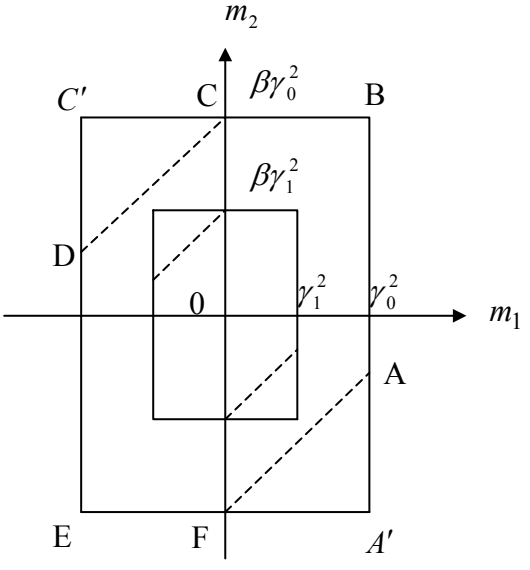

Figure 3.2. Yield condition for a circumferentially reinforced plate

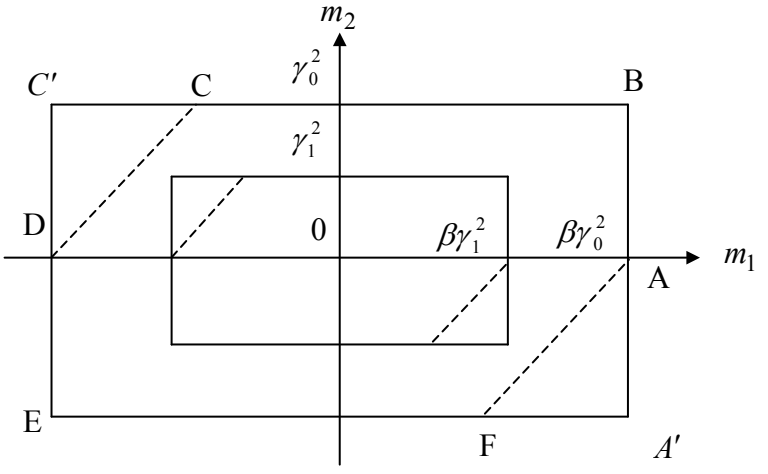

Figure 3.3. Yield condition for a radial arrangement of fibers

We are looking for the design of the plate corresponding to the minimum of the maximal residual deflection of the plate. Evidently, if the initial velocity distribution does not differ substantially from the uniform distribution then the maximum of deflections is attained at the outer edge of the plate. Thus, the cost criterion to be minimized can be taken as

$$J = W\left(a_0, t_f\right)$$

where t_f is the time instant when the motion of the plate is completed. It will be shown that the maximal residual deflection depends not only on the design parameters $h_0,...,h_n$ and $a_1,...,a_n$ but on the acceleration of the free edge $\dfrac{\partial^2 W_0}{\partial t^2}$, as well, e.g.

$$J = \Phi_*\left(\frac{\partial^2 W_0}{\partial t^2}, a_1,...,a_n, h_0,...,h_n\right), \tag{2}$$

where $W_0 = W\left(a_0, t\right)$ and Φ_* is a given function which will be defined later. When minimizing the cost criterion (2) we assume the weight or volume of the plate to be given, e.g.

$$V = \pi\sum_{j=0}^{n} h_j\left(a_{j+1}^2 - a_j^2\right). \tag{3}$$

At the re-entrant corners of steps the plate has cracks of constant length. Let c_j be length of the crack located at $r = a_j$. Due to the crack the radial moment at $r = a_j$ is restricted as (provided, $h_{j-1} < h_j;\ j = 1,...,n$)

$$\left|M_1\left(a_j\right)\right| \le M_{j-1}^1 = \nu_{j-1} M_{0\,j-1}$$

for circumferential orientation of fibers and

$$\left|M_1\left(a_j\right)\right| \le M_{j-1}^2 = \nu_{j-1} \beta M_{0\,j-1}$$

for radial arrangement of fibers where $\nu_{j-1} = \left(1 - \frac{2c_j}{h_{j-1}}\right)^2$. In previous relations and henceforth $M_{0j} = \frac{\sigma_0 h_j{}^2}{4}$ ($j = 0,...,n$). Here σ_0 stands for the yield stress of the matrix material and $\beta\sigma_0$ – yield stress of the composite in the fiber direction.

3.3. Basic equations

The equilibrium equation of a plate element can be presented as (Jones, 1989)

$$\frac{\partial}{\partial r}\left(\frac{\partial}{\partial r}\left(rM_1\right) - M_2\right) = \mu h_j r \frac{\partial^2 W}{\partial t^2} \tag{4}$$

for $r \in D_j$, ($j = 0,...,n$). The curvature rates in principal directions are

$$\frac{\partial \kappa_1}{\partial t} = -\frac{\partial^3 W}{\partial r^2 \partial t}, \quad \frac{\partial \kappa_2}{\partial t} = -\frac{1}{r}\frac{\partial^2 W}{\partial r \partial t}. \tag{5}$$

It is assumed that the curvature rates satisfy associated flow law. According to the flow law the vector of curvature rates (5) is orthogonal with respect to the yield surface and it is directed towards the outward normal to the yield surface (Kaliszky, 1989). In the present study we use approximated yield surfaces which are formed by sides BC', C'E, EA', A'B (Fig. 3.2, 3.3). It appears that in the present case the admissible flow regimes are the sides BC' of rectangles presented in Fig. 3.2, 3.3. Thus

$$\frac{\partial \kappa_1}{\partial t} = 0$$

and

$$\frac{\partial \kappa_2}{\partial t} \ge 0.$$

Last equation with relations (5) yields

$$\frac{\partial W}{\partial t} = \frac{\partial W_0}{\partial t}\frac{r - R}{a_0 - R} \tag{6}$$

where the boundary conditions

$$\frac{\partial W}{\partial t}(R,t)=0,\quad \frac{\partial W}{\partial t}(a_0,t)=\frac{dW_0}{dt}$$

are taken into account. It follows from (6) that the requirement $\frac{\partial \kappa_2}{\partial t}\geq 0$ is satisfied if $\frac{dW_0}{dt}\geq 0$.

It is reasonable to introduce following non-dimensional quantities

$$\begin{gathered}\rho=\frac{r}{R},\ \alpha_j=\frac{a_j}{R},\ \alpha=\frac{a}{R},\ \gamma_j=\frac{h_j}{h_*},\ m_{1,2}=\frac{M_{1,2}}{M_*},\\ w_0=\frac{W_0}{h_*},\ v=\frac{V}{\pi R^2 h_*},\ \tau=\sqrt{\frac{M_*}{\mu h_*^2 R^2}}\,t,\ K=\frac{K_0}{\pi h_* M_*}.\end{gathered}\tag{7}$$

Here h_* stands for the thickness of the reference plate of constant thickness and M_* is corresponding yield moment, e.g. $M_*=\frac{\sigma_0 h_*^2}{4}$.

Making use of (6), (7) one can present the velocity and acceleration distributions as

$$\dot w=\dot w_0\frac{1-\rho}{1-\alpha},\ \ \ddot w=\ddot w_0\frac{1-\rho}{1-\alpha},\tag{8}$$

where dots denote differentiation with respect to the variable τ. Note that the differentiation with respect to ρ will be denoted by primes.

In variables (7) the equilibrium equation (4) takes the form

$$\begin{aligned}m_1'&=-\frac{m_1}{\rho}+\frac{m_2}{\rho}+q,\\ q'&=-\frac{q}{\rho}+\gamma_j\ddot w_0\frac{\rho-1}{\alpha-1},\end{aligned}\tag{9}$$

for each segment D_j ($j=0,...,n$). Here q stands for an auxiliary variable (non-dimensional shear force) which admits to present the second order equation (4) in the form of a system of two equations.

The quantity m_2 in (9) is to be taken according to Fig. 3.2, 3.3 as

$$m_2=\beta\gamma_j^2\tag{10}$$

in the case of circumferential orientation of fibers. Alternatively, for radial arrangement of fibers one has

$$m_2=\gamma_j^2.$$

Let us consider now the case of circumferentially reinforced plate in a greater detail. The case of radial orientation of fibers can be solved in the similar way.

Boundary conditions for the plate clamped at the outer edge and free at the inner edge have the form

$$m_1(\alpha,\tau)=0,\ q(\alpha,\tau)=0,\ m_1(1,\tau)=-\gamma_n^2, \tag{11}$$

The solution of (9) corresponding to the flow regime (10) and boundary conditions (11) must be statically admissible, e.g.

$$\left|m_1(\rho,\tau)\right|\le \nu_j\gamma_j^2 \tag{12}$$

for internal points of each segment D_j ($j=0,...,n$). In the case of radial reinforcement instead of (12) one has the restriction $\left|m_1(\rho,\tau)\right|\le \beta\nu_j\gamma_j^2$ if $\rho\in D_j$ and $\rho\ne\alpha_j$, $\rho\ne\alpha_{j+1}$.

3.4. Necessary conditions of optimality

The problem posed above will be considered as a particular problem of the theory of optimal control. The cost function for the problem is given by (2) and state equations are presented by (9). The acceleration $\ddot{w}_0$ in (9) is assumed to be a constant parameter whereas m_1 and q are called as state variables. In order to derive necessary conditions of optimality let us introduce an extended functional (Bryson, 1975; Hocking, 2001)

$$\begin{aligned}
J_* &= \Phi+\lambda\left(\sum_{j=0}^{n}\gamma_j\left(\alpha_{j+1}^2-\alpha_j^2\right)-v\right)+\\
&+\sum_{j=0}^{n}\int_{\alpha_j}^{\alpha_{j+1}}\left\{\psi_1\left(q'+\frac{q}{\rho}-\gamma_j\ddot{w}_0\frac{\rho-1}{\alpha-1}\right)+\psi_2\left(m_1'+\frac{m_1}{\rho}-\frac{\beta}{\rho}\gamma_j^2-q\right)\right\}d\rho+\\
&+\mu_1 q(\alpha)+\mu_2 m_1(\alpha)+\mu_3\left(m_1(1)+\gamma_n^2\right)+\\
&+\sum_{j=1}^{n}\left\{\varphi_{j1}\left(\left|m_1(\alpha_j)\right|-\nu_{j-1}\gamma_j^2+\theta_{j1}^2\right)+\varphi_{j2}\left(\left|m_1(\alpha_j)\right|-\nu_{j-1}\gamma_{j-1}^2+\theta_{j2}^2\right)\right\}.
\end{aligned} \tag{13}$$

In (13) λ, μ_1, μ_2, μ_3, φ_{j1}, φ_{j2} stand for Lagrange multipliers whereas $\psi_1=\psi_1(\rho)$ and $\psi_2=\psi_2(\rho)$ are so-called co-state variables.

Quantities θ_{j1} and θ_{j2} are slack variables which admit to transform the inequalities (12) into equalities

$$\begin{aligned} \left| m_1(\alpha_j) \right| - \nu_{j-1}\gamma_j^2 + \theta_{j1}^2 = 0, \\ \left| m_1(\alpha_j) \right| - \nu_{j-1}\gamma_{j-1}^2 + \theta_{j2}^2 = 0, \end{aligned} \tag{14}$$

for each of $j = 1,...,n$. The function Φ in (13) is obtained from (2) when using non-dimensional quantities (7).

Necessary optimality conditions can be presented as $\Delta J_* = 0$, where ΔJ_* denotes the total variation of the functional J_* (Hocking, 2001; Hull, 2003). Calculating the total variation of J_* one obtains

$$\begin{aligned} &\Delta\Phi + \sum_{j=0}^{n} \lambda\left[\Delta\gamma_j\left(\alpha_{j+1}^2 - \alpha_j^2\right) + \gamma_j\left(2\alpha_{j+1}\Delta\alpha_{j+1} - 2\alpha_j\Delta\alpha_j\right)\right] + \\ &+ \sum_{j=0}^{n}\left\{\int_{\alpha_j}^{\alpha_{j+1}}\left\{ -\psi_1'\delta q + \psi_1\left(\frac{1}{\rho}\delta q - \Delta\gamma_j\ddot{w}_0\frac{\rho-1}{\alpha-1} - \gamma_j\Delta\ddot{w}_0\frac{\rho-1}{\alpha-1}\right) + \right.\right. \\ &\left.\left. + \psi_2(-\delta q) + \frac{\psi_2}{\rho}\delta m_1 - \psi_2'\delta m_1 - \psi_2\frac{\beta}{\rho}2\gamma_j\Delta\gamma_j \right\} d\rho + \right. \\ &\left. + \left(\psi_1\delta q + \psi_2\delta m_1\right)\Big|_{\alpha_j}^{\alpha_{j+1}}\right\} + \mu_1\Delta q(\alpha) + \mu_2\Delta m_1(\alpha) + \mu_3\left(\Delta m_1(1) + 2\gamma_n\Delta\gamma_n\right) + \\ &+ \sum_{j=1}^{n}\left\{\varphi_{j1}\left(\Delta\left| m_1(\alpha_j)\right| - 2\nu_{j-1}\gamma_j\Delta\gamma_j + 2\theta_{j1}\Delta\theta_{j1}\right) + \right. \\ &\left. + \varphi_{j2}\left(\Delta\left| m_1(\alpha_j)\right| - 2\nu_{j-1}\gamma_{j-1}\Delta\gamma_{j-1} + 2\theta_{j2}\Delta\theta_{j2}\right)\right\} = 0. \end{aligned} \tag{15}$$

Here $\Delta\Phi$ stands for the total variation of the function $\Phi = \Phi(\ddot{w}_0, \alpha_1,..., \alpha_n, \gamma_0,..., \gamma_n)$. Evidently,

$$\Delta\Phi = \frac{\partial\Phi}{\partial\ddot{w}_0}\Delta\ddot{w}_0 + \sum_{j=1}^{n}\left(\frac{\partial\Phi}{\partial\alpha_j}\Delta\alpha_j + \frac{\partial\Phi}{\partial\gamma_j}\Delta\gamma_j\right) + \frac{\partial\Phi}{\partial\gamma_0}\Delta\gamma_0. \tag{16}$$

From (15) one obtains the co-state system

$$\begin{aligned} \psi_1' &= \frac{\psi_1}{\rho} - \psi_2, \\ \psi_2' &= \frac{\psi_2}{\rho}. \end{aligned} \tag{17}$$

Due to arbitrariness of the quantity $\ddot{w}_0$ equations (15) and (16) yield

$$\frac{\partial \Phi}{\partial \ddot{w}_0} - \sum_{j=1}^{n} \int_{\alpha_j}^{\alpha_{j+1}} \psi_1 \gamma_j \frac{\rho - 1}{\alpha - 1} d\rho = 0 \tag{18}$$

The design parameters γ_j ($j = 0,...,n$) are arbitrary, as well. Thus, according to (15) and (16)

$$\frac{\partial \Phi}{\partial \gamma_j} + \lambda\left(\alpha_{j+1}^2 - \alpha_j^2\right) - \int_{\alpha_j}^{\alpha_{j+1}} \left(\psi_1 \ddot{w}_0 \frac{\rho - 1}{\alpha - 1} + \frac{2\psi_2 \beta}{\rho} \gamma_j \right) d\rho + \chi_j = 0 \tag{19}$$

where

$$\chi_j = \begin{cases} -2\varphi_{12}\nu_0\gamma_0, & j = 0; \\ -2\gamma_j\left(\varphi_{j1}\nu_{j-1} + \varphi_{j+1,2}\nu_j\right), & j = 1,...,n-1; \\ -2\varphi_{n1}\nu_{n-1}\gamma_n + 2\mu_3\gamma_n, & j = n. \end{cases} \tag{20}$$

Similarly it follows from (15) that

$$\begin{aligned} &\varphi_{j1}\theta_{j1} = 0, \\ &\varphi_{j2}\theta_{j2} = 0, \end{aligned} \tag{21}$$

for each $j = 1,...,n$.

According to (15) the transversality conditions have the form

$$\begin{aligned} &\psi_1(\alpha) = \mu_1 \,, \psi_2(1) = -\mu_3, \\ &\psi_2(\alpha) = \mu_2 \,, \psi_1(1) = 0. \end{aligned} \tag{22}$$

Substituting the total variations $\Delta m_1(\alpha_j \pm)$, $\Delta q(\alpha_j \pm)$ which are connected with weak variations as (see Hull, 2003; Lellep and Puman, 2001)

$$\begin{aligned} &\Delta m_1(\alpha_j) = \delta m_1(\alpha_j \pm) + m_1'(\alpha_j \pm)\Delta\alpha_j, \\ &\Delta q(\alpha_j) = \delta q(\alpha_j \pm) + q'(\alpha_j \pm)\Delta\alpha_j, \end{aligned}$$

into (15) one has

$$\sum_{j=1}^{n}\left\{\frac{\partial\Phi}{\partial\alpha_j}\Delta\alpha_j+2\lambda\alpha_j\left(\gamma_{j-1}-\gamma_j\right)\Delta\alpha_j+\right.$$
$$+\psi_1(\alpha_j-)\left(\Delta q(\alpha_j)-q'(\alpha_j-)\Delta\alpha_j\right)+$$
$$+\psi_2(\alpha_j-)\left(\Delta m_1(\alpha_j)-m_1'(\alpha_j-)\Delta\alpha_j\right)-$$
$$-\psi_1(\alpha_j+)\left(\Delta q(\alpha_j)-q'(\alpha_j+)\Delta\alpha_j\right)- \tag{22}$$
$$-\psi_2(\alpha_j+)\left(\Delta m_1(\alpha_j)-m_1'(\alpha_j+)\Delta\alpha_j\right)+$$
$$\left.+\varphi_{j1}\Delta\left|m_1\left(\alpha_j\right)\right|+\varphi_{j2}\Delta\left|m_1\left(\alpha_j\right)\right|\right\}=0.$$

The last equation yields jump conditions for co-state variables at $\rho=\alpha_j$ ($j=1,...,n$)

$$\begin{aligned}&\psi_2\left(\alpha_j-\right)-\psi_2\left(\alpha_j+\right)\pm\varphi_{j1}\pm\varphi_{j2}=0,\\&\psi_1\left(\alpha_j-\right)-\psi_1\left(\alpha_j+\right)=0,\end{aligned} \tag{23}$$

and equations

$$\frac{\partial\Phi}{\partial\alpha_j}+2\lambda\alpha_j\left(\gamma_{j-1}-\gamma_j\right)-\psi_1(\alpha_j-)q'(\alpha_j-)-\psi_2(\alpha_j-)m_1'(\alpha_j-)+$$
$$+\psi_1(\alpha_j+)q'(\alpha_j+)+\psi_2(\alpha_j+)m_1'(\alpha_j+)=0 \tag{24}$$

for each $j=1,...,n$.

3.5. Determination of residual deflections

When solving the optimization problem one has to solve equations (17)–(24) with (9)–(11), provided the function Φ is specified. For determination of Φ we employ the method of mode form motions (see Jones, 1989; Martin and Symonds, 1966) with velocity distribution (8).

Integrating the system (9) for $\rho\in D_j$ one obtains

$$\begin{aligned}\rho q&=\frac{\gamma_j\ddot{w}_0}{\alpha-1}\left(\frac{\rho^3}{3}-\frac{\rho^2}{2}\right)+B_j\ ,\\\rho m_1&=\beta\gamma_j^2\rho+\frac{\gamma_j\ddot{w}_0}{\alpha-1}\left(\frac{\rho^4}{12}-\frac{\rho^3}{6}\right)+B_j\rho+C_j\ ,\end{aligned} \tag{25}$$

where B_j, C_j ($j=0,...,n$) stand for arbitrary constants to be determined making use of appropriate boundary and continuity conditions. Starting from

the boundary conditions (11) at $\rho = \alpha$ and satisfying the continuity of m and q at $\rho = \alpha_j$ step by step one can define

$$B_j = \sum_{i=0}^{j} \frac{\ddot{w}_0}{\alpha - 1}\left(\gamma_{i-1} - \gamma_i\right)\left(\frac{\alpha_i^3}{3} - \frac{\alpha_i^2}{2}\right),$$
$$C_j = \sum_{i=0}^{j}\left\{\beta\alpha_i\left(\gamma_{i-1}^2 - \gamma_i^2\right) + \frac{\ddot{w}_0\left(\gamma_{i-1} - \gamma_i\right)}{12(\alpha - 1)}\left(4\alpha_i^3 - 3\alpha_i^4\right)\right\}. \tag{26}$$

In (26) $j = 0,...,n$ provided $\alpha_0 = \alpha$, $\alpha_{n+1} = 1$, $\gamma_{-1} = 0$.

The boundary condition $m_1(1,\tau) = -\gamma_n^2$ gives with (25) and (26) the acceleration

$$\ddot{w}_0 = -\frac{12(\alpha - 1)\left[\beta\sum_{i=0}^{n}\alpha_i\left(\gamma_i^2 - \gamma_{i-1}^2\right) - (\beta + 1)\gamma_n^2\right]}{\sum_{i=0}^{n}\left(\gamma_{i-1} - \gamma_i\right)\left(3\alpha_i^4 - 8\alpha_i^3 + 6\alpha_i^2\right) + \gamma_n}. \tag{27}$$

It follows from (27) that $\ddot{w}_0 = const$ and thus,

$$\dot{w}_0 = \ddot{w}_0\tau + \dot{w}_0(0) \tag{28}$$

and

$$w_0 = \ddot{w}_0\frac{\tau^2}{2} + \dot{w}_0(0)\tau, \tag{29}$$

where the initial condition $w_0(0) = 0$ has been taken into account.

Assume that the motion of the plate ceases at $\tau = \tau_1$ when $\dot{w}_0(\tau_1) = 0$. It can be easily obtained from (28) that

$$\tau_1 = -\frac{\dot{w}_0(0)}{\ddot{w}_0}. \tag{30}$$

The maximal residual deflection takes according to (29), (30) the form

$$w_0(\tau_1) = -\frac{1}{2}\frac{\dot{w}_0^2(0)}{\ddot{w}_0}. \tag{31}$$

Note that the quantity $\dot{w}_0(0)$ in (28)-(31) is unknown. On the other hand, it is assumed that the initial kinetic energy K is given.

Therefore, making use of (1), (6)-(8) one can recheck that

$$\dot{w}_0^2 = \frac{12K(1-\alpha)^2}{\sum_{i=0}^{n}\gamma_i\left[\left(6\left(\alpha_{i+1}^2-\alpha_i^2\right)-8\left(\alpha_{i+1}^3-\alpha_i^3\right)+3\left(\alpha_{i+1}^4-\alpha_i^4\right)\right)\right]}. \tag{32}$$

Equations (27) and (31), (32) give after some algebraic manipulations

$$w_1 = -\frac{1}{2}\frac{1-\alpha}{\beta\sum_{i=0}^{n}\alpha_i\left(\gamma_i^2-\gamma_{i-1}^2\right)-(\beta+1)\gamma_n^2} \tag{33}$$

where

$$w_1 = \frac{w_0(\tau_1)}{K}. \tag{34}$$

3.6. Discussion of results

Results of calculations are presented in Tables 3.1–3.4 and Fig. 3.4–3.19 for plates with a single step. In Tables 3.1–3.4 values of the coefficient of efficiency

$$e = \frac{w_1}{w_*} \tag{35}$$

are presented for different values of v and different crack lengths ν. Here w_* stands for the residual maximal deflection of the reference plate of constant thickness $h_* = h_1$. Evidently,

$$\gamma_* = \frac{v}{1-\alpha^2} \tag{36}$$

and

$$w_* = \frac{K(1-\alpha)^3(1+\alpha)^2}{2v^2(1+\beta(1-\alpha))} \tag{37}$$

Table 3.1. Coefficient of efficiency for circumferentially reinforced plates ($a = 0.2R$)

ν / ν'	0.82	0.83	0.84	0.85	0.86	0.87	0.88	0.89	0.93	0.96
0.1								0.9695	0.9853	1
0.2							0.9615	0.9646	0.9833	1
0.3							0.9560	0.9602	0.9816	1
0.4						0.9471	0.9511	0.9561	0.9800	1
0.5					0.9380	0.9416	0.9466	0.9523	0.9785	1
0.6				0.9294	0.9317	0.9366	0.9423	0.9487	0.9770	1
0.7				0.9214	0.9260	0.9318	0.9383	0.9453	0.9757	1
0.8			0.9109	0.9150	0.9208	0.9274	0.9345	0.9420	0.9744	1
0.9		0.9003	0.9034	0.9091	0.9158	0.9231	0.9308	0.9389	0.9731	1
1	0.8898	0.8913	0.8967	0.9035	0.9110	0.9189	0.9272	0.9358	0.9719	1

Table 3.2. Coefficient of efficiency for circumferentially reinforced plates ($a = 0.5R$)

ν / ν'	0.71	0.72	0.73	0.74	0.75	0.76	0.77	0.78	0.82	0.84
0.1								0.9293	0.9725	1
0.2							0.9157	0.9235	0.9721	1
0.3						0.9031	0.9105	0.9207	0.9720	1
0.4					0.8914	0.8978	0.9077	0.9190	0.9719	1
0.5					0.8854	0.8948	0.9058	0.9179	0.9718	1
0.6				0.8734	0.8822	0.8928	0.9045	0.9170	0.9718	1
0.7			0.8618	0.8698	0.8799	0.8913	0.9035	0.9164	0.9718	1
0.8		0.8507	0.8576	0.8672	0.8782	0.8901	0.9027	0.9159	0.9717	1
0.9		0.8457	0.8548	0.8653	0.8769	0.8892	0.9021	0.9155	0.9717	1
1	0.8338	0.8425	0.8526	0.8638	0.8758	0.8884	0.9016	0.9152	0.9717	1

Table 3.3. Coefficient of efficiency for radially reinforced plates ($a = 0.2R$)

ν / v	0.83	0.84	0.85	0.86	0.87	0.88	0.89	0.9	0.91	0,95	0.96
0.1									0.9517	0.9897	1
0.2								0.9390	0.9478	0.9896	1
0.3							0.9263	0.9357	0.9459	0.9894	1
0.4						0.9135	0.9233	0.9338	0.9447	0.9889	1
0.5					0.9004	0.9106	0.9212	0.9320	0.9430	0.9884	1
0.6					0.8966	0.9072	0.9182	0.9294	0.9408	0.9880	1
0.7				0.8824	0.8929	0.9040	0.9154	0.9270	0.927	0.9876	1
0.8			0.8679	0.8783	0.8894	0.9009	0.9127	0.9247	0.9369	0.9872	1
0.9		0.8531	0.8633	0.8744	0.8860	0.8980	0.9102	0.9226	0.9351	0.9868	1
1	0.8380	0.8479	0.8590	0.8707	0.8827	0.8951	0.9077	0.9205	0.9334	0.9865	1

Table 3.4. Coefficient of efficiency for radially reinforced plates ($a = 0.5R$)

ν / v	0.71	0.72	0.73	0.74	0.75	0.76	0.77	0.78	0.79	0.82	0.84
0.1									0.9191	0.9646	1
0.2								0.8997	0.9141	0.9644	1
0.3							0.8822	0.8967	0.9127	0.9643	1
0.4						0.8652	0.8796	0.8954	0.9120	0.9643	1
0.5					0.8486	0.8627	0.8783	0.8946	0.9116	0.9642	1
0.6				0.8323	0.8460	0.8613	0.8774	0.8941	0.9113	0.9642	1
0.7			0.8163	0.8294	0.8445	0.8603	0.8768	0.8938	0.9110	0.9642	1
0.8			0.8131	0.8278	0.8434	0.8597	0.8764	0.8935	0.9109	0.9642	1
0.9		0.7969	0.8113	0.8266	0.8426	0.8591	0.8761	0.8933	0.9108	0.9642	1
1	0.7809	0.7949	0.8100	0.8258	0.8420	0.8587	0.8758	0.8931	0.9107	0.9642	1

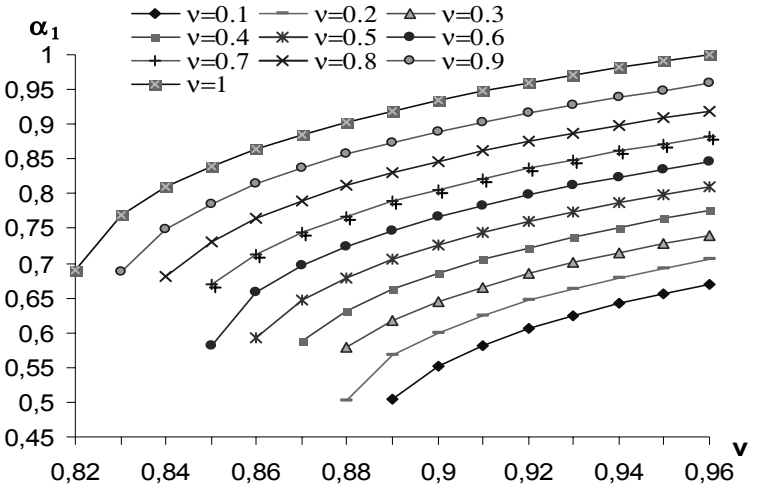

Figure 3.4. Optimal step location for $a = 0.2R$

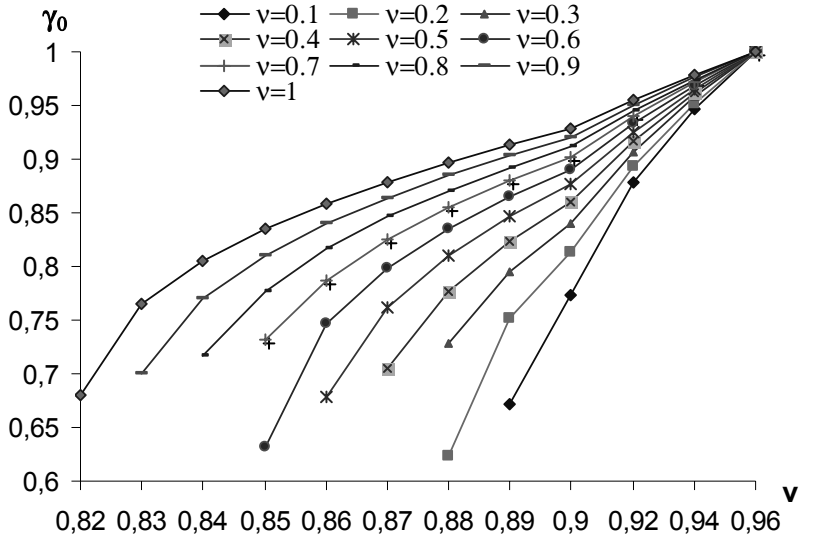

Figure 3.5. Optimal thickness for $a = 0.2R$

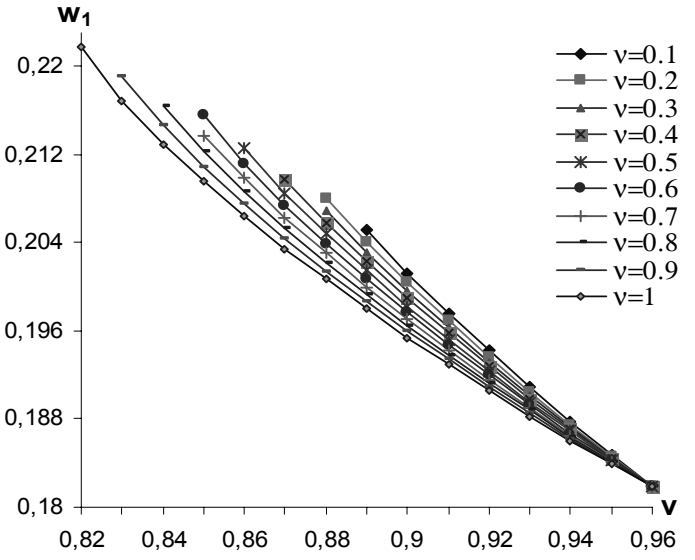

Figure 3.6. Maximal residual deflection for $a = 0.2R$

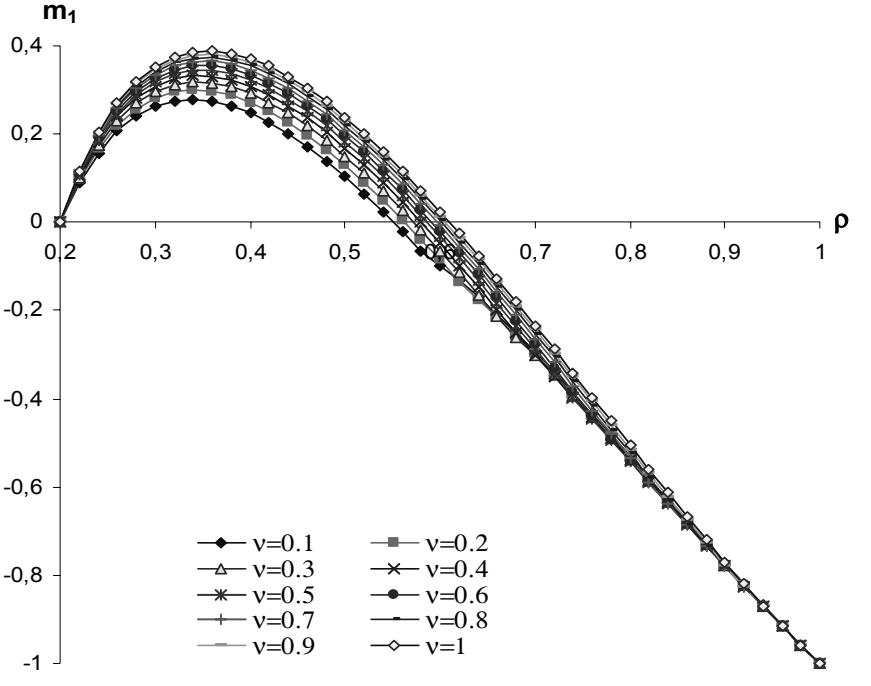

Figure 3.7. Bending moment m_1 distribution for circumferentially reinforced plates with $a = 0.2R$

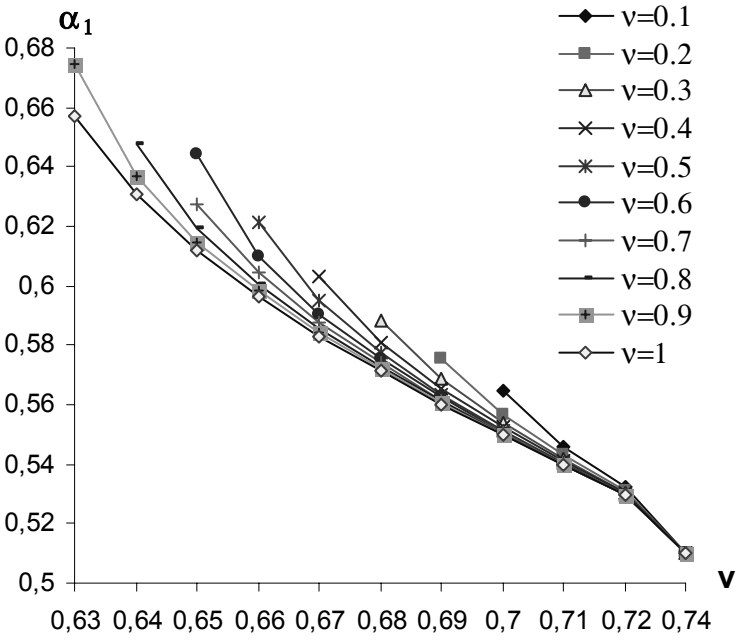

Figure 3.8. Optimal step location for $a = 0.5R$

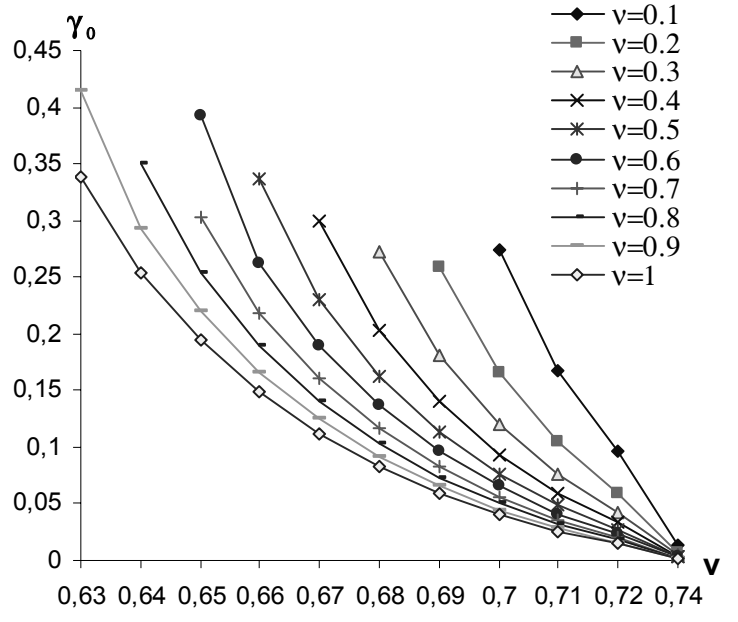

Figure 3.9. Optimal thickness for $a = 0.5R$

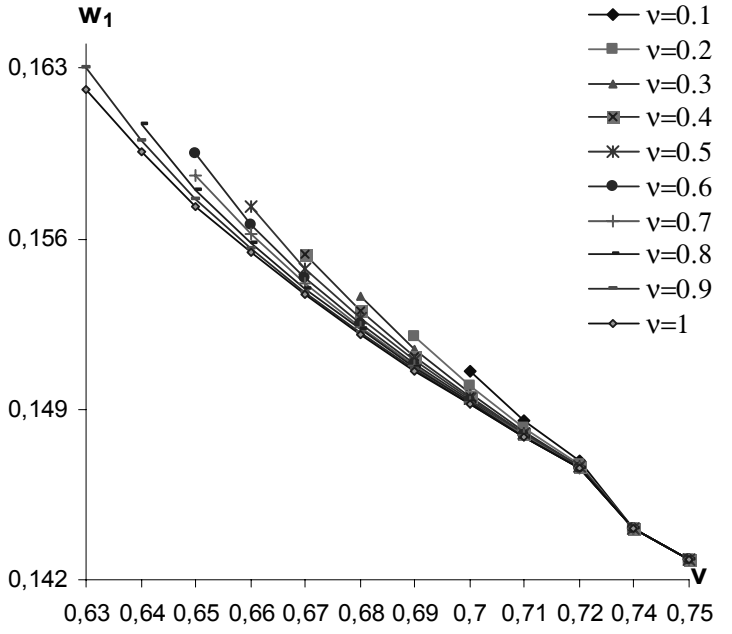

Figure 3.10. Maximal residual deflection for $a = 0.5R$

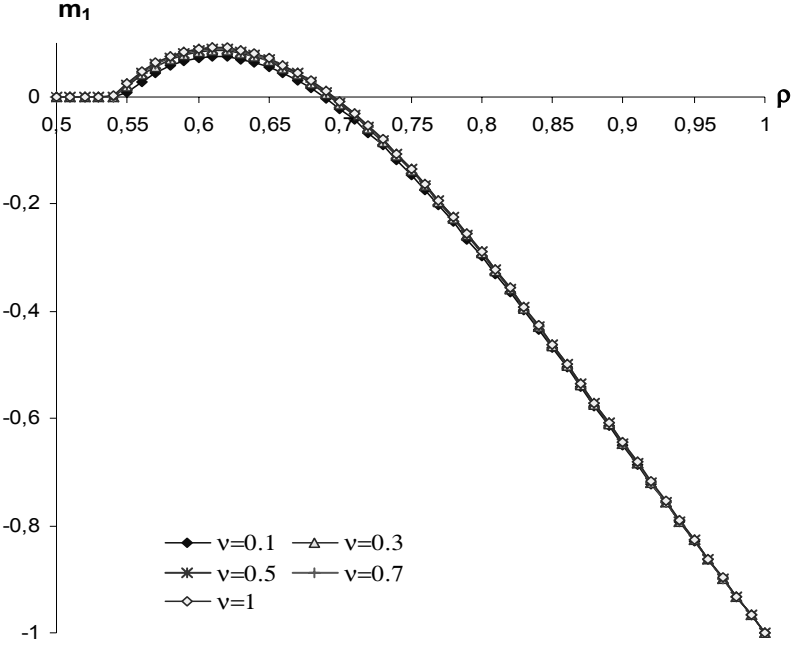

Figure 3.11. Bending moment m_1 distribution for circumferentially reinforced plates with $a = 0.5R$

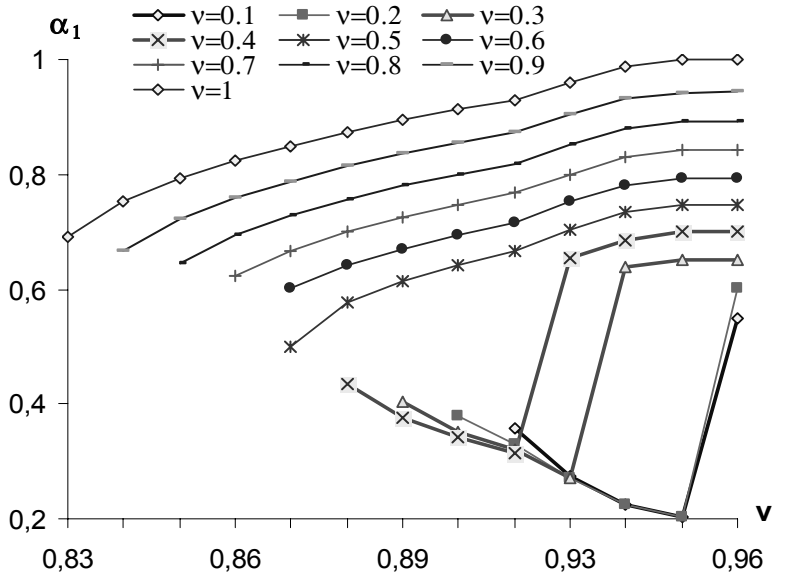

Figure 3.12. Optimal step location for $a = 0.2R$

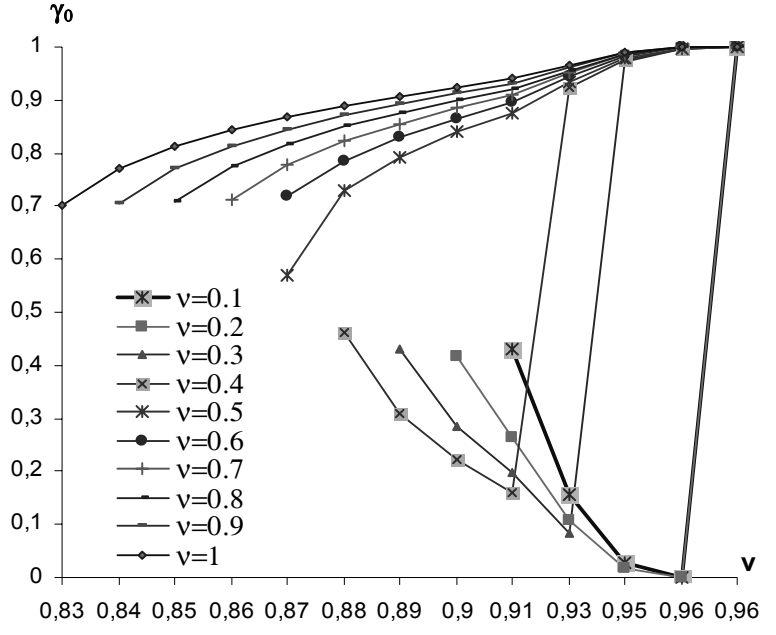

Figure 3.13. Optimal thickness for $a = 0.2R$

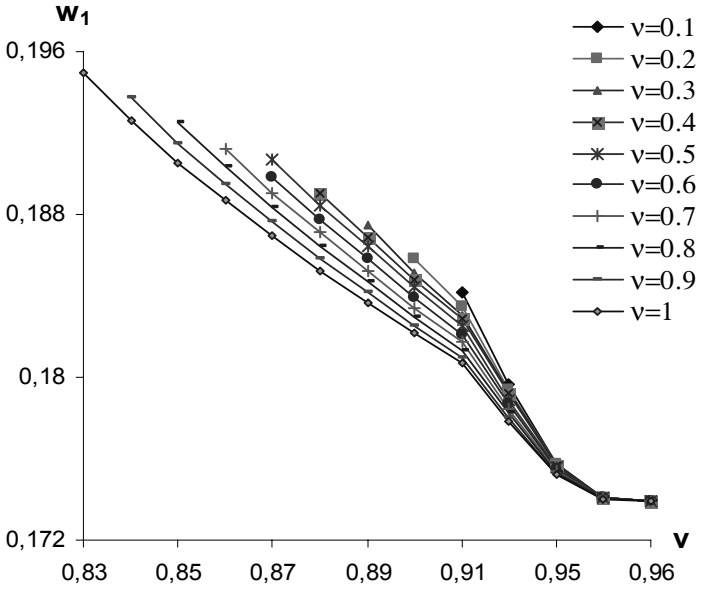

Figure 3.14. Maximal residual deflection for $a = 0.2R$

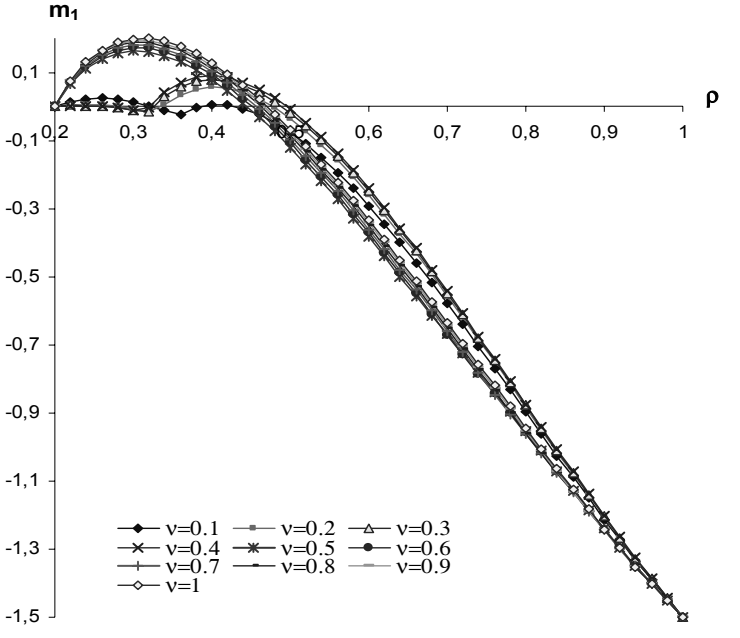

Figure 3.15. Bending moment m_1 distribution for radially reinforced plates with $a = 0.2R$

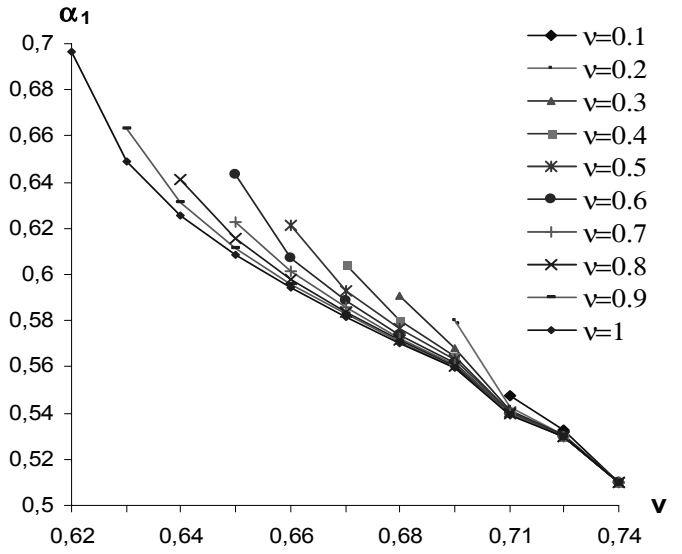

Figure 3.16. Optimal step location for $a = 0.5R$

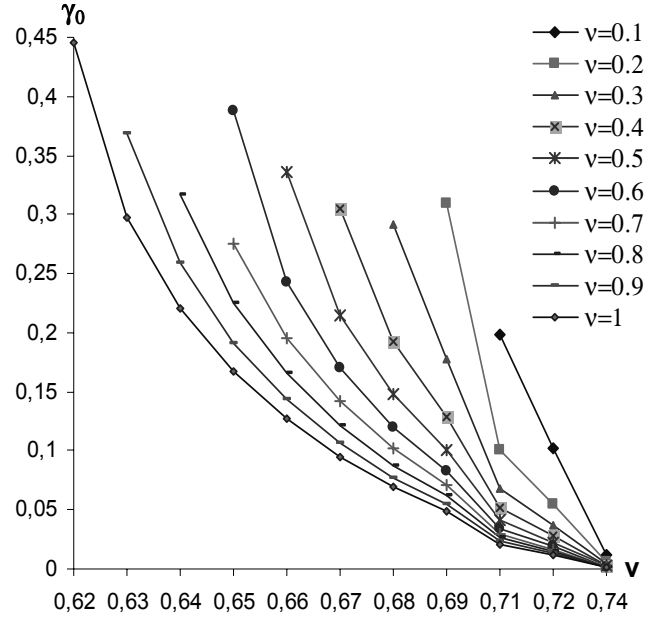

Figure 3.17. Optimal thickness for $a = 0.5R$

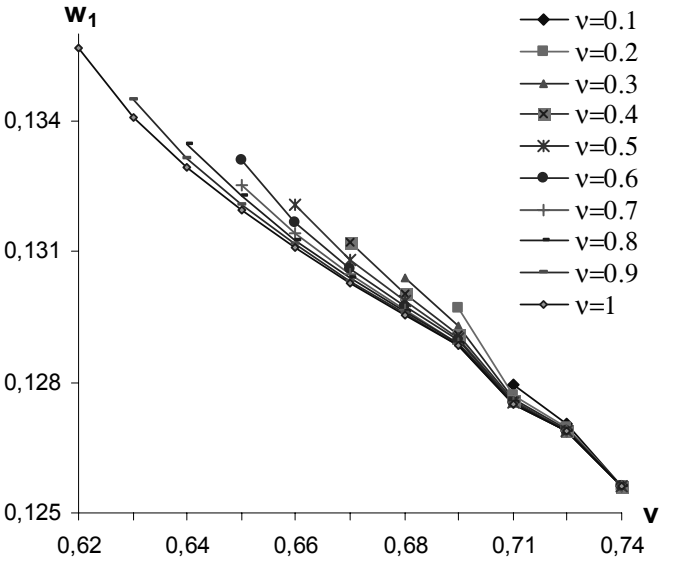

Figure 3.18. Maximal residual deflection for $a = 0.5R$

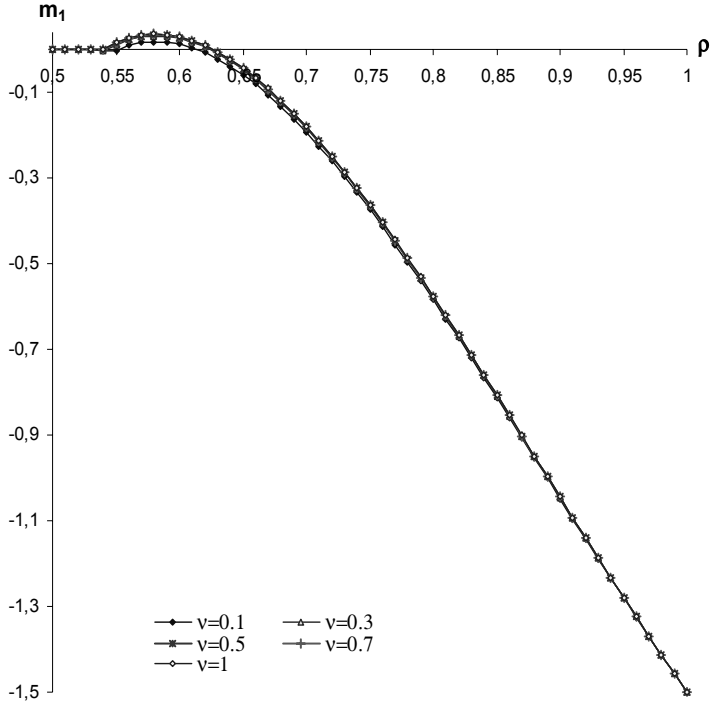

Figure 3.19. Bending moment m_1 distribution for radially reinforced plates with $a = 0.5R$

In calculations the material with $\beta = 1.5$ is considered. Tables 3.1 and 3.2 correspond to plates made of a circumferentially reinforced inelastic composite material and Tables 3.3, 3.4 are associated with radial orientation of fibers in the matrix material. Calculations carried out showed that the design parameters depend on the material and geometric parameters. It can be seen from Tables 3.1–3.4 that the efficiency of the design diminishes with decreasing ν. This means that the coefficient e increases when ν increases, provided other parameters are fixed. However, it is somewhat surprising that the coefficient (35) is not very sensitive with respect to the crack length.

Calculations carried out showed that the optimal solution does not exist for each value of v and each combination of other parameters. The places not filled up in Tables 3.1–3.4 correspond to combinations of parameters which do not lead to real optimal solutions.

In Fig. 3.4–3.11 are presented optimal values of quantities α_1, γ_0, w_1 versus v and the distribution of the bending moment m_1 for a plate with internal radius $a = 0.2R$. Fig. 3.12–3.19 correspond to plates with $a = 0.5R$. Plates made of a circumferentially reinforced material are considered in Fig. 3.4–3.7 and Fig. 3.12–3.15 whereas Fig. 3.8–3.11 and Fig. 3.16–3.19 are associated with radial orientation of fibers in the matrix material.

Optimal values of the coordinate α_1 are presented in Fig. 3.4, 3.8, 3.12, 3.16 as functions of the volume v for different values of the crack length at the re-entrant corner of the step.

Calculations carried out showed that in the range of small values of α optimal values of α_1, γ_0 increase with respect to v for given ν (Fig. 3.4, 3.5) whereas α_1, γ_0 decrease (Fig. 3.12, 3.13) for given crack length in the range of moderate values of internal radius α in the case of circumferential orientation of fibers.

In the case of radial orientation of fibers these trends take place, as well. It reveals from Fig. 3.16, 3.17 that for fixed ν quantities α_1 and γ_0 decrease monotonically if $a = 0.5R$. However, the results for plates with $a = 0.2R$ (Fig. 3.8, 3.9) show that the type of behaviour of curves α_1 versus v and γ_0 versus v strongly depends on the crack length ν. For $\nu > 0.5$ the curves reflect the behaviour typical to plates with small holes (Fig. 3.8, 3.9). However, if $\nu < 0.5$ ie in the case of longer cracks the plates with $a = 0.2R$ belong to the intermediate or transition zone.

Minimal values of maximal residual deflections are presented in Fig. 3.6 and 3.14 for circumferentially reinforced plates and in Fig. 3.10, 3.18 for plates with radial orientations of fibers. Figures 3.6 and 3.10 correspond to plates with internal radius $a = 0.2R$ whereas Fig. 3.14, 3.18 are associated with

$a = 0.5R$. It can be seen from Fig. 3.6, 3.10, 3.14, 2.18 that the maximal residual deflection is not very sensitive with respect of the crack length.

Distributions of the radial bending moment are presented for a circumferentially reinforced plate in Fig. 3.7, 3.15 and for a radially reinforced plate in Fig. 3.11, 3.19. Figures 3.7 and 3.11 correspond to plates with $a = 0.2R$ and Fig. 3.15, 3.19 to $a = 0.5R$.

Calculations carried out showed that the efficiency of the design is higher in the case of radially reinforced plates. For instance, in the case $a = 0.5R$ and single step of the thickness the optimized design enables to shorten maximal residual deflections up to 21.9 % for a radially reinforced material and 16.6 % for a circumferentially reinforced material. The maximal efficiency is obtained for a plate without any cracks. For the case $a = 0.5R$ the most efficient designs correspond to $v = 0.71$. It is worth while to mention that the efficiency of both, radially and circumferentially reinforced plates increases when the internal radius of the plate increases with other parameters remaining unchanged.

3.7. Concluding remarks

An optimization technique based on the variational methods of the theory of optimal control has been developed in the present paper. Annular plates clamped at the outer edge subjected to the initial impulsive loading have been studied. Calculations carried out showed that the maximal residual deflection can be remarkably shortened by the way of re-distributing the material in the plate. In the case of plates with a single step of the thickness the efficiency of the optimal design is maximally more than 20 %. Calculations showed that the efficiency of the design increases together with the internal radius of the plate. It appeared that the coefficient of efficiency is more sensitive with respect to the crack length in the case of small values of the internal radius of the plate.

Acknowledgements
The support from Estonian Science Foundation through the grant № 5693 is acknowledged.

3.8. References

Bryson A, Ho Yu-Chi (1975) Applied Optimal Control. Wiley, New York

Hocking LM (2001) Optimal Control. An Introduction to the Theory with Applications. Clarendon Press, Oxford

Hull DG (2003) Optimal Control Theory for Applications. Springer, Berlin Heidelberg New York

Jones N (1989) Structural Impact. Cambridge University Press, Cambridge
Jones RM (1999) Mechanics of Composite Materials. Taylor and Francis, Philadelphia
Kaliszky S (1985) Dynamic plastic response of structures. In: Sawczuk A, Bianchi G (eds) Plasticity Today: Modelling, Methods and Applications. Elsevier, London New York, pp 787–820
Kaliszky S (1989) Plasticity. Theory and Engineering Applications. Elsevier, Amsterdam
Lance RH, Robinson DN (1972) Limit analysis of ductile fiber-reinforced structures. Proc ASCE 98: 195–209
Lellep J, Hannus S (1995) Optimization of plastic cylindrical shells with stepwise varying thickness in the case of von Mises material 10: 122–127
Lellep J, Hein H (2002) Optimization of clamped plastic shallow shells subjected to initial impulsive loading. Eng Optim 34: 545–556
Lellep J, Mürk A (2004) Inelastic behaviour of stepped square plates. In: Kienzler R, Altenbach H, Ott I (eds) Theories of Plates and Shells. Critical Review and New Applications (Euromech Colloquium 444 held in Bremen 2002), Springer, Berlin Heidelberg New York, pp 133–140
Lellep J, Mürk A (2003) Inelastic stepped plates under impulsive loading. In: Gupta NK (ed) Plasticity and Impact Mechanics (Implast 2003 held in New Delhi), Phoenix Publishing House, New Delhi, pp 577–588
Lellep J, Puman E (1999) Optimization of plastic conical shells of piece wise constant thickness. Struct Optim 18: 74–79
Lellep J, Puman E (2000) Optimization of plastic conical shells loaded by a rigid central boss. Int J Solids Struct 37: 2695–2708
Lellep J, Puman E (2001) Optimization of conical shells of Mises material. Struct Multidisc Optim 22: 149–156
Lellep J, Tungel E (2005) Optimization of plastic spherical shells of von Mises material. Struct Multidisc Optim 30: 381–387
Lepik Ü (1982) Optimal Design of Inelastic Sructures under Dynamic Loading. Valgus, Tallinn (in Russian)
Lepik Ü, Mroz Z (1977) Optimal design of plastic structures under impulsive and dynamic pressure loading. Int J Solids Struct 13: 657–674
Martin JB, Symonds PS (1966) Mode approximation for impulsively loaded rigid-plastic structures. Proc ASCE 92: 43–66
Nurick GN, Martin JB (1989) Deformation of thin plates subjected to impulsive loading — a review. Part I: Theoretical considerations. Int J Impact Eng 8: 159–170

4. OPTIMIZATION OF AXISYMMETRIC PLATES WITH CRACKS

J. Lellep, A. Mürk
Institute of Applied Mathematics, University of Tartu, Liivi 2,
Tartu 50409, Estonia
Telephone: +372 737 5868
Fax: +372 737 5862
E-mail addresses: jaan.lellep@ut.ee, annely.murk@ut.ee

ABSTRACT

The behaviour of stepped annular plates made of a fiber reinforced composite material is studied making use of the method of mode form motions. At the re-entrant corners of the steps stable crack of prescribed maximal deepness are located. The plates under consideration are subjected to an initial impact and the subsequent motion is due to inertia. Variational methods of the theory of optimal control are used in order to get necessary conditions of optimality for plates with piece wise constant thickness. The designs of stepped plates are established which minimize maximal residual deflections under given material consumption. Numerical results are presented for the plate with single step.

Keywords: Annular plate, impulsive loading, ductile material, optimization, crack.

4.1. Introduction

Thin walled plates and shells have a lot of practical applications in civil engineering and machinery. Annular plates are used as internal watertight bulkheads in submersibles in order to isolate a damaged compartment in the case of an accident.

The dynamic plastic response of annular and circular plates to dynamic loadings was studied by several authors. Reviews of earlier investigations in this field can be find in the monograph books by Jones (1989) and Kaliszky (1989). A review of failure modes and criteria of plastic beams, plates and shells is presented by Yu and Chen (1998). Dynamic response of fully clamped and simply supported circular plates to impact and distributed pressure loading is investigated by Jones (1989), Liu and Stronge (1996), in the case of a Tresca material. Wang et al. (2005), Ma et al. (1999) studied circular plates on the base of unified strength theory. The unified yield criterion includes as particular cases both, the Tresca and Mises yield criteria. Clamped circular plates subjected to impulsive loading were examined by Wen, Yu, Reddy (1995).

Shen and Jones (1993) developed an approximate analysis of dynamic plastic deformations of fully clamped circular plates under impulsive loading. The analysis employs an interaction yield surface and uses the Cowper – Symonds constitutive equation which enables to prescribe the strain rate sensitivity of the material. Li and Jones (1994), also Liu and Stronge (1996); Jones, Kim and Li (1997) investigated shear and bending behaviour of circular plates subjected to various types of loading. Li and Jones (1994) considered blast loaded plates and Liu and Stronge (1996) plates subjected to a distributed pressure loading applied in a central area of the plate. Jones, Kim and Li (1997) presented a theoretical analysis to predict the dynamic behaviour of circular plates struck normally by blunt solid cylindrical masses at the centre.

In the papers mentioned above circular and annular plates of constant thickness have been investigated. Plastic response and optimization of beams, plates and shells were investigated by Lepik (1982) in the case of dynamic loading and variable thickness of structures. Methods of optimization of stepped shells based on the variational approach were developed by Lellep and Puman (2000, 2001), Lellep and Tungel (2005) for the case of quasistatic loading. In the present paper this approach is extended to stepped annular plates with cracks at the re-entrant corners of steps whereas plates are subjected to the initial impulsive loading.

4.2. Formulation of the problem

Consider an axisymmetric plate clamped at the inner edge of radius a. The outer edge of radius R is absolutely free (Fig. 4.1). Assume that the thickness of the plate is piece wise constant, e.g.

$$h = h_j$$

for $r \in \left(a_j, a_{j+1}\right)$ where $j = 0,...,n$ and r stands for the current radius. It is reasonable to introduce the notations $D_j = \left(a_j, a_{j+1}\right)$ whereas $j = 0,...,n$; $a_0 = a$; $a_{n+1} = R$. Here h_j ($j = 0,...,n$) and a_j ($j = 1,...,n$) are the design parameters to be defined so that the cost criterion

$$J = W\left(R, t_f\right) \tag{1}$$

attains the minimal value for given weight or material volume of the plate

$$V = \pi \sum_{j=0}^{n} h_j \left(a_{j+1}^2 - a_j^2\right). \tag{2}$$

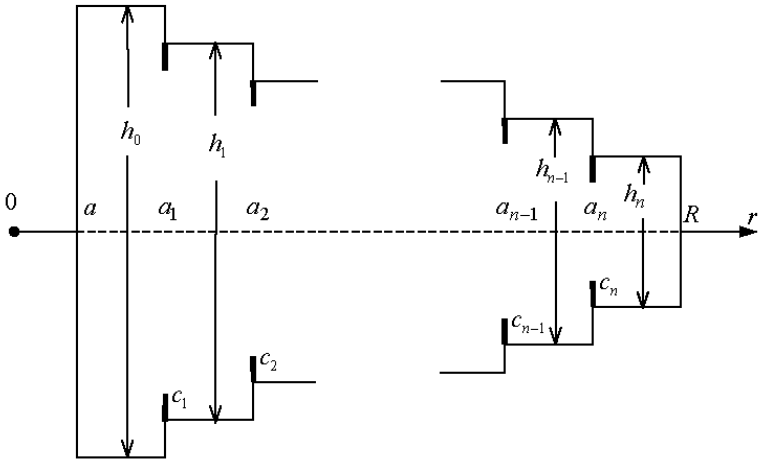

Figure 4.1. Annular plate with cracks

In (1) W stands for the transverse deflection and t_f is the response time of the plate. Thus we are looking for the design of the plate of given weight so that the maximal residual deflection attains the minimal value.

It is assumed that at the re-entrant corners of steps (Fig. 4.1) symmetrical cracks of length c_j ($j = 1,...,n$) are located.

The cracks are assumed to be stable cracks; we neglect the crack propagation during the process of deformation. Generally speaking, the crack located at $r = a_j$ is not of constant length for each $\theta \in [0,2\pi]$, where θ stands for the polar angle. We call the length c_j of the crack the maximal length of this circular crack over $\theta \in [0,2\pi]$.

The plate under consideration is subjected to the initial impulsive loading. Instead of the initial transverse velocity field we shall use the initial kinetic energy K_0 defined as

$$K_0 = \pi \sum_{j=0}^{n} \int_{D_j} \mu h_j \left(\frac{\partial W}{\partial t} \right)^2 \Big|_{t=0} r dr , \tag{3}$$

where μ is the density of the material.

In the present paper residual deflections of the plate are evaluated with the method of mode form motions. This approach enables to present the maximal

residual deflection as a function of design parameters and the acceleration at the free edge $\frac{\partial^2 W_0}{\partial t^2}$. Thus

$$J = \Phi_* \left(\frac{\partial^2 W_0}{\partial t^2}, a_1, ..., a_n, h_0, ..., h_n \right), \tag{4}$$

where $W_0 = W(R,t)$ and Φ_* is a given function which will be defined later.

4.3. Basic equations and assumptions

The equilibrium equation and deformation rates of a plate element can be presented as (Jones, 1989)

$$\begin{aligned} &\frac{\partial}{\partial r}\left(\frac{\partial}{\partial r}(rM_1) - M_2 \right) = rQ \\ &\frac{\partial}{\partial r}(rQ) = \mu h_j r \frac{\partial^2 W}{\partial t^2} \end{aligned} \tag{5}$$

for $r \in (a_j, a_{j+1})$; $j = 0,...,n$ and

$$\frac{\partial \kappa_1}{\partial t} = -\frac{\partial^3 W}{\partial r^2 \partial t}, \quad \frac{\partial \kappa_2}{\partial t} = -\frac{1}{r}\frac{\partial^2 W}{\partial r \partial t}. \tag{6}$$

Here M_1, M_2 stand for principal moments and κ_1, κ_2 — principal curvatures.

The material of the plate is assumed to be an ideal rigid plastic material. Plastic yielding of the material is controlled by the yield condition suggested by Lance and Robinson (1972). These yield hexagons correspond to unidirectionally reinforced ductile composites with ductile fibers and ductile matrix. In the foregoing analysis we assume that the stress profile corresponds to horizontal sides EA' of rectangles A'BC'E. The rectangles are considered as circumscribed approximations to hexagons presented by Lance and Robinson (Fig. 4.2, 4.3). Fig. 4.2 corresponds to a composite reinforced in the circumferential direction whereas Fig. 4.3 is associated with a radially reinforced plate.

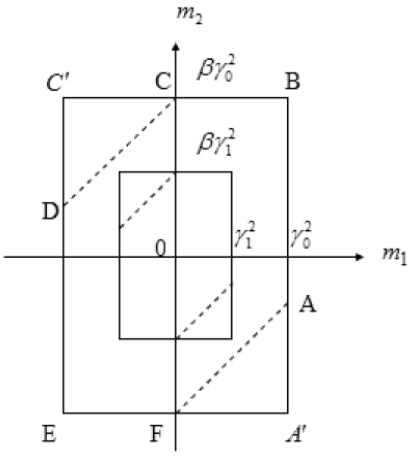

Figure 4.2. Yield condition for a circumferentially reinforced plate

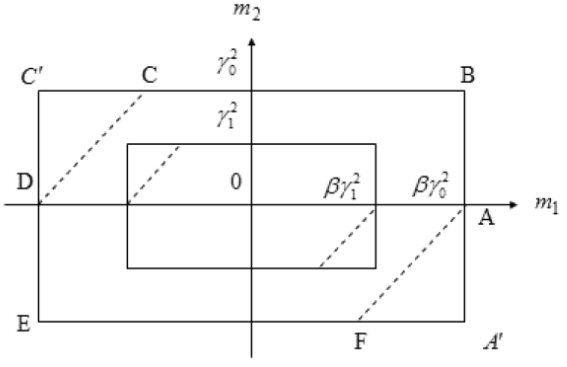

Figure 4.3. Yield condition for a radial arrangement of fibers

According to the associated flow law $\frac{\partial \kappa_1}{\partial t} = 0$. Thus, taking (6) into account one has

$$\frac{\partial W}{\partial t} = \frac{\partial W_0}{\partial t} \frac{r-a}{R-a}. \tag{7}$$

When deriving (7) the kinematical boundary condition

$$\frac{\partial W}{\partial t}(a,t) = 0$$

is satisfied, as well. It is expected that $\frac{\partial W_0}{\partial t} \geq 0$ in (7). Taking now (7) and (6) into account one can recheck that the inequality $\frac{\partial \kappa_2}{\partial t} \leq 0$ is satisfied as it is expected by the associated flow law.

Let us introduce following non-dimensional quantities

$$\begin{aligned} &\rho = \frac{r}{R},\ \alpha_j = \frac{a_j}{R},\ \alpha = \frac{a}{R},\ \gamma_j = \frac{h_j}{h_*},\ m_{1,2} = \frac{M_{1,2}}{M_*}, \\ &w_0 = \frac{W_0}{h_*},\ v = \frac{V}{\pi R^2 h_*},\ \tau = \sqrt{\frac{M_*}{\mu h_*^2 R^2}}\, t,\ K = \frac{K_0}{\pi h_* M_*}. \end{aligned} \tag{8}$$

In (8) and henceforth h_* denotes the thickness of the reference plate of constant thickness and M_* is corresponding yield moment, e.g. $M_* = \frac{\sigma_0 h_*^2}{4}$, σ_0 being the yield stress of the matrix material. The yield stress in the fiber direction will be denoted by $\beta\sigma_0$.

Assuming that the stress state of the plate corresponds to the flow regime EA' (Fig. 4.2, 4.3) one has

$$m_2 = -\beta\gamma_j^2 \tag{9}$$

in the case of circumferential orientation of fibers and

$$m_2 = -\gamma_j^2 \tag{10}$$

for $\rho \in (a_j, a_{j+1});\ j = 0,...,n$ in the case of radially reinforced plate.

It is reasonable to assume that starting from the clamped edge and moving towards the free edge thicknesses in corresponding segments decrease, e.g. $h_{j-1} > h_j$ for each $j = 1,...,n$. At the corners of steps due to stress concentration circular cracks are located. We assume that at $\rho = \alpha_j$ the cracks of maximal length c_j are located on both, upper and lower sides of the plate. The maximal moment which can be carried by the damaged plate at this point is evaluated as

$$|m_1(\rho,\tau)| \leq \nu_j \gamma_j^2 \tag{11}$$

for a plate with circumferential orientation of fibers, where $j = 1,...,n$ and

$$\nu_j = \left(1 - \frac{2c_j}{h_j}\right)^2, \tag{12}$$

if $\gamma_j \le \gamma_{j-1}$ for each $j = 1,...,n$.

In the case when fibers are oriented radially in the plate instead of (11) one has

$$\left| m_1(\rho,\tau) \right| \le \beta \nu_j \gamma_j^2$$

where β is the ratio of yield stresses in radial and circumferential direction, respectively.

Making use of (8) the transverse velocities (7) and accelerations can be presented as

$$\dot{w} = \dot{w}_0 \frac{\rho - \alpha}{1 - \alpha}, \quad \ddot{w} = \ddot{w}_0 \frac{\rho - \alpha}{1 - \alpha} \tag{14}$$

Equations of motion (5) can be presented in non-dimensional variables (8) as

$$\begin{aligned} q' &= -\frac{q}{\rho} + \gamma_j \ddot{w}_0 \frac{\rho - \alpha}{1 - \alpha}, \\ m_1' &= -\frac{m_1}{\rho} + \frac{m_2}{\rho} + q, \end{aligned} \tag{15}$$

for $\rho \in [\, a_j, a_{j+1} \,]$; $j = 0,...,n$. The solution of (15) has to satisfy following boundary conditions at the free edge

$$q(1,\tau) = 0,\ m_1(1,\tau) = 0. \tag{16}$$

From kinematical considerations it is evident that there is a plastic hinge circle at the clamped edge. Thus the radial moment attains minimal admissible value at $\rho = \alpha$ and in the case of circumferentially and radially reinforced plate

$$\begin{aligned} m_1(\alpha,\tau) &= -\beta\gamma_0^2, \\ m_1(\alpha,\tau) &= -\gamma_0^2, \end{aligned} \tag{17}$$

respectively.

It appears to be reasonable to introduce an attribute k as follows. We assume that $k = \beta$ in the case of circumferential orientation of fibers and $k = 1$ in the case of radially embedded fibers in the matrix. Thus (17) can be written together as

$$m_1(\alpha,\tau) = -\frac{\beta}{k}\gamma_0^2. \tag{18}$$

Substituting (9) and (10) in (15) one can present the equations of motion as

$$q' = -\frac{q}{\rho} + \gamma_j \ddot{w}_0 \frac{\rho - \alpha}{1 - \alpha},$$
$$m_1' = -\frac{m_1}{\rho} - \frac{k}{\rho}\gamma_j^2 + q, \tag{19}$$

for $\rho \in [\ a_j, a_{j+1}\ ];\ j = 0,...,n$.

4.4. Necessary conditions of optimality

The problem posed above consists in the minimization of the cost function with differential constraints (19), inequality constraints (11), (13) and boundary conditions (16)–(18). In order to get necessary conditions of optimality we have to compile the extended functional (Bryson, 1975; Hull, 2003; Lellep and Puman, 2001; Lellep and Tungel, 2005)

$$\begin{aligned} J_* = \Phi &+ \lambda\left(\sum_{j=0}^{n}\gamma_j\left(\alpha_{j+1}^2 - \alpha_j^2\right) - v\right) + \\ &+ \sum_{j=0}^{n}\int_{\alpha_j}^{\alpha_{j+1}}\left\{\psi_1\left(q' + \frac{q}{\rho} - \gamma_j\ddot{w}_0\frac{\rho-\alpha}{1-\alpha}\right) + \psi_2\left(m_1' + \frac{m_1}{\rho} - \frac{k}{\rho}\gamma_j^2 - q\right)\right\}d\rho + \\ &+ \sum_{j=1}^{n}\varphi_j\left(\left|m_1(\alpha_j,\tau)\right| - \nu_j\frac{\beta}{k}\gamma_j^2 + \theta_j^2\right) + \\ &+ \mu_1 q(1,\tau) + \mu_2\left(m_1(\alpha,\tau) + \frac{\beta}{k}\gamma_0^2\right) + \mu_3 m_1(1,\tau) \end{aligned} \tag{20}$$

where Φ is the cost criterion (4) written in non-dimensional quantities (8).

Here ψ_1, ψ_2 stand for co-state variables whereas λ, μ_1, μ_2, μ_3, φ_j are unknown Lagrange multipliers. The quantities θ_j are to be considered as slack variables employed in order to transform inequality constraints (11), (13) into equalities

$$\left|m_1(\alpha_j,\tau)\right| - \nu_j\frac{\beta}{k}\gamma_j^2 + \theta_j^2 = 0 \tag{21}$$

for each of $j = 1,...,n$. When calculating the total variation of (20) it is worthwhile to perceive that quantity $\ddot{w}_0$ can be considered as a constant. In fact, transverse velocity (14) corresponds to the method of mode form motions

(Jones, 1989). However, it is well known that the method of mode form motions leads to constant accelerations (Jones, 1989; Stronge, Yu, 1993).

The total variation of the extended functional (20) gives the following equation

$$\begin{aligned}
&\frac{\partial\Phi}{\partial\ddot{w}_0}\Delta\ddot{w}_0+\sum_{j=1}^{n}\left(\frac{\partial\Phi}{\partial\alpha_j}\Delta\alpha_j+\frac{\partial\Phi}{\partial\gamma_j}\Delta\gamma_j\right)+\frac{\partial\Phi}{\partial\gamma_0}\Delta\gamma_0+\\
&+\sum_{j=0}^{n}\Bigg\{\lambda\left[\Delta\gamma_j\left(\alpha_{j+1}^2-\alpha_j^2\right)+\gamma_j\left(2\alpha_{j+1}\Delta\alpha_{j+1}-2\alpha_j\Delta\alpha_j\right)\right]+\\
&+\int_{\alpha_j}^{\alpha_{j+1}}\Bigg(-\psi_1'\delta q+\psi_1\left(\frac{1}{\rho}\delta q-\Delta\gamma_j\ddot{w}_0\frac{\rho-\alpha}{1-\alpha}-\gamma_j\Delta\ddot{w}_0\frac{\rho-\alpha}{1-\alpha}\right)-\\
&-\psi_2'\delta m_1+\psi_2\left(\frac{1}{\rho}\delta m_1+\frac{k}{\rho}2\gamma_j\Delta\gamma_j-\delta q\right)\Bigg)d\rho+\left(\psi_1\delta q+\psi_2\delta m_1\right)\Big|_{\alpha_j}^{\alpha_{j+1}}\Bigg\}+\\
&+\sum_{j=1}^{n}\varphi_j\left(\Delta\left|m_1(\alpha_j,\tau)\right|-2\nu_j\frac{\beta}{k}\gamma_j\Delta\gamma_j+2\theta_j\Delta\theta_j\right)+\\
&+\mu_1\Delta q(1,\tau)+\mu_2\left(\Delta m_1(\alpha,\tau)+\frac{2\beta}{k}\gamma_0\Delta\gamma_0\right)+\mu_3\Delta m_1(1,\tau)=0
\end{aligned}\tag{22}$$

Considering δq, δm_1 as independent variations one easily obtains the co-state (adjoint) equations

$$\begin{aligned}
\psi_1'&=\frac{\psi_1}{\rho}-\psi_2\\
\psi_2'&=\frac{\psi_2}{\rho}
\end{aligned}\tag{23}$$

for $\rho\in[\ a_j,a_{j+1}\ ];\ j=0,...,n$.

Due to arbitrariness of variations $\Delta\ddot{w}_0$ one can write

$$\frac{\partial\Phi}{\partial\ddot{w}_0}-\sum_{j=0}^{n}\int_{\alpha_j}^{\alpha_{j+1}}\psi_1\gamma_j\frac{\rho-\alpha}{1-\alpha}d\rho=0\,.\tag{24}$$

Arbitrary variations of parameters γ_j ($j = 0,...,n$) yield

$$\frac{\partial \Phi}{\partial \gamma_j} + \lambda\left(\alpha_{j+1}^2 - \alpha_j^2\right) - \int_{\alpha_j}^{\alpha_{j+1}} \left(\psi_1 \ddot{w}_0 \frac{\rho - \alpha}{1-\alpha} + \psi_2 \frac{2k}{\rho}\gamma_j\right) d\rho + \chi_j = 0 \quad (25)$$

where $j = 0,...,n$. Here the quantity χ_j can be expressed as

$$\chi_j = \begin{cases} \mu_2 \dfrac{2\beta}{k}\gamma_0 & , j = 0; \\ -2\varphi_j \nu_j \dfrac{\beta}{k}\gamma_j & , j = 1,...,n-1. \end{cases} \quad (26)$$

Variations of slack variables θ_j lead to the equations

$$\varphi_j \theta_j = 0 \quad (27)$$

for each $j = 1,...,n$.

At the boundary points $\rho = \alpha$ and $\rho = 1$ variations $\delta m_1(\alpha,\tau)$, $\delta q(\alpha,\tau)$ and $\delta m_1(1,\tau)$, $\delta q(1,\tau)$ are arbitrary. Therefore it follows from (22) that

$$\begin{aligned} &\psi_1(\alpha,\tau) = 0 \\ &-\psi_2(\alpha,\tau) + \mu_2 = 0 \\ &\psi_1(1) + \mu_1 = 0 \\ &\psi_2(1) + \mu_3 = 0 \end{aligned} \quad (28)$$

Since intermediate points $\rho = \alpha_j$ of the optimal trajectory are not fixed one has to use total variations of quantities m_1 and q defined as (see Hull, 2003; Lellep and Puman, 2001; Lellep and Tungel, 2005)

$$\begin{aligned} \Delta m_1(\alpha_j) &= \delta m_1(\alpha_j \pm) + m_1'(\alpha_j \pm)\Delta\alpha_j, \\ \Delta q(\alpha_j) &= \delta q(\alpha_j \pm) + q'(\alpha_j \pm)\Delta\alpha_j. \end{aligned} \quad (29)$$

Here $\Delta m_1(\alpha_j)$, $\Delta q(\alpha_j)$ stand for the total variations of m_1 and q whereas $\delta m_1(\alpha_j \pm)$, $\delta q(\alpha_j \pm)$ denote the right-hand and left-hand weak variations, respectively, e.g.

$$\delta q(\alpha_j \pm) = \lim_{\rho \to \alpha \pm 0} \delta q(\rho,\tau)$$

$$\delta m_1(\alpha_j \pm) = \lim_{\rho \to \alpha \pm 0} \delta m_1(\rho,\tau)$$

The distinction of right-and left-hand variations is essential because according to (15) the state variables q and m_1 satisfy different equations in regions $[\ a_{j-1}, a_j\ ]$ and $[\ \alpha_j, \alpha_{j+1}\ ]$, respectively.

Taking (23)–(29) into account one can rewrite (22) as

$$\sum_{j=1}^{n}\left\{\frac{\partial\Phi}{\partial\alpha_j}\Delta\alpha_j+2\lambda\alpha_j\left(\gamma_{j-1}-\gamma_j\right)\Delta\alpha_j+\right.$$
$$+\psi_1(\alpha_j-)\left(\Delta q(\alpha_j,\tau)-q'(\alpha_j-,\tau)\Delta\alpha_j\right)+$$
$$+\psi_2(\alpha_j-)\left(\Delta m_1(\alpha_j,\tau)-m_1'(\alpha_j-,\tau)\Delta\alpha_j\right)-$$
$$-\psi_1(\alpha_j+)\left(\Delta q(\alpha_j,\tau)-q'(\alpha_j+,\tau)\Delta\alpha_j\right)- \tag{30}$$
$$-\psi_2(\alpha_j+)\left(\Delta m_1(\alpha_j,\tau)-m_1'(\alpha_j+,\tau)\Delta\alpha_j\right)+$$
$$\left.+\varphi_j\Delta\left|m_1\left(\alpha_j,\tau\right)\right|\right\}=0.$$

In (30) $\Delta q\left(\alpha_j,\tau\right)$ and $\Delta m_1\left(\alpha_j,\tau\right)$ are arbitrary variations, therefore

$$\begin{aligned}&\psi_1\left(\alpha_j-\right)-\psi_1\left(\alpha_j+\right)=0,\\&\psi_2\left(\alpha_j-\right)-\psi_2\left(\alpha_j+\right)\pm\varphi_j=0,\end{aligned} \tag{31}$$

for each $j=1,...,n$.

Finally, arbitrariness of $\Delta\alpha_j$ in (30) yields

$$\frac{\partial\Phi}{\partial\alpha_j}+2\lambda\alpha_j\left(\gamma_{j-1}-\gamma_j\right)-\psi_1(\alpha_j-)q'(\alpha_j-,\tau)-\psi_2(\alpha_j-)m_1'(\alpha_j-,\tau)+$$
$$+\psi_1(\alpha_j+)q'(\alpha_j+,\tau)+\psi_2(\alpha_j+)m_1'(\alpha_j+,\tau)=0 \tag{24}$$

for $j=1,...,n$.

4.5. Residual deflections

In order to define residual deflections of a stepped plate subjected to initial impulsive loading the method of mode form motions will be employed. Originally this method was suggested by Martin and Symonds (1966). Later it was shown by several researchers (see Jones, 1989; Lepik, 1982; Stronge and Yu, 1993) that the method enables to evaluate the dynamic plastic response of structures with reasonable exactness.

Integrating the set of equations (19) in the segment $\left[\alpha_j,\alpha_{j+1}\right]$ ($j=0,...,n$) one obtains

$$\rho q=\frac{\gamma_j\ddot{w}_0}{1-\alpha}\left(\frac{\rho^3}{3}-\alpha\frac{\rho^2}{2}\right)+B_j \tag{33}$$

and

$$\rho m_1 = -k\gamma_j^2\rho + \frac{\gamma_j \ddot{w}_0}{1-\alpha}\left(\frac{\rho^4}{12} - \alpha\frac{\rho^3}{6}\right) + B_j\rho + C_j \ . \tag{34}$$

For determination of arbitrary constants of integration B_j ($j = 1,...,n$) one can use the boundary condition (16) accounting for the continuity of the shear force

$$q(\alpha_j -, \tau) = q(\alpha_j +, \tau) \tag{35}$$

for each $j = 1,...,n$. It can be rechecked that (16) and (35) lead to results

$$B_j = -\frac{\ddot{w}_0}{1-\alpha}\left\{\sum_{i=j+1}^{n}\gamma_i\left(\frac{1}{3}\left(\alpha_{i+1}^3 - \alpha_i^3\right) - \frac{\alpha}{2}\left(\alpha_{i+1}^2 - \alpha_i^2\right)\right) + \gamma_j\left(\frac{\alpha_{j+1}^3}{3} - \frac{\alpha}{2}\alpha_{j+1}^2\right)\right\} \tag{36}$$

for each $j = 0,...,n-1$ whereas

$$B_n = -\gamma_n\frac{\ddot{w}_0}{1-\alpha}\left(\frac{1}{3} - \frac{\alpha}{2}\right) \ . \tag{37}$$

The continuity of the bending moment, e.g.

$$m_1(\alpha_j -, \tau) = m_1(\alpha_j +, \tau)$$

with the boundary condition (16) admits to define constants

$$\begin{aligned} C_j = \frac{\ddot{w}_0}{1-\alpha}\Bigg\{ & \sum_{i=j+1}^{n}\gamma_i\left(\frac{1}{4}\left(\alpha_{i+1}^4 - \alpha_i^4\right) - \frac{\alpha}{3}\left(\alpha_{i+1}^3 - \alpha_i^3\right)\right) + \\ & + \gamma_j\left(\frac{1}{4}\alpha_{j+1}^4 - \frac{1}{3}\alpha_{j+1}^3\right)\Bigg\} - k\sum_{i=j+1}^{n}\left(\gamma_i^2 - \gamma_{i-1}^2\right)\alpha_i + k\gamma_n^2 \end{aligned} \tag{38}$$

for $j = 0,...,n-1$ and

$$C_n = \frac{\ddot{w}_0}{1-\alpha}\gamma_n\left(\frac{1}{4} - \frac{\alpha}{3}\right) + k\gamma_n^2 \ . \tag{39}$$

Substituting (36)–(39) in (33) and (34) leads the relations

$$q(\rho,\tau)=\frac{\ddot{w}_0}{12(1-\alpha)}\left\{\gamma_j\left(4\left(\rho^3-\alpha_{j+1}^3\right)-6\alpha\left(\rho^2-\alpha_{j+1}^2\right)\right)-\right.$$
$$\left.-\sum_{i=j+1}^{n}\gamma_i\left(4\left(\alpha_{i+1}^3-\alpha_i^3\right)-6\alpha\left(\alpha_{i+1}^2-\alpha_i^2\right)\right)\right\},$$

$$m_1(\rho,\tau)=-k\gamma_j^2+\frac{\ddot{w}_0}{12(1-\alpha)}\left\{\gamma_j\left(\left(\rho^3-2\alpha\rho^2\right)-\gamma_j\left(4\alpha_{j+1}^3-6\alpha\alpha_{j+1}^2\right)\right)+\right. \tag{40}$$
$$+\sum_{i=j+1}^{n}\gamma_i\left(4\left(\alpha_i^3-\alpha_{i+1}^3\right)+6\alpha\left(\alpha_{i+1}^2-\alpha_i^2\right)+\frac{3}{\rho}\left(\alpha_{i+1}^4-\alpha_i^4\right)-\frac{4\alpha}{\rho}\left(\alpha_{i+1}^3-\alpha_i^3\right)\right)+$$
$$\left.+\frac{\gamma_j}{\rho}\left(3\alpha_{j+1}^4-4\alpha\alpha_{j+1}^3\right)\right\}-\frac{k}{\rho}\sum_{i=j+1}^{n}\left(\gamma_i^2-\gamma_{i-1}^2\right)\alpha_i+\frac{k\gamma_n^2}{\rho}$$

for $\rho\in\left[a_j,a_{j+1}\right]$; $j=0,...,n-1$ and

$$q(\rho,\tau)=\frac{\ddot{w}_0\gamma_n}{12(1-\alpha)\rho}\left(4\rho^3-6\alpha\rho^2-4+6\alpha\right),$$
$$m_1(\rho,\tau)=-k\gamma_n^2\left(\frac{1}{\rho}-1\right)+\frac{\ddot{w}_0\gamma_n}{12(1-\alpha)}\left(\rho^3-2\alpha\rho^2+\frac{1}{\rho}(3-4\alpha)-4+6\alpha\right) \tag{41}$$

for $\rho\in\left[a_n,a_{n+1}\right]$.

It can be easily rechecked that the bending moment given by (40) for $j=0$ satisfies the boundary condition (18) if

$$-k\gamma_0^2+\frac{\ddot{w}_0}{12(1-\alpha)}\left\{-\gamma_0\alpha^3-\gamma_0\left(4\alpha_1^3-6\alpha\alpha_1^2\right)+\frac{\gamma_0}{\alpha}\left(3\alpha_1^4-4\alpha\alpha_1^3\right)+\right.$$
$$\left.+\sum_{i=1}^{n}\gamma_i\left(-8\left(\alpha_i^3-\alpha_{i+1}^3\right)+6\alpha\left(\alpha_{i+1}^2-\alpha_i^2\right)+\frac{3}{\alpha}\left(\alpha_{i+1}^4-\alpha_i^4\right)\right)\right\}- \tag{42}$$
$$-\frac{k}{\alpha}\sum_{i=1}^{n}\left(\gamma_i^2-\gamma_{i-1}^2\right)\alpha_i+\frac{k\gamma_n^2}{\alpha}+\frac{\beta}{k}\gamma_0^2=0.$$

From (42) one easily obtains

$$\ddot{w}_0 = -\frac{12(1-\alpha)\left[k\sum_{j=0}^{n}\alpha_j\left(\gamma_j^2-\gamma_{j-1}^2\right)-k\gamma_n^2-\frac{\beta}{k}\gamma_0^2\alpha+k\alpha\gamma_0^2\right]}{\sum_{j=0}^{n}\gamma_j\left[3\left(\alpha_{j+1}^4-\alpha_j^4\right)-8\alpha\left(\alpha_{j+1}^3-\alpha_j^3\right)+6\alpha^2\left(\alpha_{j+1}^2-\alpha_j^2\right)\right]}. \qquad (43)$$

It follows from (43) as it might be expected that $\ddot{w}_0 = const$. Thus by integration one obtains

$$\dot{w}_0 = \ddot{w}_0\tau + \dot{w}_0(0) \qquad (44)$$

and

$$w_0(\tau) = \ddot{w}_0\frac{\tau^2}{2} + \dot{w}_0(0)\tau. \qquad (45)$$

The motion of the plate is completed at $\tau = \tau_1$ when $\dot{w}_0(\tau_1) = 0$. Thus it follows from (45) that

$$\tau_1 = -\frac{\dot{w}_0(0)}{\ddot{w}_0}. \qquad (46)$$

Substituting (46) in (45) yields the maximal residual deflection

$$w_0(\tau_1) = -\frac{1}{2}\frac{\dot{w}_0^2(0)}{\ddot{w}_0}. \qquad (47)$$

It is assumed that the plate under consideration is subjected to the initial impulsive loading whereas the initial kinetic energy K_0 of the plate is given. Calculating the kinetic energy corresponding to the transverse velocity distribution (14) at the moment $\tau = 0$ gives

$$K_0 = \frac{\dot{w}_0^2(0)}{(1-\alpha)^2}\sum_{j=0}^{n}\int_{\alpha_j}^{\alpha_{j+1}}\gamma_j(\rho-\alpha)^2\rho d\rho.$$

The latter yields the initial velocity at the free edge of the plate

$$\dot{w}_0^2(0) = \frac{12K(1-\alpha)^2}{\sum_{j=0}^{n}\gamma_j\left[6\alpha^2\left(\alpha_{j+1}^2-\alpha_j^2\right)-8\alpha\left(\alpha_{j+1}^3-\alpha_j^3\right)+3\left(\alpha_{j+1}^4-\alpha_j^4\right)\right]}. \qquad (48)$$

Maximal residual deflection can be defined according to (47) when the acceleration and the initial velocity $\dot{w}_0(0)$ are substituted from (43) and (48) as

$$w_1 = -\frac{1}{2}\frac{1-\alpha}{k\sum_{j=0}^{n}\alpha_j\left(\gamma_j^2-\gamma_{j-1}^2\right)-k\left(\gamma_n^2-\alpha\gamma_0^2\right)-\frac{\beta\alpha}{k}\gamma_0^2} \tag{49}$$

where

$$w_1 = \frac{w_0(\tau_1)}{K}. \tag{50}$$

4.6. Discussion of results

Results of calculations are presented in Tables 4.1–4.4 and Fig. 4.4–4.21.The curves depicted in Figures are calculated for plates with a single step, whereas the material parameter $\beta = 1.5$.

Figures 4.4–4.11 and 4.12–4.19 correspond to plates with internal radii $a = 0.2R$ and $a = 0.4R$, respectively. From figures of the first group Fig. 4.4–4.7, and of the second group Fig. 4.12–4.15, correspond to plates made of a ductile material reinforced in the circumferential direction. The rest of the figures are associated with the radially reinforced plates.

Optimal values of the coordinate $\rho = \alpha_1$ where the thickness varies rapidly are presented in Fig. 4.4, 4.8, 4.12, 4.16 versus v for different values of the crack length parameter ν. As it can been seen in (12) the value $\nu = 1.0$ presents the case of a plate without any crack. However, if $\nu = 0$, then the crack has reached trough the thickness. In the case of a crack of constant length this value corresponds to the failure of the plate. That is why in the present paper we assume that $\nu > 0$. The results of the calculation show that the location of the step moves towards the free edge when the material volume of the plate v increases. The same tendency can be revealed when the parameter ν increases, e.g. the crack length decreases.

It is worthwhile to emphasize the behaviour of α_1 versus v is quite similar in the cases of circumferential and radial arrangement of fibers in the matrix material.

Optimal values of the thickness of the outward annulus γ_1 versus v are depicted in Fig. 4.5, 4.9, 4.13, 4.17 for several values of the crack parameter ν. It reveals from Fig. 4.5, 4.9, 4.13, 4.17 that the qualitative behaviour of γ_1 is similar for plates with different radii of the clamped edge and for both types of arrangements of fibers. The thickness γ_1 decreases when the volume v increases. Similarly, in the case of a fixed value of v the thickness γ_1 is greater if the parameter ν is smaller, e.g. the crack is larger.

Table 4.1. Coefficient of efficiency for circumferentially reinforced plates ($a = 0.2R$)

ν / ν	0,64	0,65	0,66	0,68	0,69	0,7	0,71	0,73	0,75	0,77	0,85	0,9	0,95
0.1										0,7729	0,8403	0,9095	0,9846
0.2									0,7368	0,7452	0,8381	0,9091	0,9846
0.3								0,7133	0,7197	0,7377	0,8371	0,9090	0,9846
0.4							0,7015	0,6966	0,7128	0,7337	0,8366	0,9089	0,9846
0.5						0,6764	0,6763	0,6894	0,7088	0,7312	0,8362	0,9088	0,9846
0.6					0,6604	0,6621	0,6679	0,6851	0,7061	0,7295	0,8360	0,9088	0,9846
0.7				0,6468	0,6490	0,6550	0,6629	0,6821	0,7042	0,7283	0,8358	0,9087	0,9846
0.8			0,6477	0,6368	0,6426	0,6504	0,6594	0,6799	0,7028	0,7274	0,8356	0,9087	0,9846
0.9		0,6368	0,6236	0,6308	0,6383	0,6471	0,6568	0,6783	0,7017	0,7266	0,8355	0,9087	0,9846
1	0,6327	0,6136	0,6145	0,6266	0,6351	0,6446	0,6548	0,6770	0,7009	0,7260	0,8354	0,9087	0,9846

Table 4.2. Coefficient of efficiency for circumferentially reinforced plates ($a = 0.4R$)

ν / ν	0,59	0,6	0,61	0,62	0,63	0,64	0,65	0,67	0,69	0,71	0,75	0,8	0,83
0.1										0,7983	0,8478	0,9292	0,9820
0.2									0,7653	0,7870	0,8454	0,9290	0,9820
0.3								0,7373	0,7565	0,7831	0,8444	0,9289	0,9820
0.4							0,7161	0,7281	0,7527	0,7811	0,8438	0,9288	0,9820
0.5						0,6970	0,7023	0,7237	0,7504	0,7798	0,8435	0,9288	0,9820
0.6					0,6811	0,6870	0,6967	0,7210	0,7489	0,7790	0,8432	0,9288	0,9820
0.7				0,6669	0,6725	0,6819	0,6933	0,7192	0,7479	0,7783	0,8431	0,9288	0,9820
0.8			0,6539	0,6587	0,6677	0,6787	0,6909	0,7179	0,7471	0,7779	0,8429	0,9288	0,9820
0.9		0,6421	0,6456	0,6539	0,6645	0,6763	0,6892	0,7168	0,7465	0,7775	0,8428	0,9287	0,9820
1	0,6318	0,6332	0,6407	0,6507	0,6621	0,6746	0,6878	0,7160	0,7460	0,7772	0,8427	0,9287	0,9820

Table 4.3. Coefficient of efficiency for radially reinforced plates ($a = 0.2R$)

ν / ν	0,6	0,61	0,62	0,64	0,65	0,67	0,69	0,71	0,73	0,77	0,85	0,9	0,95
0.1										0,7358	0,8298	0,9044	0,9838
0.2									0,6897	0,7202	0,8283	0,9042	0,9838
0.3								0,6543	0,6696	0,7159	0,8277	0,9041	0,9838
0.4							0,6276	0,6428	0,6640	0,7139	0,8274	0,9041	0,9838
0.5						0,6044	0,6176	0,6379	0,6611	0,7126	0,8273	0,9041	0,9838
0.6					0,5854	0,5940	0,6127	0,6350	0,6592	0,7118	0,8271	0,9040	0,9838
0.7				0,5680	0,5723	0,5888	0,6097	0,6330	0,6579	0,7112	0,8270	0,9040	0,9838
0.8			0,5563	0,5586	0,5663	0,5855	0,6076	0,6316	0,6570	0,7108	0,8270	0,9040	0,9838
0.9		0,5403	0,5402	0,5534	0,5625	0,5832	0,6061	0,6306	0,6563	0,7104	0,8269	0,9040	0,9838
1	0,5272	0,5278	0,5334	0,5500	0,5598	0,5814	0,6049	0,6297	0,6557	0,7101	0,8269	0,9040	0,9838

Table 4.4. Coefficient of efficiency for radially reinforced plates ($a = 0.4R$)

ν / ν	0,57	0,58	0,59	0,6	0,61	0,63	0,64	0,66	0,68	0,71	0,77	0,8	0,83
0.1										0,7719	0,8674	0,9228	0,9804
0.2									0,7216	0,7631	0,8668	0,9227	0,9804
0.3								0,6877	0,7137	0,7609	0,8665	0,9227	0,9804
0.4							0,6575	0,6812	0,7110	0,7599	0,8664	0,9226	0,9804
0.5						0,6384	0,6503	0,6785	0,7095	0,7593	0,8663	0,9226	0,9804
0.6					0,6127	0,6335	0,6472	0,6768	0,7086	0,7589	0,8663	0,9226	0,9804
0.7				0,5958	0,6052	0,6309	0,6453	0,6758	0,7079	0,7586	0,8662	0,9226	0,9804
0.8			0,5802	0,5896	0,6017	0,6292	0,6440	0,6750	0,7075	0,7584	0,8662	0,9226	0,9804
0.9		0,5655	0,5746	0,5864	0,5994	0,6279	0,6430	0,6744	0,7071	0,7582	0,8662	0,9226	0,9804
1	0,5515	0,5600	0,5714	0,5842	0,5978	0,6270	0,6423	0,6739	0,7068	0,7581	0,8662	0,9226	0,9804

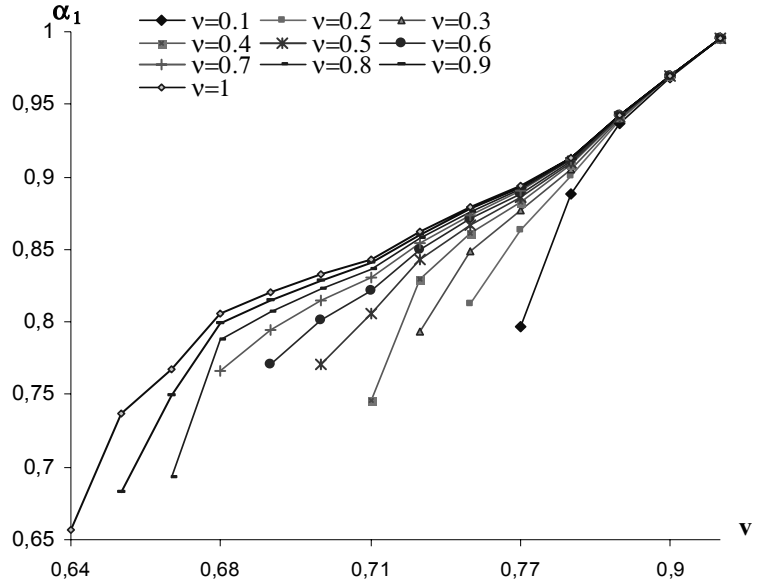

Figure 4.4. Optimal step location for $a = 0.2R$

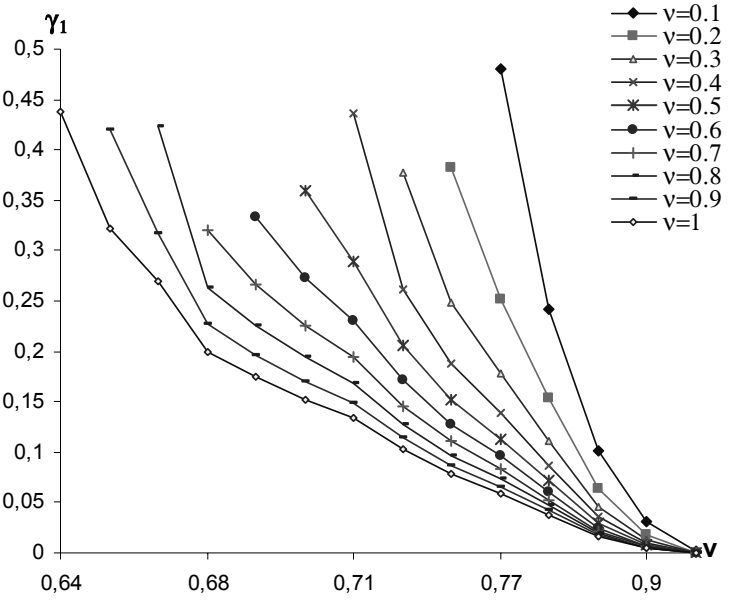

Figure 4.5. Optimal thickness for $a = 0.2R$

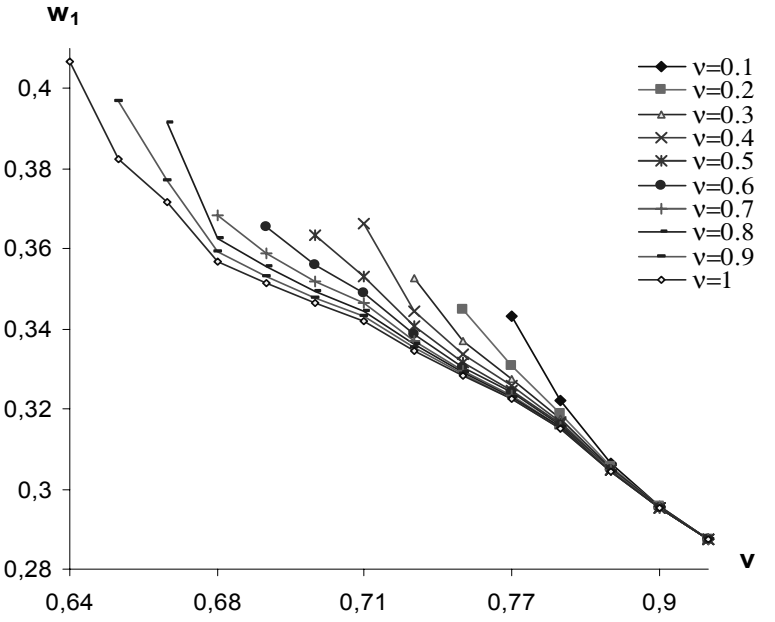

Figure 4.6. Maximal residual deflection for $a = 0.2R$

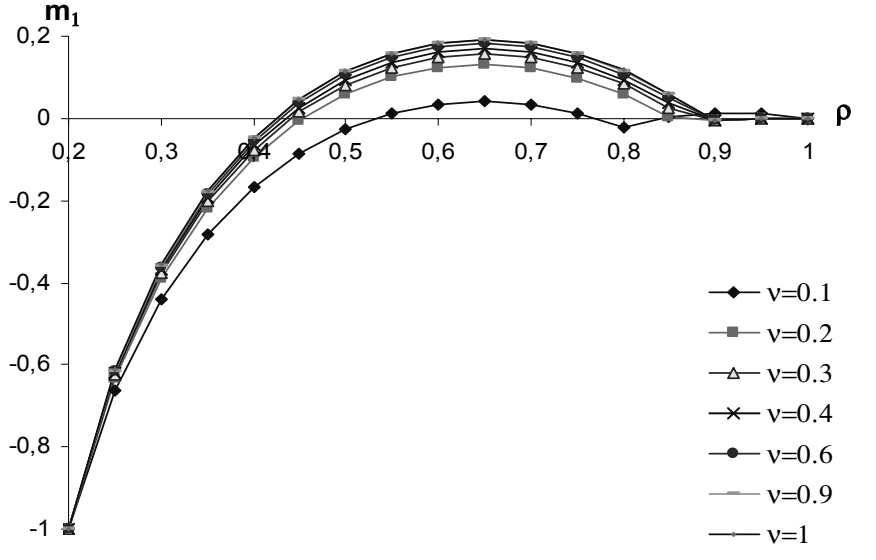

Figure 4.7. Bending moment m_1 distribution for circumferentially reinforced plates with $a = 0.2R$

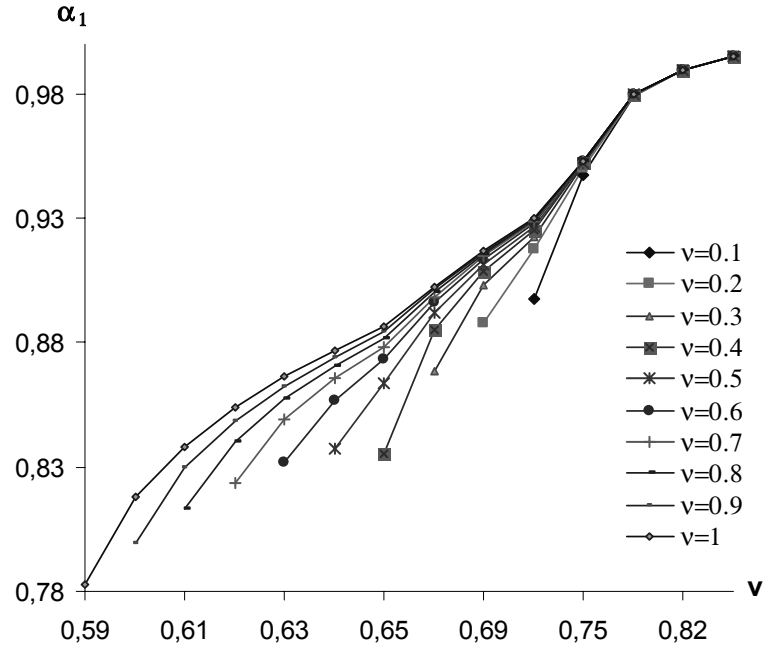

Figure 4.8. Optimal step location for $a = 0.4R$

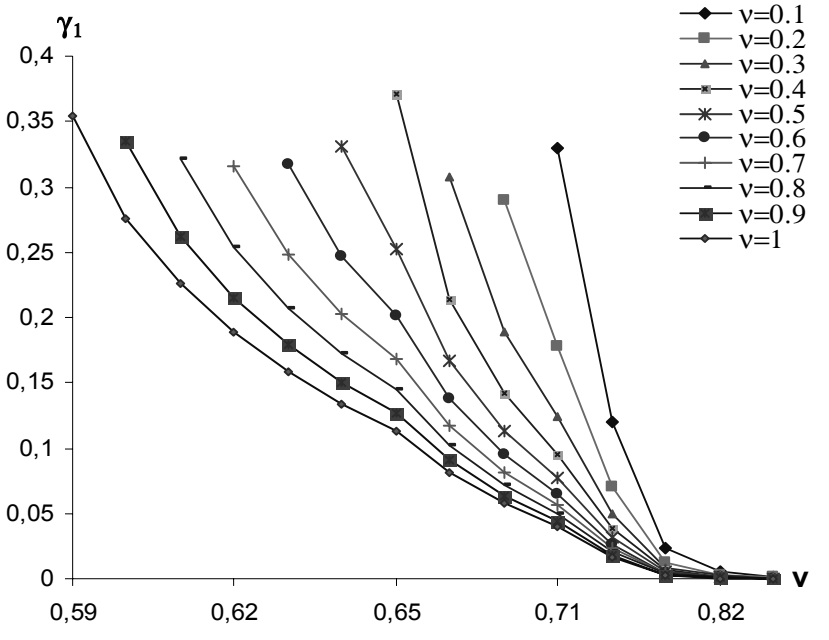

Figure 4.9. Optimal thickness for $a = 0.4R$

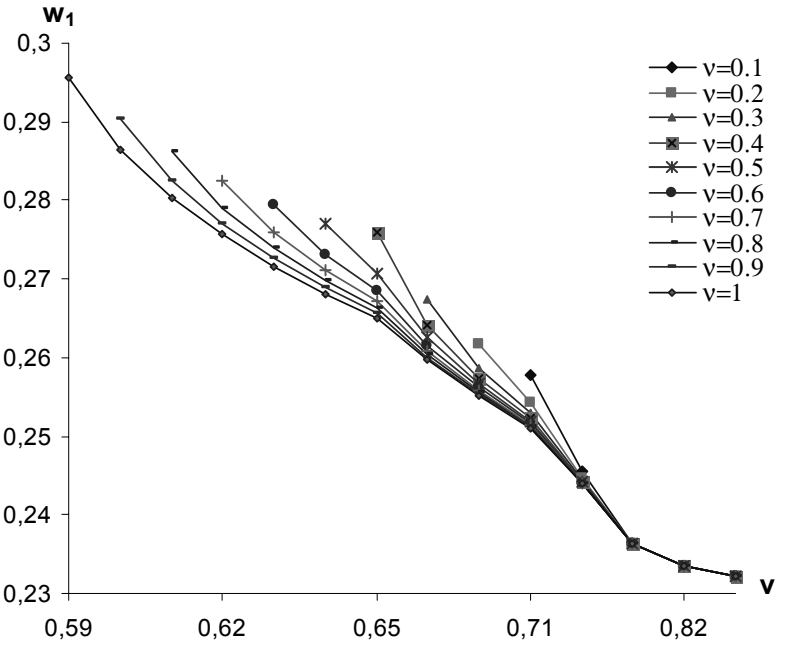

Figure 4.10. Maximal residual deflection for $a = 0.4R$

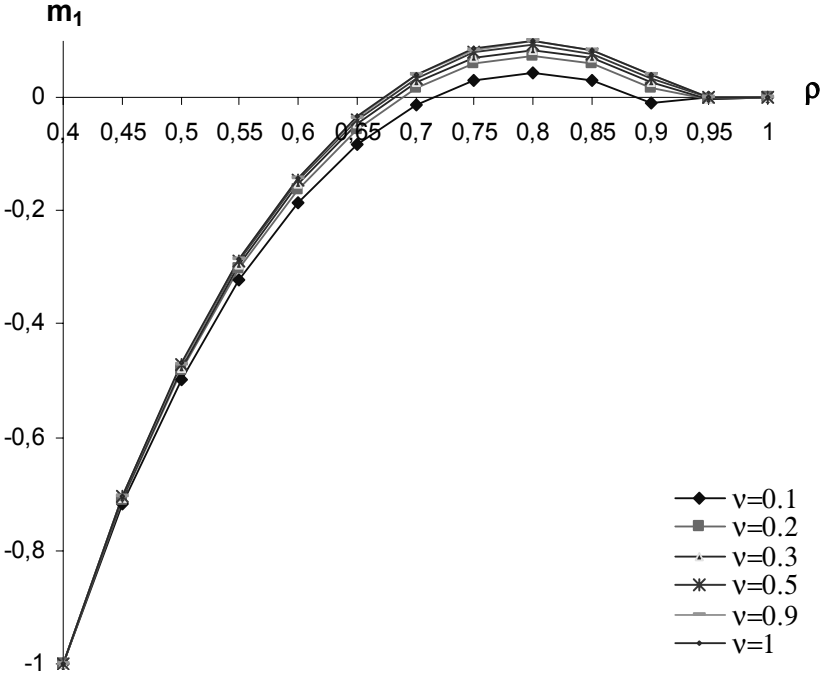

Figure 4.11. Bending moment m_1 distribution for circumferentially reinforced plates with $a = 0.4R$

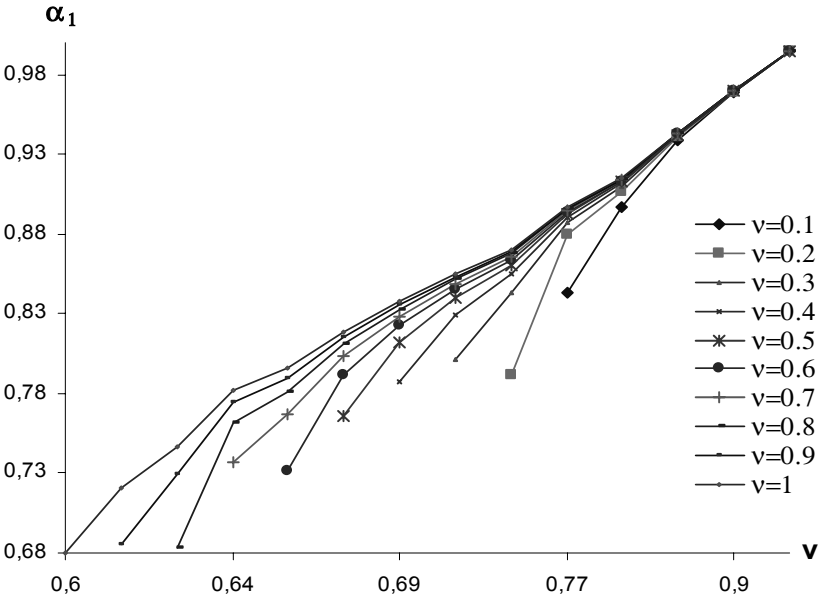

Figure 4.12. Optimal step location for $a = 0.2R$

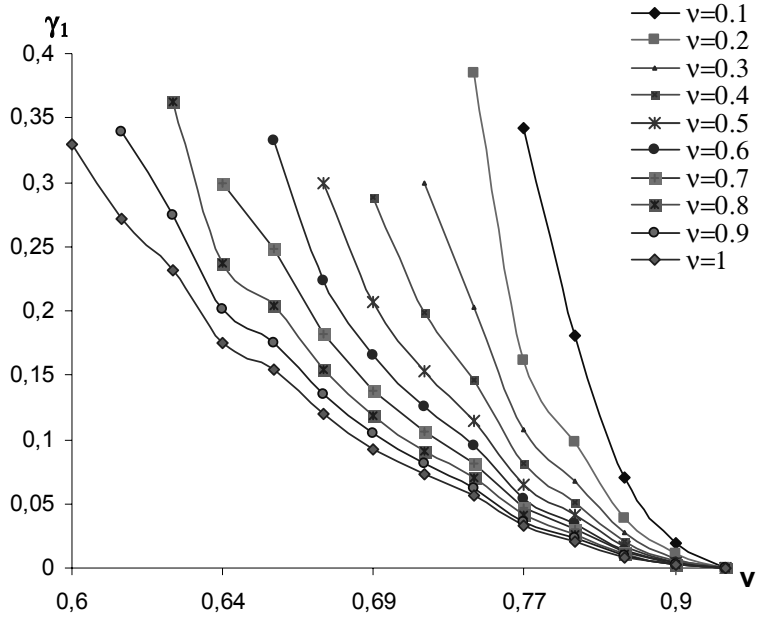

Figure 4.13. Optimal thickness for $a = 0.2R$

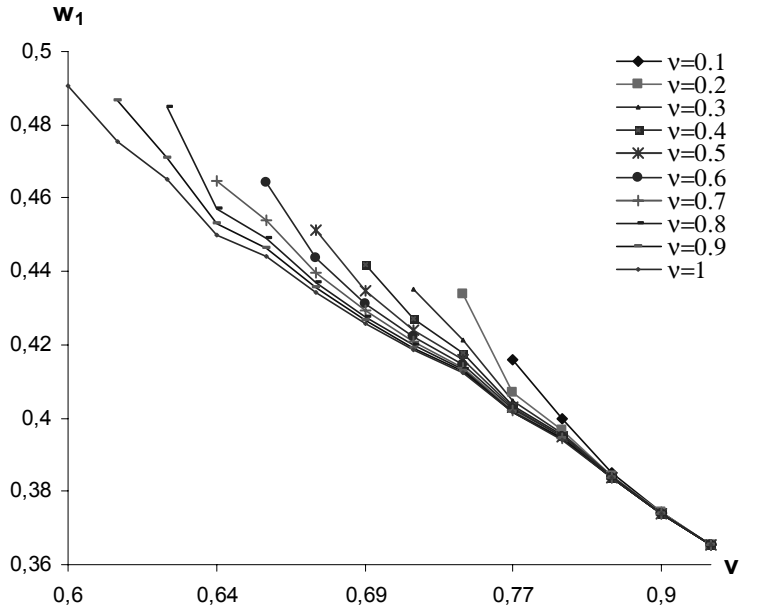

Figure 4.14. Maximal residual deflection for $a = 0.2R$

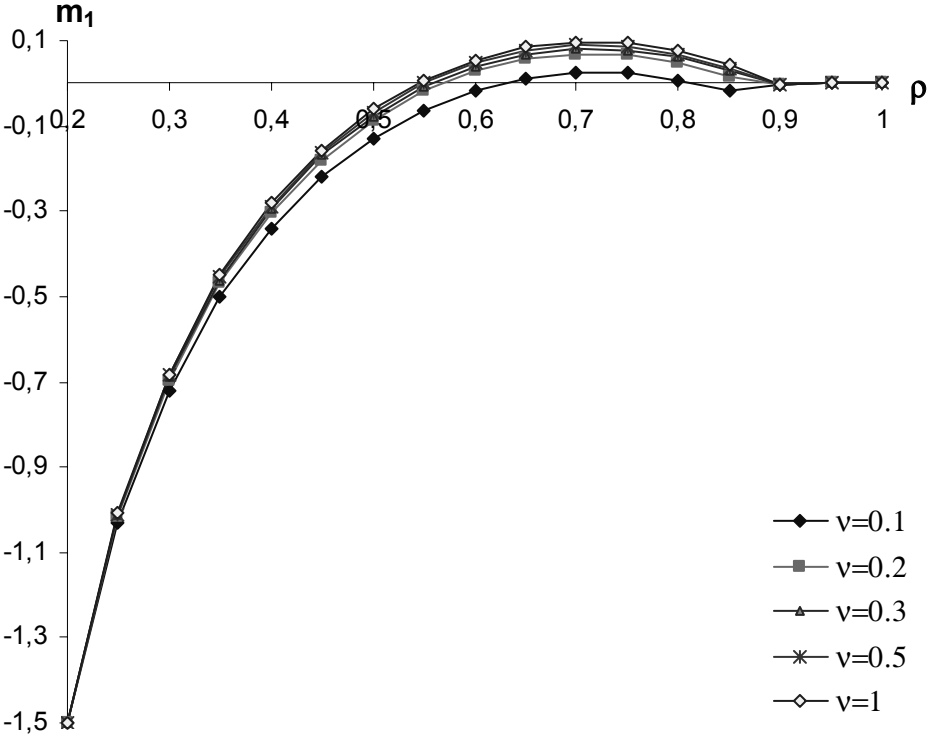

Figure 4.15. Bending moment m_1 distribution for radially reinforced plates with $a = 0.2R$

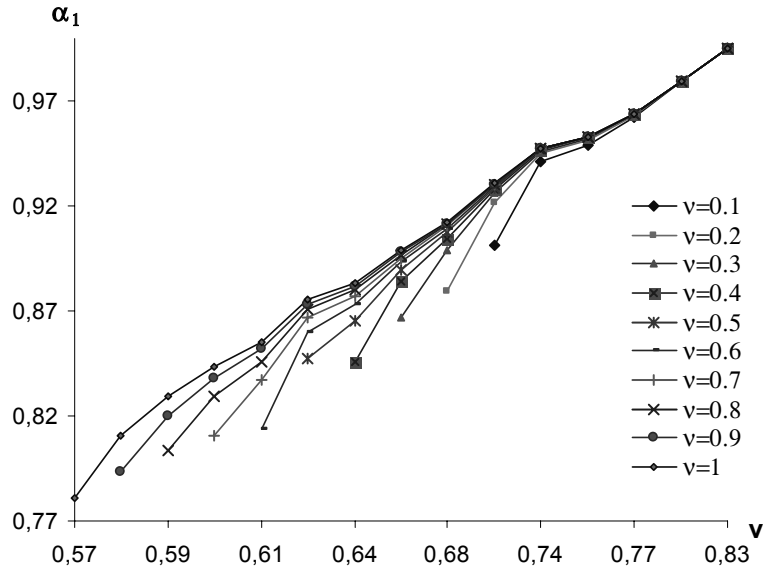

Figure 4.16. Optimal step location for $a = 0.4R$

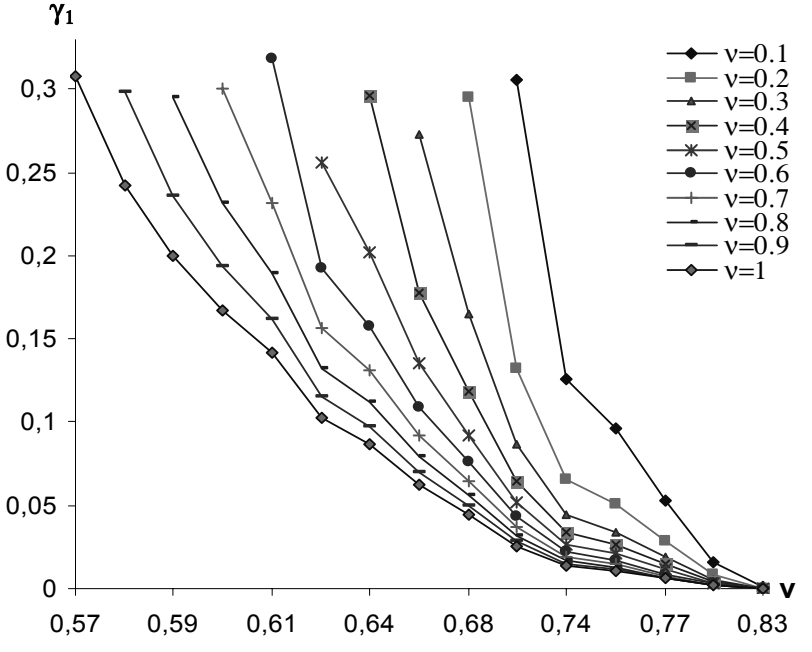

Figure 4.17. Optimal thickness for $a = 0.4R$

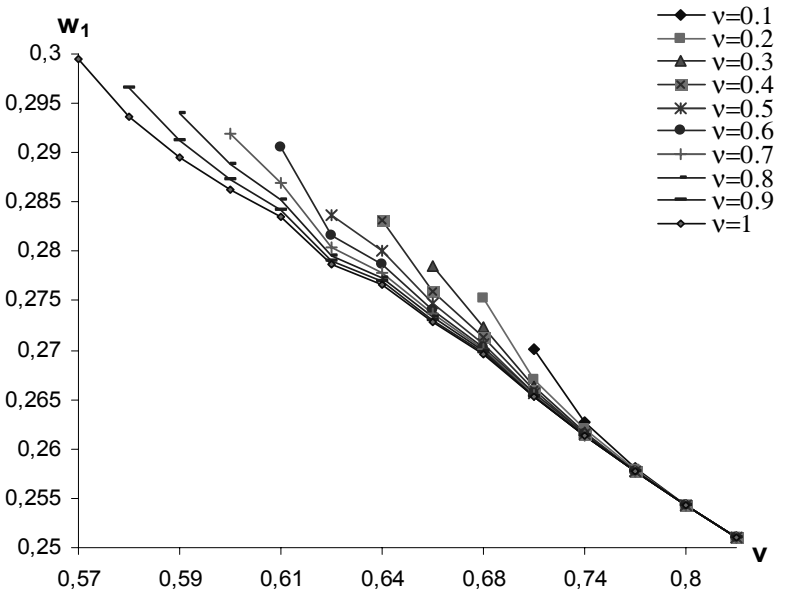

Figure 4.18. Maximal residual deflection for $a = 0.4R$

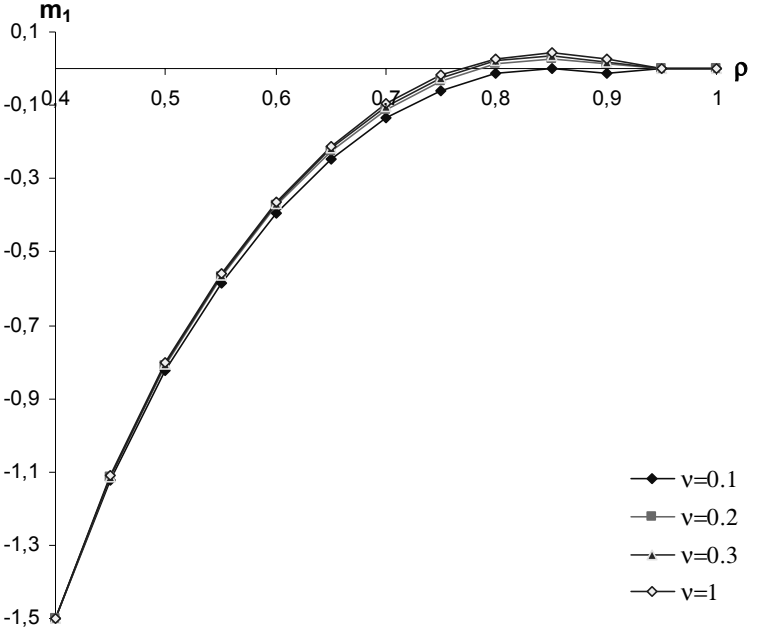

Figure 4.19. Bending moment m_1 distribution for radially reinforced plates with $a = 0.4R$

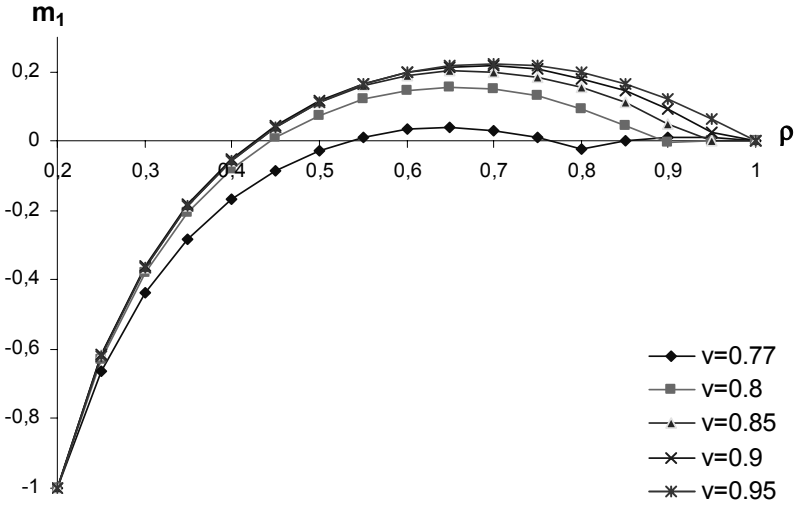

Figure 4.20. Bending moment m_1 distribution for $\nu = 0.1$

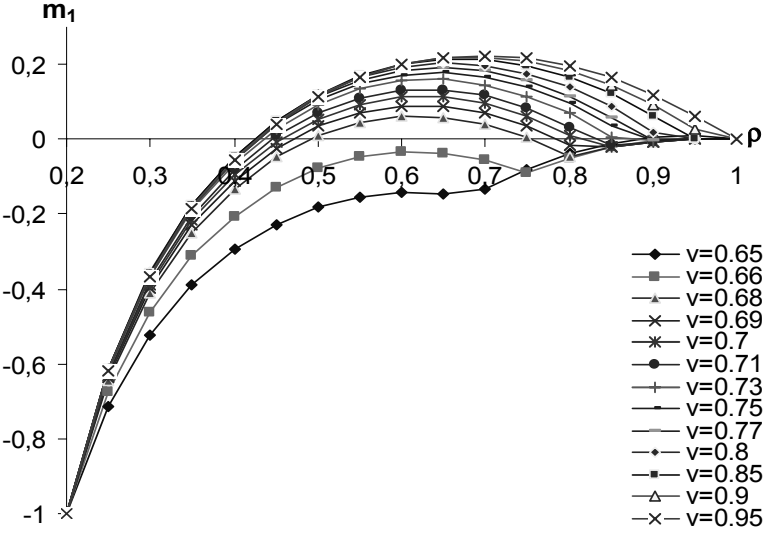

Figure 4.21. Bending moment m_1 distribution for $\nu = 0.9$

Minimal values of the residual deflection at the free edge of plates are presented in Fig. 4.6, 4.10, 4.14, 4.18 for different values of the crack parameter ν. Comparing Fig. 4.6 and 4.10, also Fig. 4.14 and 4.18 one can see that in the case of plates with smaller internal radius a the residual deflection at the free edge is larger, as it might be expected. For instance, if one compares plates with

circumferential reinforcement and the crack parameter $\nu = 0.2$ then $w_1 = 0.345$, if $a = 0.2R$ and $w_1 = 0.245$, if $a = 0.4R$.

It is somewhat surprising that the curves presented in Fig. 4.6, 4.10, 4.14, 4.18 for different values of ν are comparatively close to each other.

However, it reveals from Fig. 4.6, 4.10, 4.14, 4.18 that regions of existence of optimal solutions with respect to the volume v are substantially different for different values of the crack length. This matter reflects in Tables 4.1–4.4, as well.

The efficiency of designs is evaluated as

$$e = \frac{w_1}{w_*} \tag{51}$$

where w_* stands for the deflection at the free edge of a reference plate of constant thickness $h_* = \gamma_* h_0$. We assume herein that the reference plate of constant thickness h_* and the optimized plate of stepped shape have common weight. Therefore the non-dimensional thickness can be expressed as

$$\gamma_* = \frac{v}{1-\alpha^2}\,. \tag{52}$$

In the case of the reference plate the stress-strain state can be evaluated by (19) where $\gamma_j = \gamma_*$ for each $\rho \in [\alpha,1]$. Thus the residual deflection is expressed by (49), (50), (52) as

$$w_* = \frac{(1-\alpha)^3(1+\alpha)^2}{2\nu^2\left(k(1-\alpha)+\dfrac{\beta\alpha}{k}\right)}\,. \tag{53}$$

Values of the coefficient of efficiency (51) are accommodated in Tables 4.1–4.4 for different values of the crack parameter ν. It can be seen from Tables 4.1–4.4 that the coefficient e increases when the parameter ν decreases. This means that the design is always the best among the designs of the same weight if there is no any crack ($\nu = 1.0$). It would be mentioned that the coefficient of efficiency is comparatively insensitive with respect to the crack size ν.

Comparing the deflections of plates made of materials with radial and circumferential orientation of fibers, respectively, one can see that the deflections of circumferentially reinforced plates are less than that of radially reinforced plates, if $a < 0.5R$. When $a > 0.5R$ then radially reinforced material gives smaller deflections than a circumferentially reinforced material does. Thus for a narrow annulus clamped at the inner edge the use of a radial reinforcement seems to be preferable if the deflections are restricted.

In order to assess the statical admissibility of solutions established above radial bending moments are calculated for various values of the internal radius

α and the crack length ν. For $a = 0.2R$ the bending moment distributions are presented in Fig. 4.7, 4.11 and for $a = 0.4R$ in Fig. 4.15, 4.19. Figures 4.7 and 4.15 correspond to plates made of a circumferentially reinforced material whereas Fig. 4.11 and 4.19 are associated with radial orientation of fibers in the matrix material. It is somewhat surprising that the curves presented in these figures do not differ drastically. This matter seems to be paradoxical at the first sight as the curves correspond to different values of the crack length. However, one has to take into account that curves presented in the same figure correspond to the common weight or material volume v. Fig. 4.15, 4.19 correspond to $v = 0.71$; Fig. 4.7, 4.11 to $v = 0.77$.

The variation of bending moments with the volume v is demonstrated in Fig. 4.20 and 4.21 for plates with $\alpha = 0.2$. The curves in Fig. 4.20 are obtained for $v = 0.1$ and in Fig. 4.21 for $v = 0.9$ respectively, whereas the material is a circumferentially reinforced composite. In Fig. 4.21 the material volume varies in the interval (0.65; 0.95) and in Fig. 4.20 corresponds to the interval (0.77; 0.95).

Calculations carried out show that the stress distributions are statically admissible. It can be seen from Fig. 4.21 that in plates with low material consumption (the curves corresponding to $v = 0.65$ and $v = 0.66$) bending moments are negative at each point of the plate.

4.7. Concluding remarks

Annular plates with step wise varying thickness have been studied in the case of initial impulsive loading. A method resorting to the variational methods of the theory of optimal control has been developed for minimization of maximal residual deflections of the plates among those having common weight or material volume. The plates under consideration have been made from a ductile composite reinforced in radial or circumferential direction and clamped at the inner edge whereas the outer edge is completely free. Necessary optimality conditions are presented for a general case with n steps in the thickness. Computations carried out showed that the residual deflections of circumferentially reinforced plates are less than those corresponding to the radial orientation of fibers, if the internal radius is less than half of the outer one. If $a > 0.5R$ then, via versa, the radial orientation of fibers is more preferable. When comparing deflections we assume that the plates have common material volume.

It was shown that in the case of plates with single step the residual deflection can be reduced up to two times when choosing optimal values for thickness and the location of the step. Calculations carried out showed that the efficiency of designs established depends on the material parameters and on the geometry of

the plate. The results revealed a surprising matter that the efficiency of the design quite weakly depends on the crack length. Of course, deflections of cracked plates and the ability to sustain the impulsive loading do depend on the lengths of cracks.

Acknowledgement
The support from Estonian Science Foundation through the grant № 5693 is acknowledged.

4.8. References

Bryson A, Ho Yu-Chi (1975) Applied Optimal Control. Wiley, New York
Hull DG (2003) Optimal Control Theory for Applications. Springer, Berlin Heidelberg New York
Jones N (1989) Structural Impact. Cambridge University Press, Cambridge
Jones N, Kim SB, Li OM (1997) Response and failure of ductile circular plates struck by a mass. Trans. ASME, 119, 332–342
Kaliszky S (1989) Plasticity. Theory and Engineering Applications. Elsevier, Amsterdam
Lance RH, Robinson DN (1972) Limit analysis of ductile fiber-reinforced structures. Proc ASCE 98, 195–209
Lellep J, Hannus S (1995) Optimization of plastic cylindrical shells with stepwise varying thickness in the case of von Mises material 10, 122–127
Lellep J, Hein H (2002) Optimization of clamped rigid-plastic shallow shells of piece wise constant thickness. Int J Non-Linear Mech, 29, 625–636
Lellep J, Puman E (2000) Optimization of plastic conical shells loaded by a rigid central boss. Int J Solids Struct, 37, 2695–2708
Lellep J, Puman E (2001) Optimization of conical shells of Mises material. Struct Multidisc Optim, 22, 149–156
Lellep J, Tungel E (2005) Optimization of plastic spherical shells of von Mises material. Struct Multidisc Optim 30, 381–387
Lepik Ü (1982) Optimal Design of Inelastic Sructures under Dynamic Loading. Valgus, Tallinn (in Russian)
Li QM, Jones N (1994) Blast loading of fully clamped circular plates with transverse shear effects. Int J Solids Struct 31, 1861–1876
Liu D, Stronge W (1996) Shear and bending deformations of rigid-plastic circular plates by central pressure pulse. Int J Impact Eng, 18, 383–402
Ma G, Iwasaki Shoji, Miyamoto Y, Deto H (1999) Dynamic plastic behaviour of circular plate using unified yield criterion. Int J Solids Struct, 36, 3257–3275
Martin JB, Symonds PS (1966) Mode approximation for impulsively loaded rigid-plastic structures. Proc ASCE EM92, 43–66
Pinch E (1993) Optimal Control and the Calculus of Variations. Oxford Univ. Press, Oxford
Sage AP, White CC (1977) Optimum Systems Control. Prentice Hall, New Jersey
Shen WQ, Jones N (1993) Dynamic response and failure of fully clamped circular plates under impulsive loading. Int J Impact Eng, 13, 259–278

Stronge WJ, Yu TX (1993) Dynamic Models for Structural Plasticity. Springer, New York
Wang Y, Yu M, Xiao Y, Li L (2005) Dynamic plastic response of a circular plate based on unified strength theory. Int J Impact Eng, 31, 25–40
Wen HM, Yu TX, Reddy TY (1995) A note on circular clamped plates under impulsive loading. Mech Struct Mach, 23, 331–342
Yu TX, Chen FL (1998) Failure modes and criteria of plastic structures under intense dynamic loading: a review. Metals and Materials, 4, 219–226

5. INELASTIC BEHAVIOUR OF STEPPED SQUARE PLATES

J. Lellep and A. Mürk

Institute of Applied Mathematics, Tartu University
2 Liivi str., Tartu, Estonia

ABSTRACT

The plastic behaviour of square plates subjected to initial impulsive loading is studied. The plates under consideration have piece wise constant thickness and the material obeys Johansen's yield condition. An approximate method of mode form motions resorting to the energy balance is used in order to predict maximal residual transverse deflections. According to this concept the initial kinetic energy is assumed to be given whereas the motion of the plate is due to inertia.

5.1. INTRODUCTION

The most of the work in dynamic plasticity is dedicated to the dynamic behaviour of beams and axisymmetric plates (see Jones, 1989; Yu and Chen, 2000; Stronge, 1993). The only exact theoretical solution on dynamic response of a non- axisymmetric plastic plate is obtained by Cox and Morland (1959).

In the present paper the method of mode form motions is used in the case of small deflections of stepped square plates subjected to impulsive loadings.

5.2. FORMULATION OF THE PROBLEM AND GOVERENING EQUATIONS

Consider a square plate with a side length *2L* (Fig. 5.1). The plates with and without cutout will be studied. It is assumed that the plate is subjected to the initial impact loading. We assume that the initial kinetic energy K_0 is given whereas the initial transverse velocity field may be unknown. The dynamic response of the plate will be studied within the concept of a rigid- plastic body.

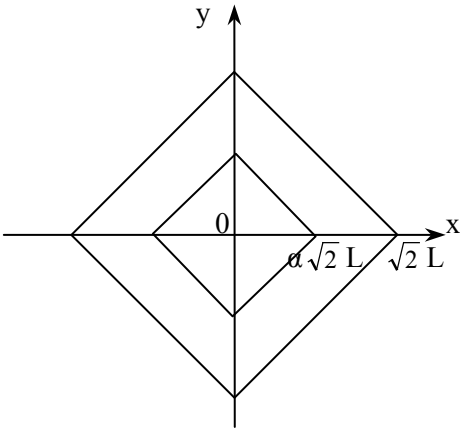

Fig. 5.1. Square plate

Let the plate thickness be piece wise constant, e.g.

$$h = h_j \tag{1}$$

for $(x, y) \in D_j$; $j = 0,...,n$. We restrict our attention to the concentric case when the inner and outer boundaries of regions D_j are squares. Let the boundaries of regions of constant thickness intersect *x*- and *y*- axis at points $\alpha_0\sqrt{2}L$, $\alpha_1\sqrt{2}L$,..., $\alpha_{n+1}\sqrt{2}L$. Here

$$\alpha_0 = \frac{a}{L}, \quad \alpha_{n+1} = 1, \tag{2}$$

provided *2a* is the length on the internal edge of the plate. Note that in the case of a full plate without cutout $\alpha_0 = a = 0$.

It is assumed that the initial kinetic energy is high enough to cause plastic strains. Moreover, we assume that elastic stains are small in comparison with plastic strains so that elastic counterparts of strains can be neglected. The material of plates is an isotropic homogeneous material which can be treated as an ideal plastic material obeying Johansen's yield condition (Fig. 5.2). Here M_1, M_2 stand for the principal moments

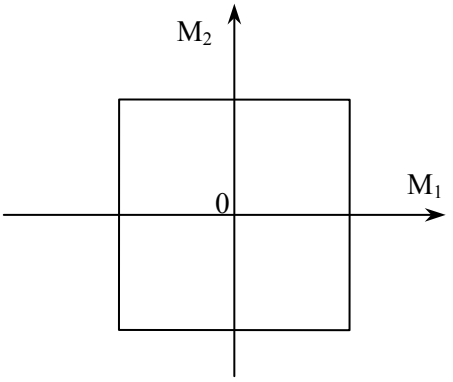

Fig. 5.2. Johansen's yield condition

The equation of motion can be presented as

$$\frac{\partial^2 M_x}{\partial x^2} + 2\frac{\partial^2 M_{xy}}{\partial x \partial y} + \frac{\partial^2 M_y}{\partial y^2} = \mu\, h \frac{\partial^2 W}{\partial t^2}. \tag{3}$$

The curvatures corresponding to (5) have the form

$$\kappa_x = -\frac{\partial^2 W}{\partial x^2}, \kappa_y = -\frac{\partial^2 W}{\partial y^2}, \kappa_{xy} = -\frac{\partial^2 W}{\partial x \partial y}. \tag{4}$$

It is reasonable to assume that the deformation process is symmetrical with respect to coordinate axis. Thus we can restrict our attention to the first quadrant only. Following Cox and Morland (1959) we introduce a new variable

$$z = \frac{1}{\sqrt{2}L}(x + y). \tag{5}$$

Evidently, in the first quadrant $0 \le z \le 1$. The method of mode form motions will be used in the present paper. This method was suggested by Martin and Symonds (1966). It was established that the approximate theoretical predictions are in good correlation with exact solutions and experimental results.

Perhaps the simplest kinematically admissible transverse velocity distribution is

$$\frac{\partial W}{\partial t} = V(t)\frac{1-z}{1-\alpha} \tag{6}$$

for a plate with cutout. If there is no cutout one can take $\alpha = 0$. Here $V(t)$ stands for an unknown function of time.

5.3. DETERMINATION OF THE ACCELERATION

Substituting (1) and (6) in (3) leads to the equation

$$\frac{\partial^2 M_x}{\partial x^2} + 2\frac{\partial^2 M_{xy}}{\partial x \partial y} + \frac{\partial^2 M_y}{\partial y^2} = \frac{\mu\, h_j \dot{V}}{1-\alpha}(1-z) \tag{7}$$

which holds good in the region D_j ($j = 0,...,n$). Let us interpret D_j as the region in the first quadrant where $z \in (\alpha_j, \alpha_{j+1})$.

In (7) $\dot{V}$ stands for the acceleration of the free edge of the plate ($z = \alpha$) or of the central point of the plate ($z = 0$) in the case of the plate without cutout. It is assumed herein that the outer edge of the plate is simply supported or clamped whereas the inner edge is free (in the case of the plate with cutout).

Boundary conditions at the edge can be obtained from the relation for the moment with respect to an inclined edge Cox and Morland (1959)

$$M_n = M_x \sin^2\beta + M_y \cos^2\beta + M_{xy} \sin 2\beta \tag{8}$$

where β stands for the angle of inclination with respect to the *x*-axis. Similar relation can be derived for the shear force as well

$$Q_n = Q_x \sin\beta + Q_y \cos\beta \tag{9}$$

We are looking for the solution of (7) in the form

$$\begin{aligned} M_x &= M_j + x^2 F_j(z) \\ M_y &= M_j + y^2 F_j(z) \\ M_{xy} &= xy F_j(z) \end{aligned} \tag{10}$$

for $(x, y) \in D_j$ ($j = 0,...,n$).

Here M_j stands for the limit moment for the part D_j of the plate. Thus $M_j = \sigma_0 h_j^2 / 4$, σ_0 being the yield stress of the material. Functions F_j ($j = 0,...,n$) in (10) are unknown functions of *z* which have to be defined so that the equation (7) is satisfied in each region D_j ($j = 0,...,n$).

Substituting (10) in (7) gives after appropriate transformations

$$z^2 \frac{\partial^2 F_j}{\partial z^2} + 6z\frac{\partial^2 F_j}{\partial z} + 6F_j = \frac{\mu\, h_j \dot{V}(t)}{1-\alpha}(1-z) \tag{11}$$

for $z \in D_j$ ($j = 0,...,n$). The equation (13) has a solution

$$F_j = \frac{\mu h_j \dot{V}}{12(1-\alpha)}(2-z) + \frac{B_j}{z^2} + \frac{C_j}{z^3} \tag{12}$$

B_j and C_j being arbitrary constants.

Consider the plate with clamped outer edge and free inner edge in a greater detail. At the outer edge one has $M_n\big|_1 = -M_n$ whereas at the free edge $M_n\big|_\alpha = 0$, $Q_n\big|_\alpha = 0$. Thus according to (8) - (10) boundary conditions can be presented as

$$\begin{aligned} F_0(\alpha) &= -\frac{M_0}{\alpha^2 L^2}, \\ F_0'(\alpha) &= \frac{3M_0}{\alpha^3 L^2}. \end{aligned} \tag{13}$$

At the outer edge one has

$$F_n(1) = -\frac{2M_n}{L^2} \tag{14}$$

Due to the continuity of M_n and Q_n at $z = \alpha_j$ ($j = 0,...,n$) following requirements must be met by the set functions F_j

$$\begin{aligned} F_j(\alpha_{j+1} - 0) &= F_{j+1}(\alpha_{j+1} + 0) + \frac{M_{j+1} - M_j}{\alpha_j{}^2 L^2}, \\ F_j'(\alpha_{j+1} - 0) &= F_{j+1}'(\alpha_{j+1} + 0) - 3\frac{M_{j+1} - M_j}{\alpha_j{}^3 L^2}. \end{aligned} \tag{15}$$

For determination of *2n+3* unknown constants B_j, C_j ($j = 1,...,n$) and $\dot{V}$ one has *2n+3* requirements which are given by (13) – (15). The solution of the non- linear system (13)–(15) in general case is quite complicated.

However, in the particular case when *n=1* the system takes the form

$$\frac{\mu h_0\dot{V}}{12(1-\alpha)}(2-\alpha)+\frac{B_0}{\alpha^2}+\frac{C_0}{\alpha^3}=-\frac{M_0}{\alpha^2L^2},$$
$$\frac{\mu h_0\dot{V}}{12(1-\alpha)}+\frac{2B_0}{\alpha^3}+\frac{3C_0}{\alpha^4}=-\frac{3M_0}{\alpha^3L^2},$$
$$\frac{\mu h_1\dot{V}}{12(1-\alpha)}+B_1+C_1=-\frac{2M_1}{L^2}, \tag{16}$$
$$\frac{\mu h_0\dot{V}}{12(1-\alpha)}(2-\theta)+\frac{B_0}{\theta^2}+\frac{C_0}{\theta^3}=\frac{\mu h_1\dot{V}}{12(1-\alpha)}(2-\theta)+\frac{B_1}{\theta^2}+\frac{C_1}{\theta^3},$$
$$\frac{\mu h_0\dot{V}}{12(1-\alpha)}+\frac{2B_0}{\theta^3}+\frac{C_0}{\theta^4}=\frac{\mu h_1\dot{V}}{12(1-\alpha)}+\frac{2B_1}{\theta^3}+\frac{3C_1}{\theta^4}.$$

In (16) the notation $\theta=\alpha_1$ is used. From (16) one readily obtains that

$$\dot{V}=\frac{12(1-\alpha)\left[M_0(\alpha-\theta)+M_1(\theta-2)\right]}{\mu L^2\left[(h_0-h_1)\left(3\theta^4-8\theta^3+6\theta^2\right)-h_0\left(3\alpha^4-8\alpha^3+6\alpha^2\right)+h_1\right]} \tag{17}$$

5.4. RESIDUAL DEFLECTIONS

As it might be expected the acceleration of the free edge is a constant (see (17)). Thus one can easily integrate the acceleration which gives

$$\dot{W}(\alpha)=V(t)=\dot{V}t+V_0. \tag{18}$$

Integrating once more one obtains

$$W(\alpha,t)=\frac{\dot{V}}{2}t^2+V_0t \tag{19}$$

when deriving (18) and (19) initial conditions $\dot{W}(\alpha,0)=V_0$, $W(\alpha,0)=0$ have been taken into account.

It follows from (18) that the motion ceases at the moment

$$t_1=-\frac{V_0}{\dot{V}} \tag{20}$$

and the maximal residual deflection is

$$W_1=W(\alpha,t_1)=-\frac{V_0^2}{2\dot{V}}. \tag{21}$$

Note that we are employing the method of mode form motions. Thus the velocity distribution (6) holds good at each moment of time during the motion

of the plate. Therefore, the initial kinetic energy of a plate with a single step can be calculated as

$$K_0 = \frac{2\mu V}{(1-\alpha)^2}\left\{ \int_0^{\sqrt{2}\alpha L} dx \int_{-x+\sqrt{2}\alpha L}^{-x+\sqrt{2}\theta L} h_0 (1-z)^2\, dy + \int_{\sqrt{2}\alpha L}^{\sqrt{2}\theta L} dx \int_0^{-x+\sqrt{2}\theta L} h_0 (1-z)^2\, dy + \right.$$

$$\left. + \int_0^{\sqrt{2}\theta L} dx \int_{-x+\sqrt{2}\theta L}^{-x+\sqrt{2}L} h_1 (1-z)^2\, dy + \int_{\sqrt{2}\theta L}^{\sqrt{2}L} dx \int_0^{-x+\sqrt{2}L} h_1 (1-z)^2\, dy \right\}. \tag{22}$$

If the number of steps in the thickness exceeds unity the relation (22) must be accommodated appropriately. It easily follows from (22) that the initial velocity can be presented as

$$V_0^2 = \frac{12 K_0 (1-\alpha)^2}{4\mu L^2 \left\{ (h_1 - h_0)(1-\theta)^3 (3\theta+1) + h_0 (1-\alpha)^3 (3\alpha+1) \right\}}. \tag{23}$$

Substituting (17) and (23) in (21) leads to the maximal residual displacement

$$W_1 = \frac{K_0 (1-\alpha)}{8\left[M_0 (\theta-\alpha) + M_1 (2-\theta) \right]}. \tag{24}$$

It follows from (24) that in the case of a plate of constant thickness h_* the maximal deflection is

$$W_1 = \frac{K_0 (1-\alpha)}{8 M_* (2-\alpha)}.$$

Here M_* stands for the limit moment of the plate of constant thickness h_*, e.g. $M_* = \sigma_0 h_*^2 / 4$.

5.5. NUMERICAL RESULTS

Maximal residual deflections for plates with a single step are depicted in Fig. 5.3- 5.5. The results presented in Fig. 5.3 correspond to plates simply supported at the edge whereas Fig. 5.4 is associated with the clamped plates.

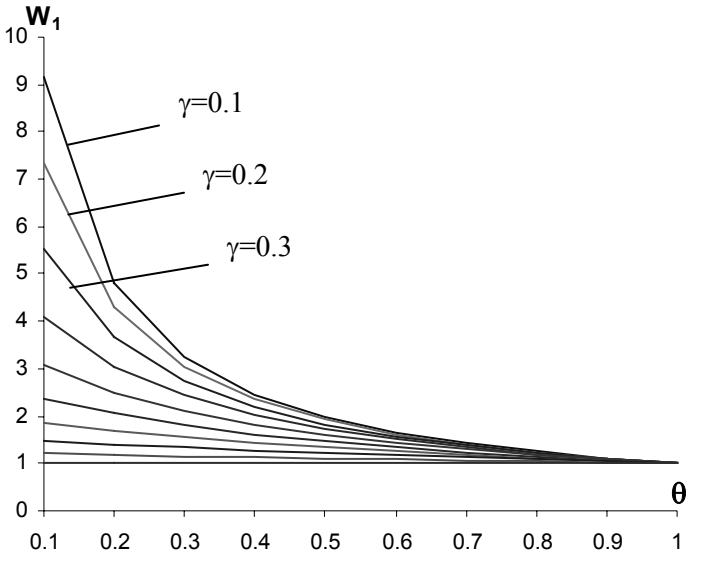

Fig. 5.3. Maximal deflections of a simply supported plate

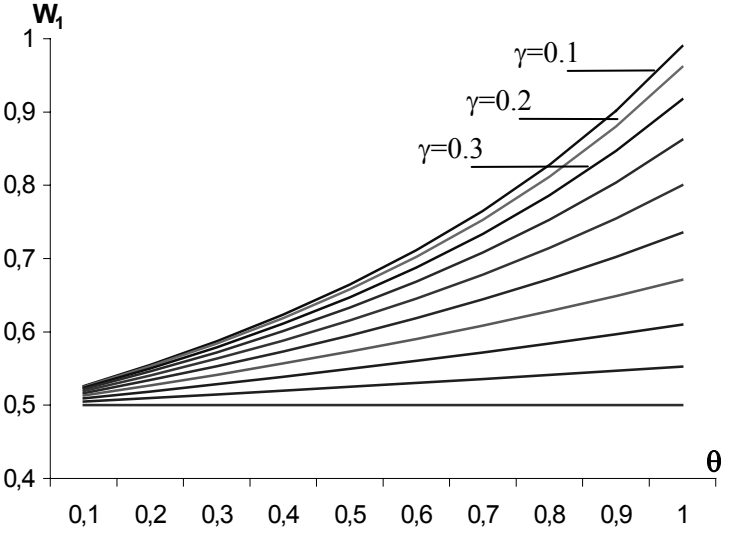

Fig. 5.4. Deflections of a clamped plate

The results of Fig. 5.5 are obtained for clamped plates with cutout. In the latter case the transverse deflection attains its maximal value at the internal edge of the plate.

It can be seen from Fig. 5.3- 5.5 that the maximal residual deflection tends to that of the reference plate of constant thickness when the step tends to the outer edge (Fig. 5.3) or to the center of the plate (Fig. 5.4) or to the inner edge of the plate (Fig. 5.5)

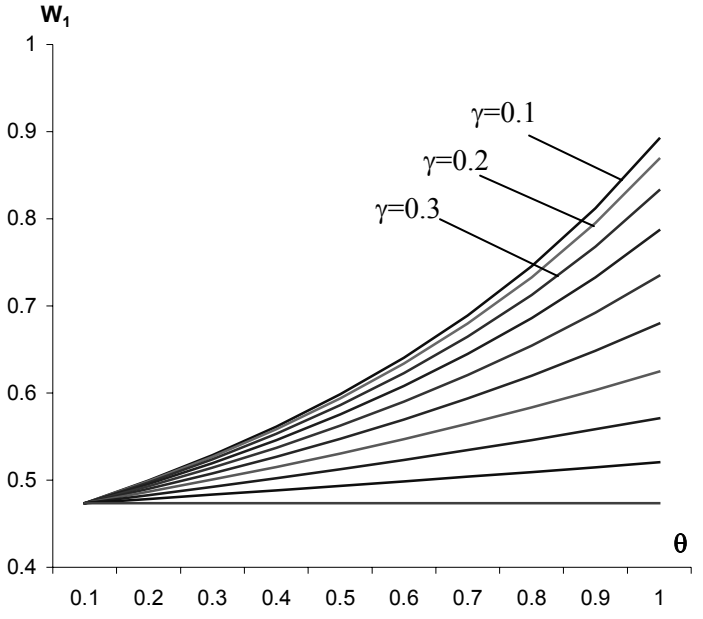

Fig. 5.5. Deflections of a plate with cutout

5.6. CONCLUDING REMARKS

A method for prediction of the behaviour of rigid- plastic square plates under initial impulsive loading has been developed. The plates under consideration have piece wise constant thickness and obey Johansen's yield condition.

Numerical analysis showed that the method of mode form motions leads to results which are close to the exact solution in case of plates of constant thickness. The statical admissibility of solutions for stepped plates was established numerically.

5.7. REFERENCES

1. Cox AD, Morland LM (1959) Dynamic plastic deformations of simply supported square plates. J Mech Phys Solids, 7, 229–241
2. Jones N (1989) Structural Impact. Cambridge University Press, 1989
3. Stronge W, Yu TX (1993) Dynamic Models of Structural Plasticity. Springer, New York London
4. Yu TX, Chen FL (2000) Failure of plastic structures under intense dynamic loading: modes criteria and thresholds. Int J Mech Sci, 42, 1537–1554

6. OPTIMIZATION OF INELASTIC SQUARE PLATES WITH CRACKS

J. Lellep, A. Mürk
Institute of Applied Mathematics, University of Tartu,
Tartu 50409, Estonia
Telephone: +372 737 5868
Fax: +372 737 5862
E-mail addresses: jaan.lellep@ut.ee, annely.murk@ut.ee

Abstract

Problems of optimization of inelastic square plates are studied in the case of the material obeying Johansen's yield condition. The plates under consideration are subjected to initial impulsive loading and have piece wise constant thickness. Edges of the plate can be both, simply supported or clamped. It is assumed that the plates have cracks at the re-entrant corners of steps. Maximal residual transverse deflections are predicted by the approximate method of mode form motions resorting to the energy balance. According to this concept the initial kinetic energy which is absorbed during plastic deformations is assumed to be given whereas the motion of the plate is due to inertia. An optimal design which corresponds to the minimum of residual deflections is developed for given material consumption.

Keywords: Rectangular plate. Impulsive loading. Inelastic material. Optimization. Crack

.

6.1. Introduction

There is a quite rich literature on the dynamic plasticity of structural elements. Various authors have studied the dynamic behaviour of beams and axisymmetric plates (see Jones, 1989; Yu and Chen, 1992, 2000; Stronge, 1993). However, the only exact theoretical solution on dynamic response of a non-axisymmetric plastic plate is obtained by Cox and Morland (1959) who investigated within the framework of thin plate theory the behaviour of square plates subjected to rectangular pressure pulse.

Several authors (among these Cox and Morland) have studied square plates of constant thickness made of a Johansen's material. Blast loaded square plates are investigated by Olson et. al (1993). Approximate techniques are presented by Baker (1975). Zhu (1996) obtained both, theoretical numerical predictions and experimental results for transient deformation modes of square plates

subjected to explosive loadings. Numerical predictions showed a good agreement with experimental results.

The phenomenon of saturated impulse in elastic- plastic square plates is studied by Zhu and Yu (1997) in the case of a fully clamped plate.

Approximate procedures for investigation of rigid- plastic rectangular plates subjected to dynamic loadings are developed by Jones et. al (1970, 1971), Yu and Chen (1992). Theoretical predictions suggested by Jones (1970, 1971) and Symonds (1980, 1982) give surprisingly good agreement with corresponding experimental results.

Lellep and Mürk (2003, 2004) used this approach for determination of residual deflections of stepped annular and square plates subjected to impulsive loadings.

Inelastic behaviour and optimal design of beams, plates and shells was investigated by Lepik (1982) in the case of dynamic loading. Various approaches to the optimization of thin-walled structures are discussed in review by Kruzelecki and Życzkowski (1985), Lellep and Lepik (1984), Życzkowski (1992). In the work by Lepik (1982) also by Lellep and Hein (2002) methods on non-linear programming have been used for optimal design of structures of piece wise constant thickness in the case of initial impulsive loading.

An alternative approach which is based on variational methods of the theory of optimal control was suggested for optimization of shells under quasistatic loading by Lellep and Puman (2001), Lellep and Tungel (2005).

In the present paper an attempt is made to accommodate the programming approach to inelastic stepped plates which have cracks emanating from the plate at corners of steps.

6.2. Formulation of the problem

Let us consider a square plate with a side length *2L* (Fig. 6.1). The plates under consideration are subjected to the initial impact loading. We assume that the initial kinetic energy K_0 is given whereas the initial transverse velocity field may be unknown. The dynamic response of the plate will be studied within the concept of a rigid- plastic body.

We are considering plates with thickness, e.g.

$$h = h_j \tag{1}$$

for $(x, y) \in D_j$; $j = 0,...,n$. We restrict our attention to the concentric case when the inner and outer boundaries of regions D_j are squares. Let the boundaries of regions of constant thickness intersect *x*- and *y*- axis at points 0, $\alpha_1\sqrt{2}L,\ldots,\ \alpha_n\sqrt{2}L,\ \sqrt{2}L$. Here $\alpha_0 = 0$, $\alpha_{n+1} = 1$.

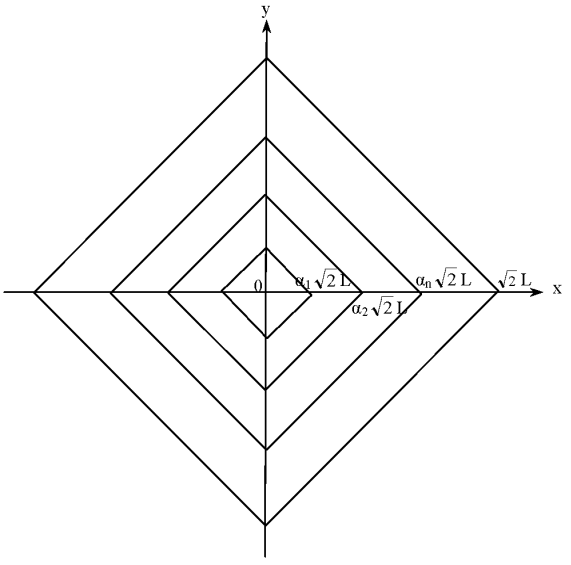

Figure 6.1. Square plate

The plate under consideration has cracks at re-entrant corners of steps. Let c_j be the length (deepness) of the straight crack located at the inner boundary of the region D_j. We assume that the cracks are stable part trough surface cracks. The development and propagation of cracks is not studied in the current paper.

The material volume of the plate is

$$V = 4L^2 \sum_{j=0}^{n} h_j \left(\alpha_{j+1}^2 - \alpha_j^2 \right) \tag{2}$$

We are looking for the design of the plate for which the maximal residual deflection W_1 attains its minimal value for fixed weight or material volume (2) of the plate.

6.3. Basic equations and hypotheses

It is assumed that elastic strains are small in comparison with plastic ones so that elastic counterparts of strains can be neglected. The material of plates is an isotropic homogeneous material which can be treated as an ideal plastic material

obeying Johansen's yield condition (Fig. 6.2). Here M_1, M_2 stand for the principal moments which are coupled with moments M_x, M_y by relations

$$M_1 = \frac{1}{2}\left[M_x + M_y + \sqrt{\left(M_x - M_y\right)^2 + 4M_{xy}^2} \right],$$
$$M_2 = \frac{1}{2}\left[M_x + M_y - \sqrt{\left(M_x - M_y\right)^2 + 4M_{xy}^2} \right]. \tag{3}$$

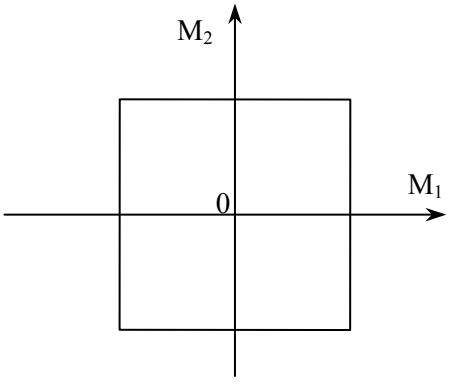

Figure 6.2. Johansen's yield condition

The moments M_x, M_y, M_{xy} with shear forces Q_x, Q_y have to satisfy equilibrium equations (2), (3)

$$\frac{\partial Q_x}{\partial x} + \frac{\partial Q_y}{\partial y} + p = \mu h \frac{\partial^2 W}{\partial t^2}$$
$$\frac{\partial M_x}{\partial x} + \frac{\partial M_{xy}}{\partial y} - Q_x = 0 \tag{4}$$
$$\frac{\partial M_y}{\partial y} + \frac{\partial M_{xy}}{\partial x} - Q_y = 0$$

Here μ stands for the material density, p is the intensity of transverse loading and W is the transverse deflection. Since we consider the motion of the plate due to inertia we can take $p = 0$. Eliminating shear forces Q_x, Q_y from (4) one obtains a single equation

$$\frac{\partial^2 M_x}{\partial x^2} + 2\frac{\partial^2 M_{xy}}{\partial x \partial y} + \frac{\partial^2 M_y}{\partial y^2} = \mu h \frac{\partial^2 W}{\partial t^2} \tag{5}$$

It is well known that the curvatures corresponding to (5) have the form

$$\kappa_x = -\frac{\partial^2 W}{\partial x^2},\ \kappa_y = -\frac{\partial^2 W}{\partial y^2},\ \kappa_{xy} = -\frac{\partial^2 W}{\partial x \partial y} \tag{6}$$

We assume that the deformation process is symmetrical with respect to coordinate axis. Thus we can restrict our attention to the first quadrant only. Following Cox and Morland (1959) we introduce a new variable

$$z = \frac{1}{\sqrt{2}L}(x + y) \tag{7}$$

Evidently, in the first quadrant $0 \le z \le 1$. The method of mode form motions will be used in the present paper. This method was suggested by Martin and Symonds (see Symonds, 1982). It was established that the approximate theoretical predictions are in good correlation with exact solutions and experimental results (see Baker, 1975; Jones, 1989).

Perhaps the simplest kinematically admissible transverse velocity distribution is

$$\frac{\partial W}{\partial t} = \dot{W}_0(t)(1 - z) \tag{8}$$

where $W_0(t)$ stands for an unknown function of time. Evidently, $\dot{W}_0(t)$ is the transverse velocity of the central point of the plate.

6.4. Integration of governing equations

Substituting (1) and (8) in (5) leads to the equation

$$\frac{\partial^2 M_x}{\partial x^2} + 2\frac{\partial^2 M_{xy}}{\partial x \partial y} + \frac{\partial^2 M_y}{\partial y^2} = \mu\, h_j \ddot{W}_0(1 - z) \tag{9}$$

which holds good in the region D_j ($j = 0,...,n$). Let us interpret D_j as the region in the first quadrant where $z \in (\alpha_j, \alpha_{j+1})$.

In (9) $\ddot{W}_0$ stands for the acceleration of the central point of the plate at $z = 0$. It is assumed herein that the outer edge of the plate is simply supported or clamped.

Boundary conditions at the edge can be obtained from the relation for the moment with respect to an inclined edge (see Ventsel and Krauthammer, 2001)

$$(M)_n = M_x \sin^2\beta + M_y \cos^2\beta + M_{xy} \sin 2\beta$$

where β stands for the angle of inclination with respect to the *x*-axis. In the case of a square plate $\beta = \pi/4$. Therefore the last relation takes the form

$$(M)_n = \frac{1}{2}(M_x + M_y)^2 + M_{xy}. \tag{10}$$

Similarly, for the shear force one has (Ventsel and Kraufthammer, 2001)

$$(Q)_n = Q_x \sin\beta + Q_y \cos\beta$$

or

$$(Q)_n = \frac{1}{\sqrt{2}}(Q_x + Q_y). \tag{11}$$

We are looking for the solution of (9) in the form

$$\begin{aligned} M_x &= M_j + x^2 F_j(z), \\ M_y &= M_j + y^2 F_j(z), \\ M_{xy} &= xyF_j(z), \end{aligned} \tag{12}$$

for $(x, y) \in D_j$ ($j = 0,...,n$).

Here M_j stands for the limit moment for the part D_j of the plate. Thus $M_j = \sigma_0 h_j^2 / 4$, σ_0 being the yield stress of the material. Functions F_j ($j = 0,...,n$) in (12) are unknown functions of *z* which have to be defined so that the equation (9) is satisfied in each region D_j ($j = 0,...,n$).

Consider now sections of the plate parallel to the edge $z = 1$ in the region $z \in D_j$. The shear forces acting on these planes can be presented by (11) or making use of (4) as

$$(Q)_n = \frac{1}{\sqrt{2}}\left(\frac{\partial M_x}{\partial x} + \frac{\partial M_{xy}}{\partial y} + \frac{\partial M_y}{\partial y} + \frac{\partial M_{xy}}{\partial x}\right). \tag{13}$$

Substituting bending moments M_x, M_y, M_{xy} from (12) into (13) one has

$$(Q)_n = Lz(3F_j + zF_j') \tag{14}$$

for $(x, y) \in D_j$, or $z \in (\alpha_j, \alpha_{j+1})$; $j = 0,...,n$. Here and henceforth prims denote the differentiation with respect to the variable z.

Similarly, substituting (12) into (10) yields for $(x, y) \in D_j$ ($j = 0,...,n$)

$$(M)_n = M_j + L^2 z^2 F_j(z). \tag{15}$$

Consider now the edge $z = 1$. In the case of the simply supported edge $(M)_n\big|_{z=1} = 0$. Bearing in mind that the edge $z = 1$ belongs to the region D_n one immediately obtains from (15) that

$$F_n(1) = -\frac{M_n}{L^2}. \tag{16}$$

In the case of the clamped edge $(M)_n\big|_{z=1} = -M_n$ and thus

$$F_n(1) = -\frac{2M_n}{L^2}. \tag{17}$$

From mechanical considerations it is evident that $(M)_n$ and $(Q)_n$ are continuous when crossing the lines $z = \alpha_j$ ($j = 1,...,n$). Continuity of $(M)_n$ yields

$$M_{j-1} + L^2\alpha_j^2 F_{j-1}(\alpha_j -) = M_j + L^2\alpha_j^2 F_j(\alpha_j +)$$

and

$$F_j(\alpha_j + 0) - F_{j-1}(\alpha_j - 0) = \frac{M_{j-1} - M_j}{L^2\alpha_j^2} \tag{18}$$

for each $j = 1,...,n$.

The continuity of the shear force $(Q)_n$ at $z = \alpha_j$ yields

$$F_j'(\alpha_j + 0) - F_{j-1}'(\alpha_j - 0) = \frac{3}{L^2\alpha_j^3}(M_j - M_{j-1}) \tag{19}$$

for each $j = 1,...,n$.

When looking for the optimal design of the simply supported plate it is reasonable to assume that

$$h_j > h_{j+1}$$

for each $j = 0,...,n-1$.

We have to check if the stress is statically admissible at each point of the plate. Since at $z = \alpha_j$ a crack with maximal deepness c_j is located the maximal bending moment sustained by the plate is $\nu_j M_j$ where

$$\nu_j = \left(1 - \frac{c_j}{h_j}\right)^2.$$

Thus at $z = \alpha_j$ we have to check if the inequality

$$(M)_n\big|_{z=\alpha_j} \le M_j \tag{20}$$

is satisfied for each $j = 1,...,n$.

Substituting (12) in (9) gives after appropriate transformations

$$z^2\frac{d^2F_j}{dz^2} + 6z\frac{dF_j}{dz} + 6F_j = \mu\, h_j\ddot{W}_0(t)(1-z) \tag{21}$$

for $z \in D_j$ ($j = 0,...,n$).

The equation (21) can be solved with the aid of transform $z = e^s$. In this case

$$\frac{\partial}{\partial z} = e^s \frac{\partial}{\partial s},$$

$$\frac{\partial^2}{\partial z^2} = e^{-2s}\left(\frac{\partial^2}{\partial s^2} - \frac{\partial}{\partial s}\right)$$

and equation (21) takes the form

$$\frac{d^2 F_j}{ds^2} + 5\frac{dF_j}{ds} + 6F_j = \mu\, h_j \ddot{W}_0\left(1 - e^s\right)$$

which has solution

$$F_j = B_j e^{-2s} + C_j e^{-3s} + \frac{1}{12}\mu\, h_j \ddot{W}_0\left(2 - e^s\right)$$

since $s = \ln z$ one has

$$F_j = \mu\, h_j \ddot{W}_0\left(2 - z\right) + \frac{B_j}{z^2} + \frac{C_j}{z^3} \tag{22}$$

where B_j and C_j being arbitrary constants.

6.5. Residual deflections

It turns out that the acceleration $\ddot{W}_0$ of the free edge is a constant. Thus one can easily integrate the acceleration which gives

$$\dot{W}_0 = \ddot{W}_0 t + \dot{W}_0(0). \tag{23}$$

Integrating once more one obtains

$$W_0(t) = \ddot{W}_0 \frac{t^2}{2} + \dot{W}_0(0)t \tag{24}$$

where initial conditions $\dot{W}_0$ and $W_0(0) = 0$ have been taken into account.

It follows from (23) that the motion ceases at the moment

$$t_1 = -\frac{\dot{W}_0(0)}{\ddot{W}_0} \tag{25}$$

and the maximal residual deflection is

$$W_1 = -\frac{\dot{W}_0^2(0)}{2\ddot{W}_0}. \tag{26}$$

Note that we are employing the method of mode form motions. Thus the velocity distribution (8) holds good at each moment of time during the motion of the plate. Therefore, the initial kinetic energy of the stepped plate with a single step can be calculated as

$$K_0 = \frac{1}{3} L^2 \mu \dot{W}_0^2(0) \left\{ \sum_{j=1}^{n} h_j \left[(\alpha_{j+1} - 1)^3 (3\alpha_{j+1} + 1) - (\alpha_{j+1} - 1)^3 (3\alpha_j + 1) \right] + \right.$$
$$\left. + h_0 \left[(\alpha_1 - 1)^3 (3\alpha_1 + 1) + 1 \right] \right\} \tag{27}$$

It immediately follows from (27) that

$$\dot{W}_0^2(0) = \frac{3K_0}{\mu L^2} \left\{ \sum_{j=1}^{n} h_j \left[(\alpha_{j+1} - 1)^3 (3\alpha_{j+1} + 1) - (\alpha_j - 1)^3 (3\alpha_j + 1) \right] + \right.$$
$$\left. + h_0 \left[(\alpha_1 - 1)^3 (3\alpha_1 + 1) + 1 \right] \right\} \tag{28}$$

For determination of residual deflections according to (26) we need the initial velocity (28) and the acceleration $\ddot{W}_0$, as well. The acceleration can be defined from boundary conditions (16) or (17) for simply supported and clamped plates, respectively, provided functions $F_j(z)$ ($j = 0,...,n$) are known. Evidently, in the central region F_0 must be finite. This yields $B_0 = C_0 = 0$ and

$$F_0 = \mu h_0 \ddot{W}_0 (2 - z). \tag{29}$$

Making use of (22) and (29) with (18), (19) one can determine step by step the arbitrary constants B_j, C_j for $j = 1,...,n$ .For instance, jump conditions (18), (19) give at $z = \alpha_j$ for a simply supported plate

$$B_1 = \frac{1}{(1 - \alpha_1)} \left\{ -\frac{1}{12} \mu \ddot{W}_0 h_1 + \frac{1}{12} \mu \ddot{W}_0 \alpha_1^3 (2 - \alpha_1)(h_1 - h_0) - \right.$$
$$\left. - \frac{1}{L^2} \left[M_0 \alpha_1 + M_1 (1 - \alpha_1) \right] \right\}, \tag{30}$$

$$C_1 = \frac{1}{(1 - \alpha_1)} \left\{ \frac{1}{12} \mu \ddot{W}_0 h_1 \alpha_1 - \frac{1}{12} \mu \ddot{W}_0 \alpha_1^3 (2 - \alpha_1)(h_1 - h_0) + \frac{M_0 \alpha_1}{L^2} \right\}.$$

If we have a plate with single step, then (22), (30) and (16) give the acceleration

$$\ddot{W}_0 = \frac{12}{\mu L^2} \frac{M_0 \alpha_1 + M_1 (1 - \alpha_1)}{\left[(h_1 - h_0)(3\alpha_1^4 - 8\alpha_1^3 + 6\alpha_1^2) - h_1 \right]} \tag{31}$$

for the simply supported plate.

In the case of a clamped plate with unique step one has

$$\ddot{W}_0 = \frac{12}{\mu L^2} \frac{M_0\alpha_1 + M_1(2-\alpha_1)}{\left[\ (h_1 - h_0)\left(3\alpha_1^4 - 8\alpha_1^3 + 6\alpha_1^2\right) - h_1\ \right]}. \tag{32}$$

Substituting (28), (31), (32) in (26) it leads to the residual deflections for simply supported and clamped plates.

The problem of optimization consists in the minimization of the final deflection under the condition that the material volume (2) is given and the stress state of the plate is statically admissible. This condition leads to inequality constraints (20) which can be taken into account with (15) and (22). Thus the problem is transformed into a problem of non-linear programming.

6.6. Numerical results

The programming problem is solved with the aid of Lagrange multipliers. The obtained system of algebraic equations is solved numerically.

Results of calculations are presented for the case of plates with single step in Fig. 6.3–6.16 and Tables 6.1–6.2.

Maximal residual deflections w_1 versus dimensionless volume v are presented in Fig. 6.3 and 6.4. Figure 6.3 corresponds to a simply supported plate and Figure 6.4 to a clamped plate. Here and in the rest illustrations

$$w_1 = \frac{8M_0W_1}{K_0}, \quad \gamma_1 = \frac{h_1}{h_0},$$

$$m_{1,2} = \frac{M_{1,2}}{M_0}, \quad v = \frac{V}{4h_0L^2}.$$

Different curves in Fig. 6.3 and 6.4 are calculated for different values of the crack parameter ν. Note that $\nu = 1$ in the case of a plate without cracks. Alternatively, if $\nu = 0$, then the crack has penetrated through the plate. It is somewhat surprising that the maximal residual deflection only slightly depends on the crack length (Fig. 6.3, 6.4). However, the existence of the solution for different values v as it can be seen from Fig. 6.3, 6.4.

Bending moment $m = (M)_n / M_0$ distributions for optimized plates are presented in Fig. 6.5–6.8. Figures 6.5, 6.6 correspond to simply supported plates and Fig. 6.7, 6.8 to clamped plates. Different curves in Fig. 6.5–6.8 are obtained for different values of the volume parameter v. Curves presented in Fig. 6.5 and Fig. 6.7 are calculated for the plates without crack (here $\nu = 1$) and Fig. 6.6 and Fig. 6.8 for $\nu = 0.7$. It can be seen from Fig. 6.5, 6.6 that the bending moment $(M)_n$ only slightly depends on the parameter v in the case of simply supported plates.

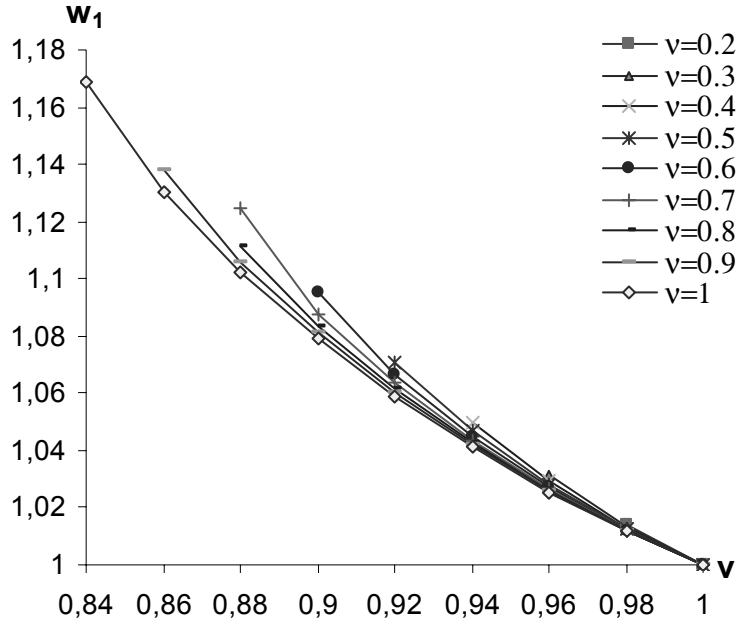

Figure 6.3. Maximal residual deflection for simply supported plate

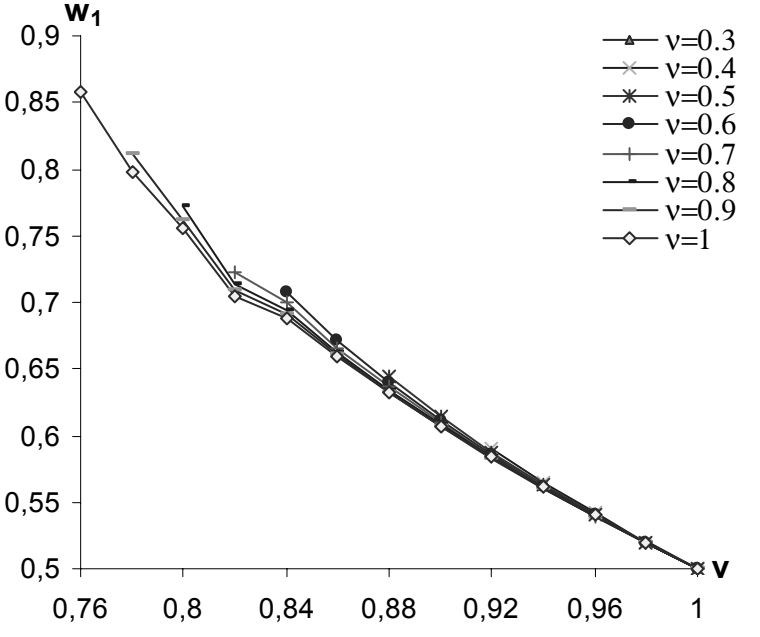

Figure 6.4. Maximal residual deflection for clamped plate

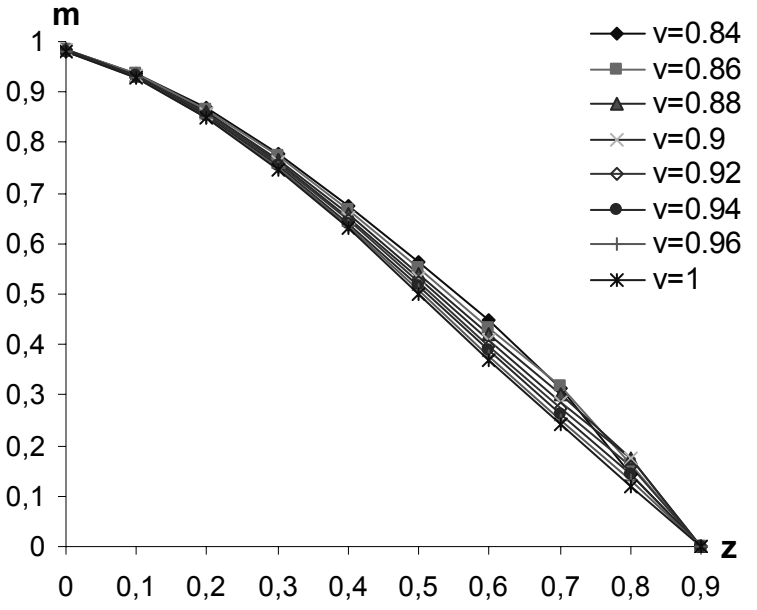

Figure 6.5. Bending moment m distribution for simply supported plates with $\nu = 1$

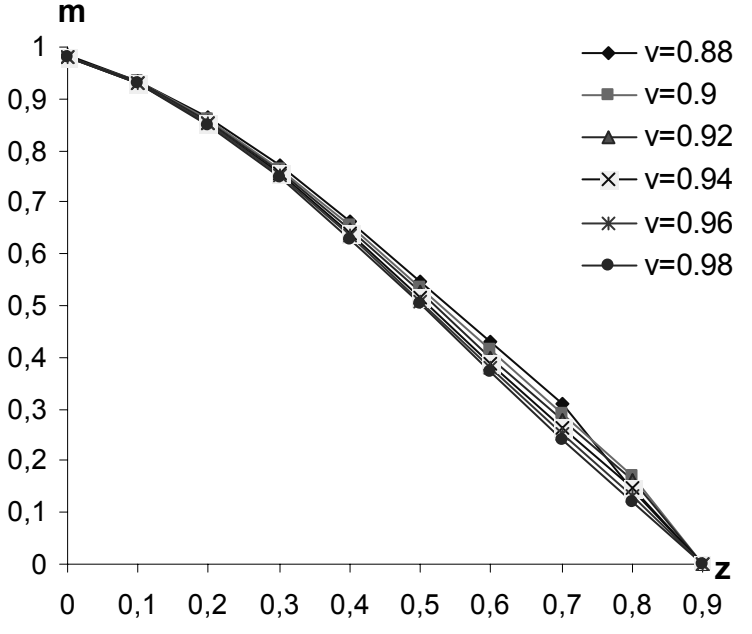

Figure 6.6. Bending moment m distribution for simply supported plates with $\nu = 0.7$

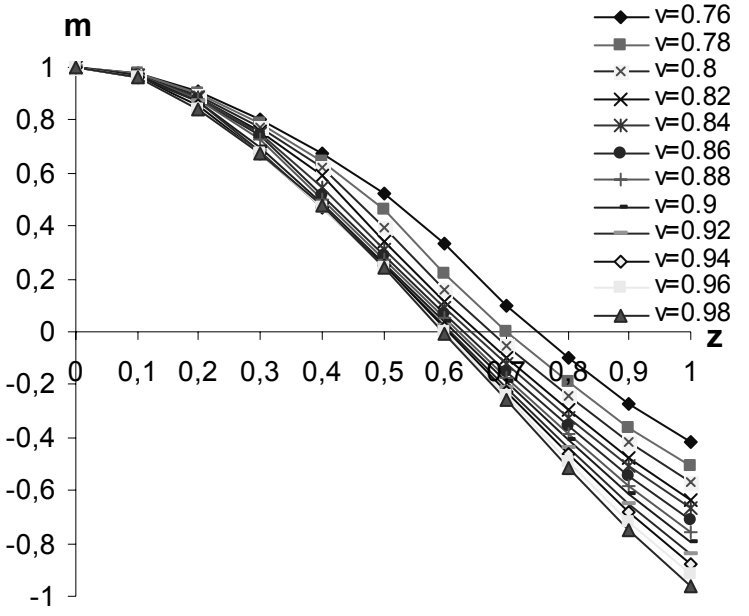

Figure 6.7. Bending moment m distribution for clamped plates with $\nu = 1$

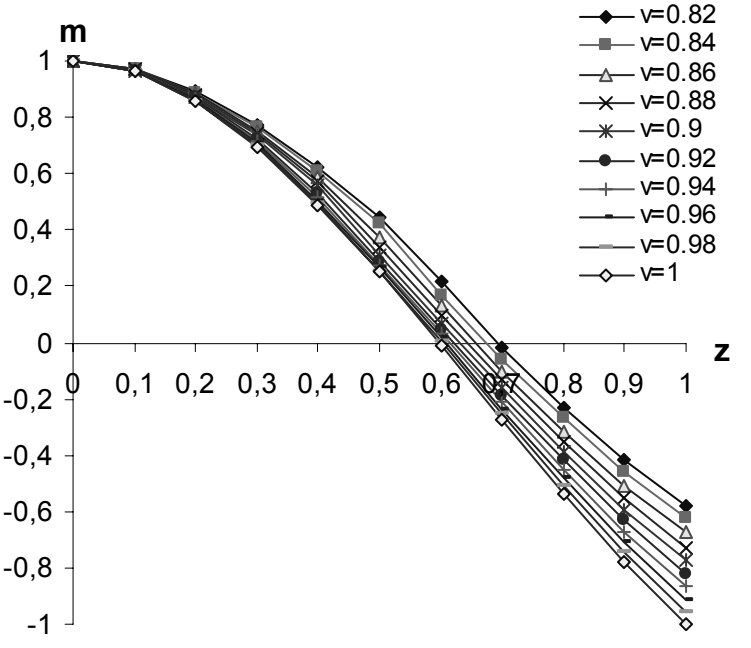

Figure 6.8. Bending moment m distribution for clamped plates with $\nu = 0.7$

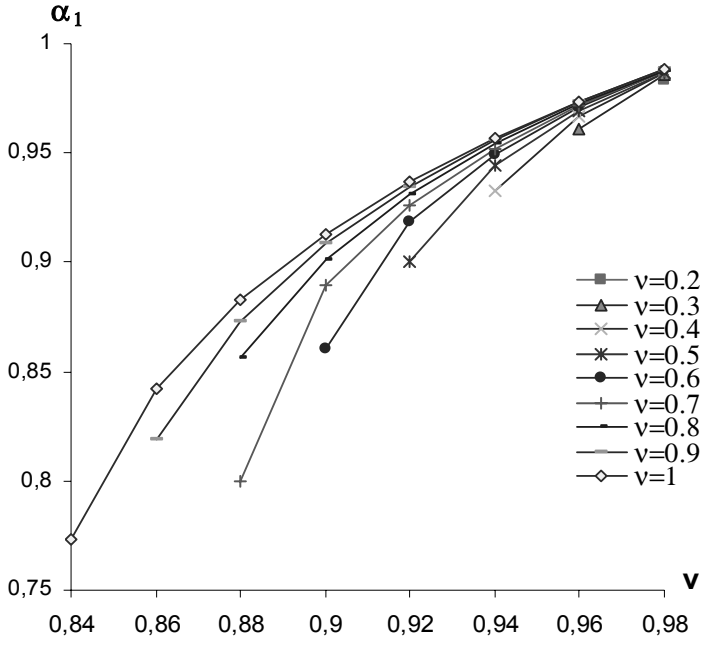

Figure 6.9. Optimal step location for simply supported plates

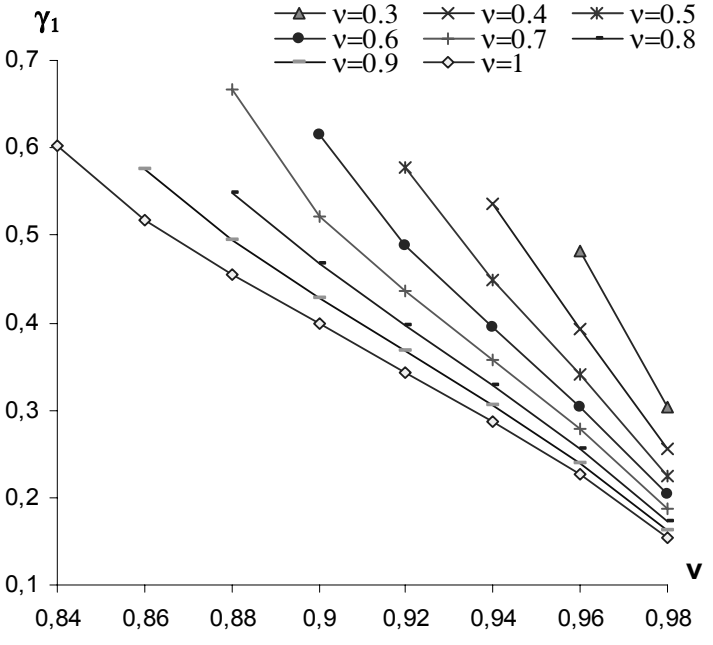

Figure 6.10. Optimal thickness for simply supported plates

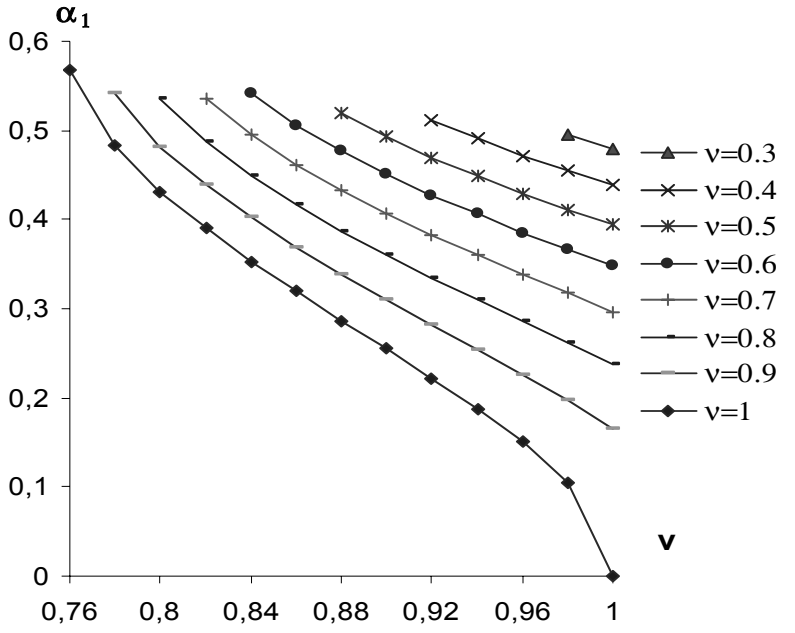

Figure 6.11. Optimal step location for clamped plates

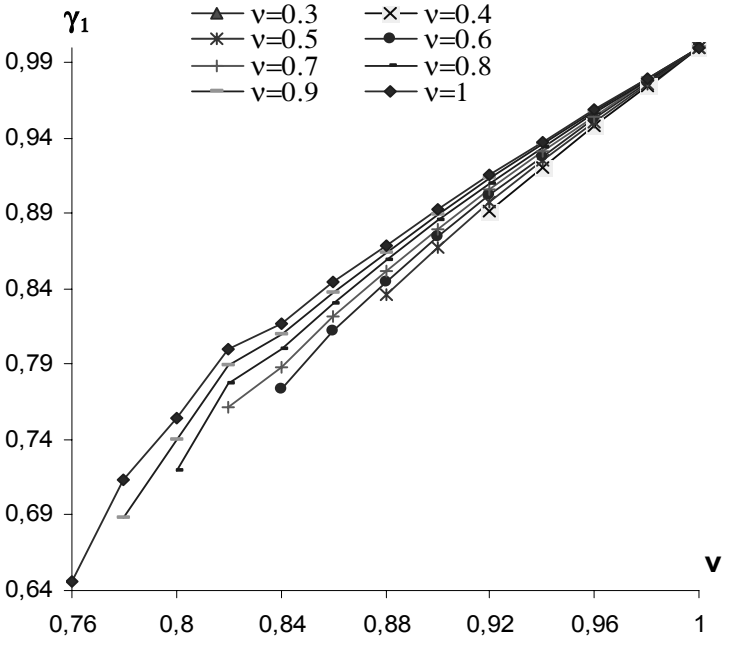

Figure 6.12. Optimal thickness for clamped plates

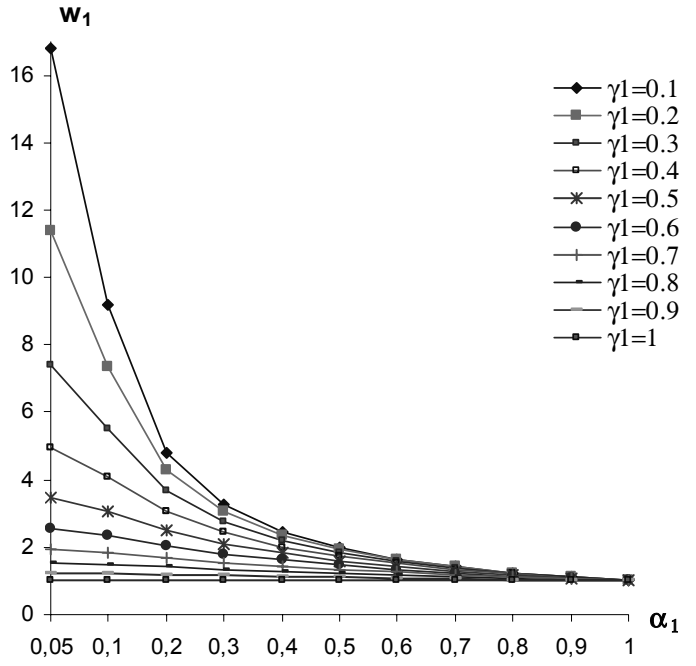

Figure 6.13. Maximal residual deflection for simply supported plates

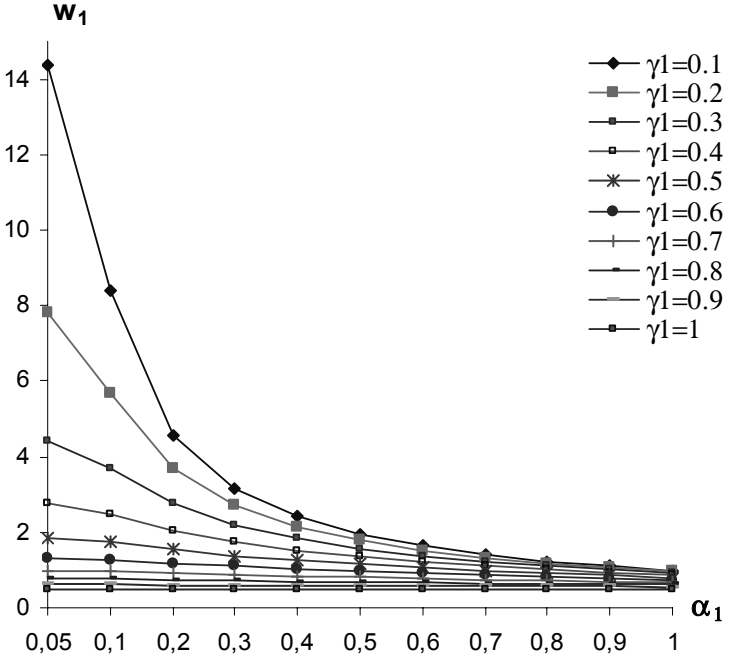

Figure 6.14. Maximal residual deflection for clamped plates

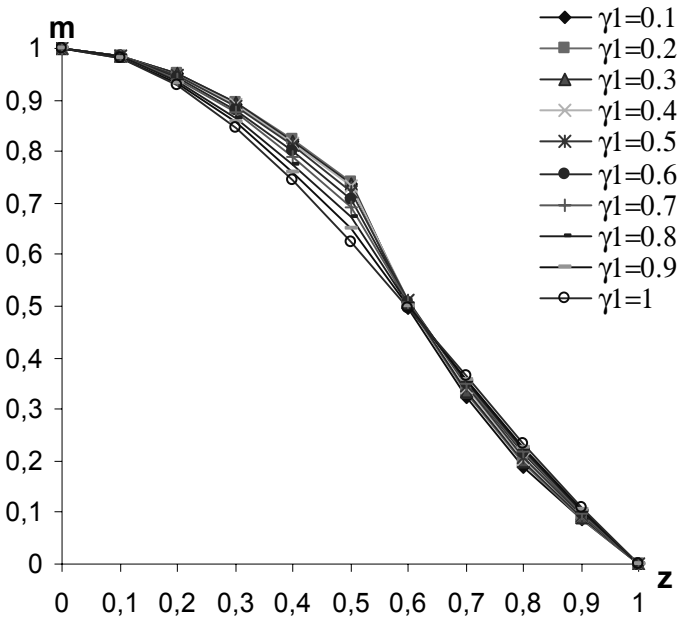

Figure 6.15. Bending moment m distribution for simply supported plates

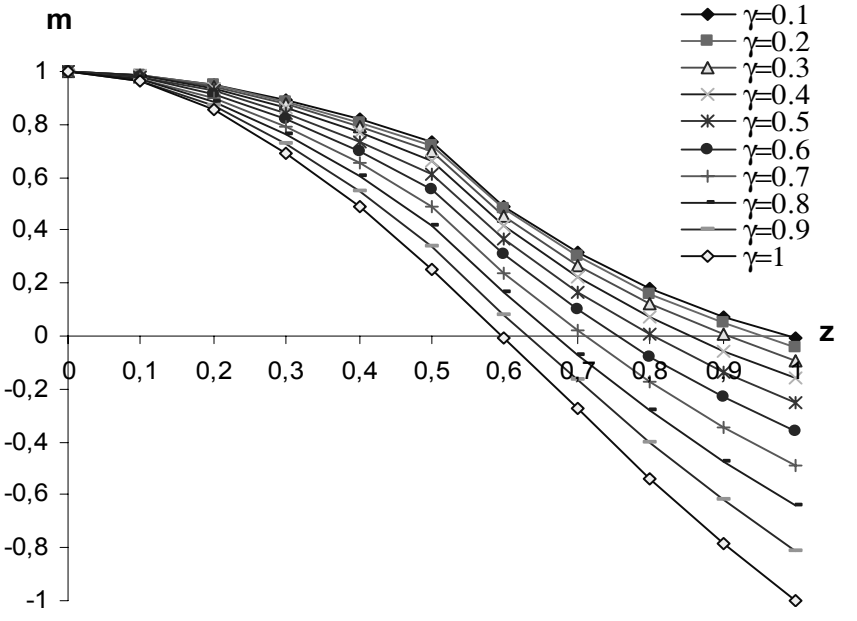

Figure 6.16. Bending moment m distribution for clamped plates

Table 6.1. Coefficient of efficiency for simply supported plates

ν / ν	0.84	0.86	0.88	0.9	0.92	0.94	0.96	0.98	1
0.1									1
0.2								0.9741	1
0.3							0.9503	0.9732	1
0.4						0.9278	0.9485	0.9727	1
0.5					0.9066	0.9250	0.9474	0.9724	1
0.6				0.8869	0.9024	0.9233	0.9467	0.9722	1
0.7			0.8712	0.8809	0.9001	0.9221	0.9461	0.9720	1
0.8			0.8606	0.8778	0.8984	0.9212	0.9457	0.9719	1
0.9		0.8417	0.8564	0.8756	0.8971	0.9205	0.9454	0.9718	1
1	0.8249	0.8361	0.8536	0.8739	0.8961	0.9199	0.9451	0.9717	1

Table 6.2. Coefficient of efficiency for clamped plates

ν / ν	0.76	0.78	0.8	0.82	0.84	0.88	0.92	0,98	1
0.1									1
0.2									1
0.3								0.9997	1
0.4							0.9988	0.9988	1
0.5						0.9971	0.9946	0.9981	1
0.6					0.9976	0.9905	0.9916	0.9976	1
0.7				0.9947	0.9870	0.9856	0.9893	0.9973	1
0.8			0.9891	0.9835	0.9795	0.9822	0.9879	0.9972	1
0.9		0.9869	0.9756	0.9759	0.9744	0.9802	0.9874	0.9974	1
1	0,9913	0.9701	0.9669	0.9709	0.9713	0.9795	0.9880	0.9983	1

Optimal values of parameters α_1 and γ_1 as functions of v are depicted in Fig. 6.9–6.12. Fig. 6.9, 6.10 are obtained for simply supported plates and Fig. 6.11, 6.12 for clamped plates. Different curves in Fig. 6.9–6.12 are obtained for different values of the crack parameter ν. It reveals from Fig. 6.9, 6.12 that α_1 for simply supported plates and γ_1 for clamped plates increase when v increases. In other cases they behave vice versa.

Maximal deflections as functions of γ_1 and α_1 are plotted in Fig. 6.13 for simply supported and in Fig. 6.14 for clamped plates. In this case no optimization procedure is applied. Bending moments for the case when $\alpha_1 = 0.5$ are presented in Fig. 6.15 for simply supported and in Fig. 6.16 for clamped plates. Different curves in Fig. 6.15, 6.16 are calculated for different values of γ_1.

The efficiency of designs established can be assessed by the ratio

$$e = \frac{w_1}{w_*}$$

where w_* stands for the maximal deflection of the reference plate of constant thickness. The latter has common weight with the optimized plate.

Values of the coefficient of efficiency e are accommodated in Tables 6.1 and 6.2. Table 6.1 corresponds to the simply supported plate and Table 6.2 to the clamped plate. It can be seen from Tables 6.1, 6.2 that the optimal designs are more efficient in the case of plates without any cracks.

6.7. Concluding remarks

A method for optimal design was developed for rigid- plastic square plates with cracks at re-entrant corners of steps which are subjected to initial impulsive loading. The plates under consideration have piece wise constant thickness and are made of a rigid-plastic material which obeys Johansen's yield condition.

For determination of residual deflections approximate method of mode form motions was used. Numerical analysis showed that the method of mode form motions leads to results which are close to exact solutions in the case of plates of constant thickness. The statical admissibility of solutions for stepped plates was established numerically.

For determination of optimality conditions variational methods of the theory of optimal control are employed. Numerical results are presented for clamped and simply supported plates with single step of the thickness. Calculations carried out showed that cracks of moderate size have relatively weak influence on the design parameters. However, the existence of a statically admissible solution does depend on the length of the crack.

Acknowledgements
The support from Estonian Science Foundation through the Grant № 5693 is acknowledged.

6.8. References

Baker WE (1975) Approximate techniques for plastic deformation of structures under impulsive loading. Shock Vibration Digest, 7, 107–117

Cox AD and Morland LM (1959) Dynamic plastic deformations of simply supported square plates. J Mech Phys Solids, 7, 229–241

Jones N (1989) Structural Impact. Cambridge University Press, Cambridge.

Jones N (1971) A theoretical study of the dynamic behaviour of beams and plates with finite deflections. Int J Solids Structures, 7, 1007–1029

Jones N, Uran T and Tekin SA (1970) The dynamic plastic behaviour of fully clamped rectangular plates. Int J Solids Structures, 6, 1499–1512

Kruželecki J and Zyczkowski M (1985) Optimal structural design of shells- asurvey. Solid Mechanics Archives, 10, 101–170

Lellep J, Hein H (2002) Optimization of clamped plastic shallow shells subjected to initial impulsive loading. Eng Optim 34, 545–556

Lellep J and Lepik Ü (1984) Analytical methods in plastic structural design. Eng Optimiz, 7, 3, 209–239

Lellep J, Mürk A (2004) Inelastic behaviour of stepped square plates. In: Kienzler R, Altenbach H, Ott I (eds) Theories of Plates and Shells. Critical Review and New Applications (Euromech Colloquium 444 held in Bremen 2002), Springer, Berlin Heidelberg New York, 133–140

Lellep J, Mürk A (2003) Inelastic stepped plates under impulsive loading. In: Gupta NK (ed) Plasticity and Impact Mechanics (Implast 2003 held in New Delhi), Phoenix Publishing House, New Delhi, 577–588

Lellep J, Puman E (2001) Optimization of conical shells of Mises material. Struct Multidisc Optim 22, 149–156

Lellep J, Tungel E (2005) Optimization of plastic spherical shells of von Mises material. Struct Multidisc Optim 30, 381–387

Lepik Ü (1982) Optimal Design of Inelastic Sructures under Dynamic Loading. Valgus, Tallinn (in Russian)

Martin JB and Symonds PS 1966 Mode approximation for impulsively loaded rigid-plastic structures. Proc ASCE, EM92, 43–66

Olson M, Nurick GN and Fagnan JR (1993) Deformation and rupture of blast loaded square plates. Predictions and experiments. Int J Impact Eng, 13, 279–291

Stronge W , Yu TX (1993) Dynamic Models of Structural Plasticity. Springer Verlag, London

Symonds PS (1982) Dynamics of Inelastic Structures. Mir, Moscow, (in Russian)

Symonds PS (1980) Finite elastic and plastic deformations of pulse loaded structures by an extended mode technique. Int J Mech Sciences, 22, 579–605

Ventsel E and Krauthammer T (2001) Thin Plates and Shells. Theory, Analysis and applications. Marcel Dekker, New York.

Yu TX , Chen FL (2000) Failure of plastic structures under intense dynamic loading: modes criteria and thresholds. Int J Mech Sci, 42, 1537–1554
Yu TX , Chen FL (1992) The large dynamic plastic response of rectangular plates. Int J Impact Eng, 12, 603–616
Zhu L (1996) Transient deformation modes of square plates subjected to explosive loadings Int J Solids Structures, 33, 301–314
Zhu L, Yu TX (1997) Saturated impulsive for pulse-loaded elastic- plastic square plates. Int J Solids Structures, 34, 1709–1718
Zyczkowski M (1992) Recent advances in optimal structural design of shells. Eur J Mech A/Solids, 11, 5–24

REFERENCES

Aggarwal HR, Ablow CM (1971) Plastic bending of an annular plate by uniform impulse. Int J Non-Linear Mech, 6, 69-80

Baker WE (1975) Approximate techniques for plastic deformation of structures under impulsive loading. Shock Vibration Digest, 7, 107–117

Bryson A, Ho Yu-Chi (1975) Applied Optimal Control. Wiley, New York

Chakrabarty J (2000) Applied Plasticity. Springer, Berlin New York

Cox AD, Morland LM (1959) Dynamic plastic deformations of simply supported square plates. J Mech Phys Solids, 7, 229–241

Florence AL (1965) Annular Plate under a Transverse Line Impulse. AIAA Journal, 3, 9, 1726-1732

Hocking LM (2001) Optimal Control. An Introduction to the Theory with Applications. Clarendon Press, Oxford

Hopkins HG, Prager W (1954) On the dynamics of plastic circular plates. ZAMP, 5, 317–330

Hull DG (2003) Optimal Control Theory for Applications. Springer, Berlin Heidelberg New York

Ich NT, Jones N (1973) The dynamic plastic behaviour of simply supported spherical shells. Int J Solids Structures, 9, 741–760

Jones N (1971) A theoretical study of the dynamic behaviour of beams and plates with finite deflections. Int J Solids Structures, 7, 1007–1029

Jones N (1980) Dynamic plastic response of structures. Recent Adv Struct Dyn Proc Int Conf Southampton, 677–689

Jones N (1989) Structural Impact. Cambridge University Press, Cambridge

Jones N, Kim SB, Li OM (1997) Response and failure of ductile circular plates struck by a mass. Trans. ASME 119, 332–342

Jones N, Ich NT (1972) The load carrying capacities of symmetrically loaded shallow shells. Int J Solids Structures 8, 1339–1351

Jones N, Uran T, Tekin SA (1970) The dynamic plastic behaviour of fully clamped rectangular plates. Int J Solids Structures, 6, 1499–1512

Jones RM (1999) Mechanics of Composite Materials. Taylor and Francis, Philadelphia

Kaliszky S (1985) Dynamic plastic response of structures. In: Sawczuk A, Bianchi G (eds) Plasticity Today: Modelling, Methods and Applications. Elsevier, London New York, 787–820

Kaliszky S (1989) Plasticity. Theory and Engineering Applications. Elsevier, Amsterdam

Kruželecki J, Zyczkowski M (1985) Optimal structural design of shells- asurvey. Solid Mechanics Archives, 10, 101–170

Lance RH, Robinson DN (1973) Plastic analysis of filled, reinforced, circular cylindrical shells. Int J Mech Sci, 15, 1, 65–79

Lance RH, Robinson DN (1972) Limit analysis of ductile fiber-reinforced structures. Proc ASCE, EM98, 195–209

Lance RH, Robinson DN (1972) A maximum shear stress theory of plastic failure of fiber-reinforced materials. J Mech Phys Solids, 19, 49–60

Lellep J, Hannus S (1995) Optimization of plastic cylindrical shells with stepwise varying thickness in the case of von Mises material. Struct Optim, 10, 122–127

Lellep J, Hein H (2002) Optimization of clamped plastic shallow shells subjected to initial impulsive loading. Eng Optim, 34, 545–556
Lellep J, Hein H (1994) Optimization of clamped rigid-plastic shallow shells of piece wise constant thickness. Int J Non-Linear Mech, 29, 625–636
Lellep J, Lepik Ü (1984) Analytical methods in plastic structural design. Eng Optim, 7, 3, 209–239
Lellep J, Mürk A Optimization of inelastic annular plates with cracks. Struct Multidisc Optim (in press)
Lellep J, Mürk A Optimization of axisymmetric plates with cracks. Int J Solids Structures (in press)
Lellep J, Mürk A Optimization of inelastic square plates with cracks. Eng Optim (in press)
Lellep J, Mürk A (2004) Inelastic behaviour of stepped square plates. In: Kienzler R, Altenbach H, Ott I (eds) Theories of Plates and Shells. Critical Review and New Applications (Euromech Colloquium 444 held in Bremen 2002), Springer, Berlin Heidelberg New York, 133–140
Lellep J, Mürk A (2003) Inelastic stepped plates under impulsive loading. In: Gupta NK (ed) Plasticity and Impact Mechanics (Implast 2003 held in New Delhi), Phoenix Publishing House, New Delhi, 577–588
Lellep J, Myrk A (2002) Optimization of stepped plates under dynamic loading. Engineering Design Optimization. Proc 4th ASMO-UK/ISSMO Conf (Ed P. Gosling). Newcastle, 119–125
Lellep J, Mürk A (1999) Optimization of axisymmetric plates of composite materials. Impact and Damage Tolerance Modelling of Composite Materials and Structures. Proc Euromech Colloq 400 (Ed Soutis C, Guz IA). Imperial Colledge of Science, Technol Medic London, 146–153
Lellep J, Mürk A (1997) Optimization of annular plates of composite materials. Polymeric Composites-Expanding the Limits. Proc 18-th Riso Int Symposium on Materials Science, (Eds Andersen SI et al.), Roskilde, 405–410
Lellep J, Puman E (2001) Optimization of conical shells of Mises material. Struct Multidisc Optim, 22, 149–156
Lellep J, Puman E (2000) Optimization of plastic conical shells loaded by a rigid central boss. Int J Solids Struct, 37, 2695–2708
Lellep J, Puman E (1999) Optimization of plastic conical shells of piece wise constant thickness. Struct Optim, 18, 74–79
Lellep J, Tungel E (2005) Optimization of plastic spherical shells of von Mises material. Struct Multidisc Optim, 30, 381–387
Lellep J, Tungel E (2005) Optimization of plastic spherical shells with a central hole. Struct Multidisc Optim, 23, 3, 233–240
Lepik Ü (1982) Optimal Design of Inelastic Sructures under Dynamic Loading. Valgus, Tallinn (in Russian)
Lepik Ü (1982) Optimal design of non-linear-viscous circular and annular plates. Tartu Ülikooli Toimetised, 627, 9–16 (in Russian)
Lepik Ü, Mroz Z (1977) Optimal design of plastic structures under impulsive and dynamic pressure loading. Int J Solids Struct, 13, 657–674
Li QM, Jones N (1994) Blast loading of fully clamped circular plates with transverse shear effects. Int J Solids Struct, 31, 1861–1876

Liu D, Stronge W (1996) Shear and bending deformations of rigid-plastic circular plates by central pressure pulse. Int J Impact Eng, 18, 383–402
Ma G, Iwasaki Shoji, Miyamoto Y, Deto H (1999) Dynamic plastic behaviour of circular plate using unified yield criterion. Int J Solids Struct, 36, 3257–3275
Martin, JB (1975) Plasticity. Fundamentals and General Results. MIT Press, Cambridge
Martin JB, Symonds PS (1966) Mode approximation for impulsively loaded rigid-plastic structures. Proc ASCE, EM92, 43–66
Mazalov VN, Nemirovsky JuV (1976) Dynamical bending of rigid-plastic annular plates. Int J Non-Linear Mech, 11, 25-39
Nurick GN, Martin JB (1989) Deformation of thin plates subjected to impulsive loading — a review. Part I: Theoretical considerations. Int J Impact Eng, 8, 159–170
Olson M, Nurick GN, Fagnan JR (1993) Deformation and rupture of blast loaded square plates. Predictions and experiments. Int. J Impact Eng, 13, 279–291
Pinch E (1993) Optimal Control and the Calculus of Variations. Oxford University Press, Oxford
Romalis N, Tamuzs V (1989) Fracture of Non-Homogeneous Solids. Zinatne, Riga (in Russian)
Sage AP, White CC (1977) Optimum Systems Control. Prentice Hall, New Jersey
Shapiro GS (1959) On a rigid-plastic annular plate under impulsive load. Prikl Mat Mekh, 23, 172-175
Shen WQ, Jones N (1993) Dynamic response and failure of fully clamped circular plates under impulsive loading. Int J Impact Eng, 13, 259–278
Stronge WJ, Yu TX (1993) Dynamic Models for Structural Plasticity. Springer, New York, London
Symonds PS (1982) Dynamics of Inelastic Structures. Mir, Moscow, (in Russian).
Symonds (1980) Elastic, finite deflection and strain rate effects in a mode approximation technique for plastic deformation of pulse loaded structures. J Mech Eng Sci, 22, 4, 189–197
Tamuzs V, Romalis N, Petrova V (2000) Fracture of Solids with Microdefects. Nova Science Publ, New York
Ventsel E, Krauthammer T (2001) Thin Plates and Shells. Theory, Analysis and applications. Marcel Dekker, New York
Wang Y, Yu M, Xiao Y, Li L (2005) Dynamic plastic response of a circular plate based on unified strength theory. Int J Impact Eng, 31, 25–40
Wang AJ (1955) The permanent deflection of a plastic plate under blast loading. J Appl Mech, 22, 375–376
Wang AJ, Hopkins HG (1954) On the plastic deformation of built-in circular plates under impulsive load. J Mech Phys Solids, 3, 22–37
Wen HM, Yu TX, Reddy TY (1995) A note on circular clamped plates under impulsive loading. Mech Struct Mach, 23, 331–342
Yu TX, Chen FL (2000) Failure of plastic structures under intense dynamic loading: modes criteria and thresholds. Int J Mech Sciences, 42, 1537–1554
Yu TX, Chen FL (1998) Failure modes and criteria of plastic structures under intense dynamic loading: a review. Metals and Materials, 4, 219–226
Yu TX, Chen FL (1992) The large dynamic plastic response of rectangular plates. Int J Impact Eng, 12, 603–616
Zhu L (1996) Transient deformation modes of square plates subjected to explosive loadings. Int J Solids Structures, 33, 301–314

Zhu L, Yu TX (1997) Saturated impulsive for pulse-loaded elastic- plastic square plates. Int J Solids Structures, 34, 1709–1718

Zyczkowski M (1992) Recent advances in optimal structural design of shells. Eur J Mech A/Solids, 11, 5–24

SUMMARY

Optimization of inelastic plates with cracks

In the present study problems of optimization of stepped plates with cracks are investigated. The plates are subjected to the initial impulsive loading.

Current thesis consists of five original research papers of the author. In Chapter I the introduction to contributing publications is presented.

In Chapter II "Inelastic stepped plates under impulsive loading" the dynamic response of fiber reinforced inelastic annular plates is investigated. The plates of sandwich cross-section are subjected to the initial impulsive loading and clamped at the outer or at the inner edge. An approximate theoretical method resorting to the method of mode form motions is developed for predicting residual deflections. The bounds of the applicability of the approximate technique are established.

In Chapter III "Optimization of inelastic annular plates with cracks" annular plates clamped at the outer edge with free inner edge are studied. They are made of a fiber reinforced composite material and have piece wise constant thickness. At the re-entrant corners of the steps stable circular cracks with variable deepness are located. The plates under consideration are imparted initial velocity and the subsequent motion is due to inertia. An optimal design method is developed for minimization of residual deflections under the condition that the volume of the plate is fixed. Variational methods of the theory of optimal control are used in order to derive necessary optimality conditions for stepped plates. Numerical results are presented for the case of plates with single step.

Chapter IV "Optimization of axisymmetric plates with cracks" is devoted to the optimization of cracked annular plates clamped at the inner edge and free at the outer edge. Stable cracks are located at the re-entrant corners of steps. Optimal designs which correspond to the minimum of residual deflections for fixed material consumption are established. The efficiency of designs is evaluated numerically.

In Chapter V "Inelastic behaviour of stepped square plates" square plates subjected to impulsive loading are studied. The plates with and without cutout are considered. A method for determination of residual deflections of stepped plates is developed. The approach is based on the approximate method of mode form motions. Numerical results are presented for full plates and plates with cutouts whereas outer edges can be simply supported or clamped.

In Chapter VI "Optimization of inelastic square plates with cracks" an optimization procedure is developed for stepped square plates with cracks. The plates are subjected to the initial impulsive loading and the material of plates obeys Johansen's yield condition. Edges of plates can be both, simply supported or clamped. Maximal residual deflections are predicted by an approximate method of mode form motions resorting to the energy balance. An optimal design which corresponds to the minimum of residual deflections is developed under the given weight of the plate.

KOKKUVÕTE (Summary in Estonian)

Pragudega plastsete plaatide optimiseerimine

Käesolevas töös uuritakse dünaamiliselt koormatud rõngasplaate ja ruudukujulisi plaate arvestades pragusid. Vaadeldakse tükiti konstantse paksusega plaate. Optimiseerimisülesannetes leitakse niisuguste plaatide projektid, mille korral maksimaalne jääkläbipaine saavutab minimaalse väärtuse antud ruumala korral. Materjali käitumise iseloomustamiseks kasutatakse ideaalselt jäik-plastse keha mudelit. Eeldatakse, et materjal allub assotsieeritud voolavusseadusele, Johanseni ning Lance'i ja Robinsoni poolt välja töötatud voolavustingimustele. Püstitatud ülesanded lahendatakse voolavustingimuste mitmesuguste aproksimatsioonide korral. Erinevate ülesannete lahendamisel vaadeldakse mitmeid plaadi kinnitusviise.

Töö koosneb kuuest peatükist, millest igaüks kujutab endast üht autori originaalpublikatsiooni. Esimeses peatükis esitatakse autori publikatsioonides lahendatud ülesannete püstitused ning nende ülevaatlik analüüs.

Teises peatükis "Mitte-elastsete astmetega plaatide impulsiivne koormamine" uuritakse komposiitmaterjalist rõngasplaatide dünaamilist käitumist. Vaadeldakse ideaalselt kahekihilise ristlõikega ehk niinimetatud sandwich-tüüpi ristlõikega plaate, millele on rakendatud impulsskoormus. Uuritakse rõngasplaate, mille üks serv on vabalt toetatud ja teine jäigalt kinnitatud. Plaadid on armeeritud ühesuunaliste kiududega. Kasutatakse Lance'i ja Robinsoni voolavustingimust, mida võib kujutleda Tresca voolavutingimuse modifikatsioonina. Jääkläbipainete määramisel kasutatakse modaalsete lahendite meetodit. Numbrilised tulemused leitakse ühe astmega plaadi korral. Saadud tulemusi illustreerivad momentide ja läbipainete graafikud. Leitakse ka paksuste alumised piirid, mis esitatakse kahes tabelis.

Kolmandas peatükis "Pragudega mitte-elastsete rõngasplaatide optimiseerimine" uuritakse väljast jäigalt kinnitatud ja seest vabalt toetatud komposiitmaterjalist rõngasplaate. Eraldi vaadeldakse juhtusid, kui armeerivad kiud asetsevad tangentsiaalsuunas või radiaalsuunas. Plaadid on tükiti konstantse paksusega. Eeldatakse, et plaadi hüppekohtades on erineva sügavusega stabiilsed praod. Plaadile mõjub impulsiivne koormus. Eeldatakse, et materjal allub Lance'i ja Robinsoni voolavustingimusele. Leitakse plaadi optimaalne projekt, mille korral maksimaalne jääkläbipaine saavutab miinimumi fikseeritud ruumala korral. Optimaalsuse tarvilike tingimuste tuletamisel astmeliste plaatide jaoks kasutatakse optimaalse juhtimise teoorial põhinevat variatsioonmeetodit. Numbrilised tulemused on saadud ühe astmega plaadi korral.

Neljandas peatükis "Pragudega telgsümmeetriliste plaatide optimiseerimine" leitakse väljast vabalt toetatud ja seest jäigalt kinnitatud komposiitmaterjalist rõngasplaatide optimaalsed projektid. Minimiseeritakse plaadi maksimaalset jääkläbipainet etteantud ruumala korral. Plaat on impulsiivselt koormatud. Vaa-

deldakse plaate, mis on armeeritud kas tangentsiaalse või radiaalse orientatsiooniga kiududega. Kasutatakse Lance'i ja Robinsoni voolavustingimust ristküliku kujul. Optimaalsuse tarvilike tingimuste tuletamisel kasutatakse optimaalse juhtimise teoorial põhinevat variatsioonmeetodit. Numbrilised tulemused on saadud ühe astmelise plaadi korral.

Viiendas peatükis "Astmetega ruudukujuliste plaatide käitumine plastsete deformatsioonide korral" uuritakse dünaamiliselt koormatud ruudukujulisi plaate. Plaadi paksus on astmeline. Vaadeldakse nii avausega kui ilma avauseta plaate. Plaadid on külgedelt kas jäigalt kinnitatud või vabalt toetatud (ilma avauseta plaadi korral) ning seest vabalt toetatud ja väljast jäigalt kinnitatud (avausega plaadi puhul). Leitakse meetod jääkläbipainete määramiseks kasutades modaalsete lahendite meetodit. Kasutatakse Johanseni voolavustingimust ruudu kujul. Numbrilised tulemused on saadud ühe astmega plaadi korral.

Kuuendas peatükis "Pragudega mitte-elastsete ruudukujuliste plaatide optimiseerimine" on esitatud optimiseerimismeetod astmelise paksusega ruudukujulise plaadi jaoks. Plaadile mõjub impulsskoormus. Eeldatakse, et materjal allub Johanseni voolavustingimusele. Plaadi küljed on kas vabalt toetatud või jäigalt kinnitatud. Maksimaalsete jääkläbipainete määramisel kasutatakse modaalsete lahendite meetodit. Määratakse plaadi optimaalne projekt juhul, kui plaadi astmete kohtades on lokaalsed praod. Leitakse plaadi maksimaalsed jääkläbipainded fikseeritud ruumala korral. Numbrilised tulemused on saadud ühe astmega plaadi jaoks.

ACKNOWLEDGEMENTS

I am very grateful to my supervisor Professor Jaan Lellep for his advices and continuous support during my doctoral studies.

I would like to thank my colleagues for their comments and suggestions.

I am also grateful to all my friends and my relatives (especially my parents) for their support and encouragement.

The partial support of Estonian Science Foundation through grant № 5693 is acknowledged.

CURRICULUM VITAE

Annely Mürk

Born:	October 21,1971, Põlva, Estonia
Nationality:	Estonian
Marital Status:	single
Aaddress:	Liivi 2, 50409 Tartu, Estonia
Phone:	+372 737 6425, e-mail: annely.murk@ut.ee

Education

1990	Põlva Secondary School
1991–1996	Faculty of Mathematics, University of Tartu, *Baccalaureus Scientiarum* in mathematics
1996–1999	MSc student at Institute of Applied Mathematics, University of Tartu,
2000	*Magister Scientiarum* in mathematics
2000	Tartu University, Faculty of Mathematics, Teacher of Mathematics in Upper Secondary School
2000–2006	PhD student at Institute of Applied Mathematics, University of Tartu.

Professional employment

Since 10/2004 extraordinary researcher at Institute of Applied Mathematics, University of Tartu

Scientific work

Optimization of rigid-plastic plates under dynamical loading.

Special courses

February 1998, University of Sunderland, “Analysis of Dynamical Systems”, TEMPUS project.

CURRICULUM VITAE (in Estonian)

Annely Mürk

Sünniaeg ja -koht: 21. oktoober 1971, Põlva, Eesti
Kodakondsus: Eesti
Perekonnaseis: vallaline
Aadress: Liivi 2, 50409 Tartu, Estonia
Tel: +372 737 6425, e-mail: annely.murk@ut.ee

Haridus

1990	Põlva Joh.Käisi nim. Keskkool, keskharidus.
1991–1996	Tartu Ülikool, Matemaatikateaduskond, bakalaureuseõpe, *Baccalaureus Scientiarum* matemaatika erialal.
1996–1999	Tartu Ülikool, Matemaatikateaduskond, magistriõpe,
2000	*Magister Scientiarum* matemaatika erialal.
2000	Tartu Ülikool, Matemaatikateaduskond, põhikooli ja gümnaasiumi matemaatikaõpetaja kutse.
2000–2006	Tartu Ülikool, Matemaatika-informaatikateaduskond, doktoriõpe.

Teenistuskäik

Alates okt. 2004 Tartu Ülikooli rakendusmatemaatika instituudi erakorraline teadur.

Teaduslik tegevus

Teadustöö teema on dünaamiliselt koormatud jäik-plastsete plaatide optimiseerimine.

Erialane enesetäiendus

Veebruar 1998, Sunderlandi Ülikool, “Dünaamiliste süsteemide analüüs”, TEMPUS projekti raames.

LIST OF PUBLICATIONS

1. J. Lellep and A. Mürk Optimization of inelastic annular plates with cracks, Structural and Multidisciplinary Optimization (in press)
2. J. Lellep and A. Mürk Optimization of axisymmetric plates with cracks, International Journal of Solids and Structures (in press)
3. J. Lellep and A. Mürk Optimization of inelastic square plates with cracks, Engineering Optimization (in press)
4. J. Lellep and A. Mürk (2004) Inelastic behaviour of stepped plates. Lecture Notes in Applied and Computational Mechanics. Vol. 16 Theories of Plates and Shells. Critical Review and New Applications (Eds. R. Kienzler, H. Altenbach, I. Ott), Springer, 133–140.
5. J. Lellep and A. Mürk (2003) Inelastic stepped plates under impulsive loading. Proc. 8th Int. Symp. Plasticity and Impact Mechanics. Phoenix Publishing House, (Ed. N. Gupta), New Delhi, 577–588.
6. J. Lellep and A. Myrk (2002) Optimization of stepped plates under dynamic loading. Engineering Design Optimization. (Ed. P. Gosling), Proc. 4th ASMO-UK/ ISSMO Conf. Newcastle, 119–125.
7. J. Lellep and A. Mürk (1999) Optimization of axisymmetric plates of composite materials. Impact and Damage Tolerance Modelling of Composite Materials and Stuctures. Proc. Euromech. Colloquium 400, (Eds. C. Soutis and I. Guz), London, 146–153.
8. J. Lellep and A. Mürk (1997) Optimization of annular plates of composite materials. Polymeric Composites-Expanding the Limits. Proc.18-th Riso Int. Symposium on Materials Science, (Eds. S. I. Andersen et al.), Roskilde, 405–410.
9. J. Lellep and A. Mürk (1996) Optimization of fiber-reinforced plastic circular plates. 9-th Nordic Seminar on Computational Mechanics, Lyngby, 29–32.